The Official Journal of the Chinese Stomatological Association (CSA)

Chinese Journal of Dental Research

CJDR

VOLUME 27 NUMBER 4 2024

OUTSTANDING SELECTION

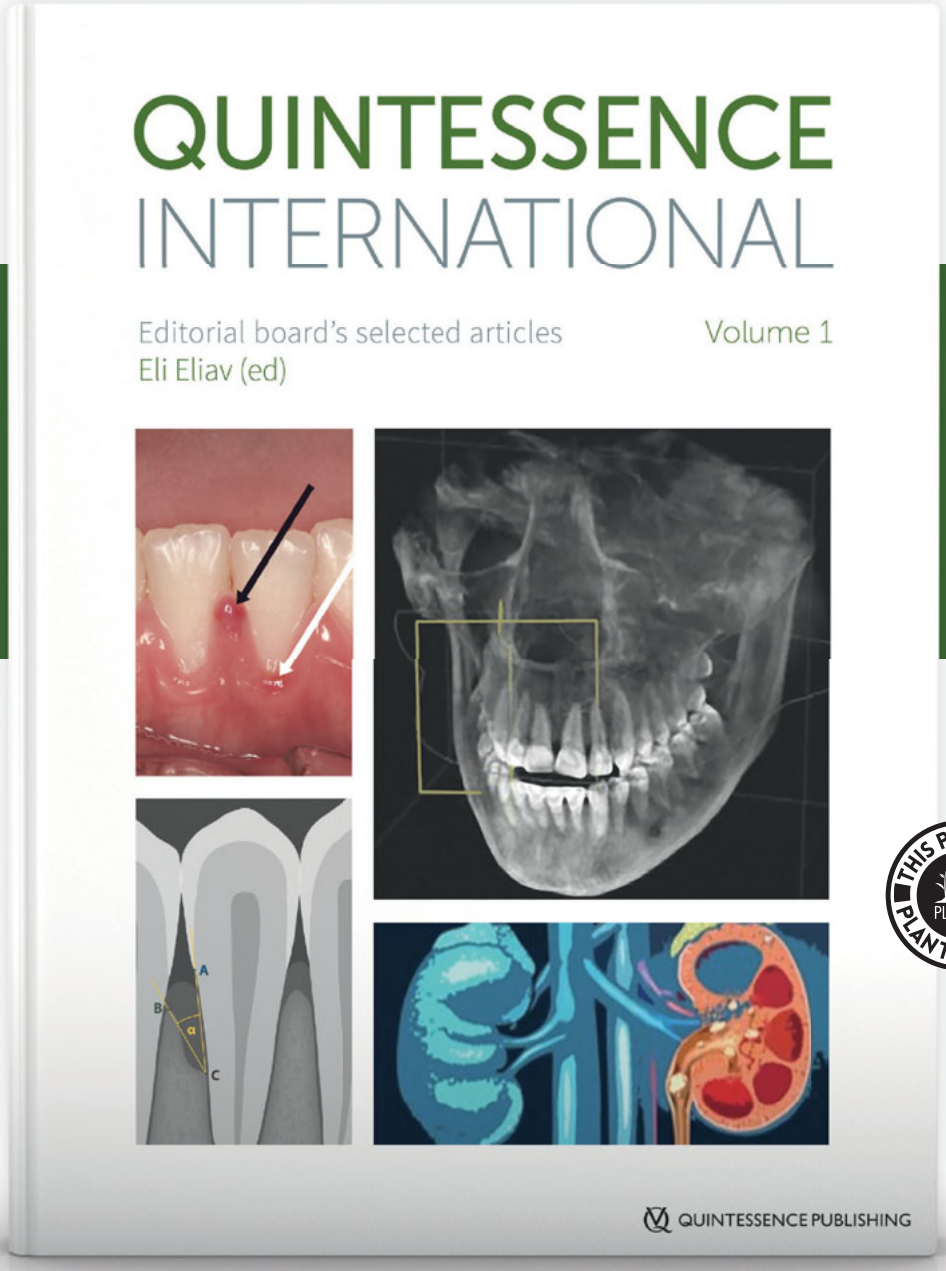

Eli Eliav (Ed)

Quintessence International Volume 1

Editorial board's selected articles

216 pages, 100 illus.
ISBN 978-1-78698-143-1, €28 ~~€98~~

THIS PRODUCT ONE TREE PLANTED PLANTS TREES

This Quintessence International (QI) annual yearbook is a compilation of selected articles representing the most significant work from the past year. Through a double-blind process that ensures anonymity and quality, our team of editors and reviewers performed the remarkable and difficult task of reviewing and evaluating many deserving submissions to present you with this outstanding selection of 20 articles. Organized by disciplines and topics, the articles provide a valuable and user-friendly resource that we hope you find enjoyable and informative.

www.quint.link/qi-vol1
books@quintessenz.de
+49 (0)30 761 80 667
QUINTESSENCE PUBLISHING

Chinese Journal of Dental Research

The Official Journal of the Chinese Stomatological Association (CSA)

Chinese Journal of Dental Research

The Official Journal of the Chinese Stomatological Association (CSA)

Review

Original articles

Original articles

Case report

Chinese Journal of Dental Research

CN 10-1194/R • ISSN 1462-6446 • eISSN 1867-5646 • Quarterly
The Official Journal of the Chinese Stomatological Association
Co-sponsor: Peking University School of Stomatology, Quintessenz Verlag

Publication Department

Production Manager: Megan Platt (London, UK)
Managing Editor: Xiao Xia ZHANG (Beijing, P.R. China)

Address: 4F, Tower C, Jia 18#, Zhongguancun South Avenue, HaiDian District, 100081, Beijing, P.R. China.
Tel: 86 10 82195785, **Fax:** 86 10 62173402
Email: editor@cjdrcsa.com

Manuscript submission: Information can be found on the Guidelines for Authors page in this issue. To submit your outstanding research results more quickly, please visit: http://mc03.manuscriptcentral.com/cjdr

Administrated by: China Association for Science and Technology
Sponsored by: Chinese Stomatological Association and Popular Science Press
Published by: Popular Science Press
Printed by: Beijing ARTRON Colour Printing Co Ltd
Subscription (domestically) by Post Office

Chinese Journal of Dental Research is indexed in MEDLINE.

For more information and to download the free full text of the issue, please visit
www.quint.link/cjdr
http://www.cjdrcsa.com

Acknowledgements

We would like to express our gratitude to the peer reviewers for their great support to the journal in 2023.

Afrashtehfar, Kelvin (Switzerland)
Agudelo-Suárez, Andrés (Colombia)
Aksoy, Merve (Turkey)
Alkan Aygor, Fehime (Turkey)
Al-Nuaimi, Nassr (United States)
An, Na (China)
Ananthaswamy, Akanksha (India)
Arpornmaeklong, Premjit (Thailand)
Arslan, Merve (Turkey)
Ateş, Melis Oya (Turkey)
Ayna, Emrah (Turkey)
Ballal, Nidambur (India)
Banerjee, Santasree (China)
Bayindir, Funda (Turkey)
Bi, Liang Jia (China)
Bilgili, Dilber (Turkey)
Brailo, Vlaho (Croatia)
Buldur, Burak (Turkey)
Cao, Zheng Guo (China)
Chabbra, Ajay (India)
Chai, Yang (United States)
Chen, Bin (China)
Chen, Chen (China)
Chen, Fa Ming (China)
Chen, Li (China)
Chen, Li Li (China)
Chen, Peng (China)
Chen, Tao (China)
Chen, Zhi (China)
Chu, Chun Hung (HK, China)
Cui, Li (United States)
Dede, Dogu Omur (Turkey)
Dehghanian, Danoosh (Iran)
Desai, Rajiv S (India)
Ding, Ming Chao (China)
Dong, Yan Mei (China)
Eaton, Kenneth (United Kingdom)
El-Bialy, Tarek (Canada)
Elias, Carlos N (Brazil)
Erber, Ralf (Germany)
Esen, Çağri (Turkey)
Fan, Yuan (China)
Fan, Zhi Peng (China)
Fathy Abo-Elmahasen, Mahmoud M (Egypt)
Feng, Chen (China)
Fu, Kai Yuan (China)
Gallo, Camila (Brazil)
Gan, Ye Hua (China)
Gao, Xue Jun (China)
Garoushi, Sufyan (Finland)
Geduk, Gediz (Turkey)
Grigorian, Mircea (Romania)
Gruber, Reinhard (Austria)
Gu, Yong Chun (China)
Gündoğar, Mustafa (Turkey)
Han, Dong (China)
Hashimoto, Kenji (Japan)
He, Miao (China)
Hong, Guang (Japan)
Hourfar, Jan (Germany)
Hu, Wen Jie (China)
Hua, Fang (China)
Huang, Zhen (China)
Jayasinghe, Ruwan D (Sri Lanka)
Ji, Yi (China)
Jiang, Hong Bing (China)
Jiang, Jiu Hui (China)
Ju, Xiang Qun (Australia)
Kaklamanos, Eleftherios G (Cyprus)
Karadas, Muhammet (Turkey)
Khan, Sher Alam (Pakistan)
Khijmatgar, Shahnawaz (India)
Kinzinger, Gero (Germany)
Kurt, Aysegul (Turkey)
Li, Gang (China)
Li, Yi Hong (United States)
Li, Yu (China)
Li, Ze Han (China)
Lin, Min Kui (China)
Lin, Xiao Ping (China)
Liu, Da Wei (China)
Liu, Da Yong (China)
Liu, Hai Bo (China)
Liu, Hong Wei (China)
Liu, Huan (China)
Liu, Jian Zhang (China)
Liu, Jia Qiang (China)
Liu, Min (China)
Liu, Yao (China)
Liu, Ya Wei (China)
Lu, Yan (China)
Lucchese, Alessandra (Italy)
Mady, Fatma (Egypt)
Mahjabeen, Wajiha (Pakistan)
Mossey, P. A. (United Kingdom)
Nassani, Mohammad zakaria (Saudi Arabia)
Nayak, Ullal Anand (Saudi Arabia)
Neves, Lucimara Teixeira das (Brazil)
Niu, Li Na (China)
Özdemir, Burcu (Turkey)
Ozturk, Taner (Turkey)
Pan, Shao Xia (China)
Pan, Ya Ping (China)
Pan, Yong Chu (China)
Park, Joo-Cheol (Korea)
Pei, Dan Dan (China)
Pereira, Jefferson Ricardo (Brazil)
Pugazhendi, Sathish kumaran (India)
Qin, Li Zheng (China)
Ren, Xiu Yun (China)
Ren, Yi Jin (Netherlands)
Ritchie, Helena H. (United States)
Rodrigues, Gabriel (Oman)
Saber, Shehabeldin Mohamed (Egypt)
Saddki, Norkhafizah (Malaysia)
Saito, Hanae (United States)
Sarialioglu Gungor, Ayça (Turkey)
Sharma, Rajinder K. (India)
Shi, Song Tao (China)
Si, Yan (China)
Song, Jin Lin (China)
Song, Xiao Meng (China)
Song, Ya Ling (China)
Sousa-Neto, Manoel D. (Brazil)
Su, Guan Yue (China)
Sui, Bing Dong (China)
Sulaiman, Ghassan M. (Iraq)
Sun, Qiang (China)
Sun, Yu Chun (China)
Sun, Zhi Peng (China)
Taneja, Pankaj (Denmark)
Tang, Qing Ming (China)
Tao, Ren Chuan (China)
Topsakal, Kubra Gulnur (Turkey)
Tsoi, James (HK, China)
Tuovinen, Olli (United States)
Uzun, Ismail (Turkey)
Wajid Hussain Chan, Malik (Pakistan)
Wang, Chun Li (China)
Wang, Fu (China)
Wang, Lin (China)
Wei, Fu Lan (China)
Wei, Xi (China)
Wu, Tao (China)
Wu, Yi Qun (China)
Xie, Shang (China)
Xu, Kang (China)
Xu, Tian Min (China)
Yu, Jin Hua (China)
Yu, Xi Jiao (China)
Yuan, Quan (China)
Zadeh, Homayoun H. (United States)
Zeng, Xiao Juan (China)
Zhang, Cheng Fei (HK, China)
Zhang, Hao (China)
Zhang, Hong Liang (China)
Zhang, Lei (China)
Zhao, Yu Ming (China)
Zheng, Shu Guo (China)
Zheng, Yun Fei (China)
Zhou, Hai Hua (China)
Zhou, Hong Mei (China)
Zhou, Ping (United States)
Zhu, Xiao Fei (China)
Zong, Chen (Belgium)

Editorial Office
Chinese Journal of Dental Research

Tooth Root Development and Homeostasis during Eruptive and Post-eruptive Movement

En Hui YAO[1], Jia Hui DU[1], Xin Quan JIANG[1]

Tooth eruption is the process whereby the developing tooth moves to its functional position in the occlusal plane and it occurs concomitantly with formation of the tooth root, which is a critical component of the tooth anchored to surrounding alveolar bone through the periodontal ligament. Post-eruptive tooth movement ensues that once occlusion is achieved, the teeth maintain their alignment within the alveolar bone to facilitate proper bite function through periodontium remodelling. Tooth overeruption presents a clinically significant issue, yet the precise mechanisms by which alterations in occlusal forces are translated into periodontal remodelling remain largely unexplored. In this review, the present authors aim to outline the latest progress on the potential mechanisms governing tooth root formation and homeostasis during tooth eruptive and post-eruptive movement. Based on recent findings using various mouse models, we provide an overview of the collaborative intercellular interaction during root formation, including Hertwig's epithelial root sheath, dental papilla and dental follicle. Moreover, we summarise the potential mechanism underlying post-eruptive movement mainly in view of the responses of periodontal tissues to vertical mechanical stimuli. In sum, the precise regulatory mechanisms during tooth eruption throughout life will shed light on disease treatment of tooth eruption defects and overeruption.

Keywords: *homeostasis, mechanotransduction, periodontium, tooth eruption, tooth root*
Chin J Dent Res 2024;27(4):273–289; doi: 10.3290/j.cjdr.b5860254

The tooth, which comprises two functionally distinct components, the crown and the root, is critical for mastication, digestion and phonation.[1,2] Tooth development begins with the dental lamina and underlying dental mesenchyme, and involves sequential, reciprocal epithelial-mesenchymal interactions. The dental lamina derives from thickened oral epithelium, giving rise to the enamel organ (epithelial component). The condensed dental mesenchyme is derived from cranial neural crest cells after their migration into the oral region of the first pharyngeal arch, and diversifies into dental papilla (DP) and dental follicle (DF) (mesenchymal components). DP gives rise to dental pulp and odontoblasts, whereas DF differentiates into periodontal tissues including the periodontal ligament (PDL), cementum and alveolar bone.[2-4]

Tooth eruption refers to the movement of the tooth from its developmental location within the arch to its functional position in the oral cavity,[2,5] a process that occurs concomitantly with root formation.[6] The process of tooth eruption can be divided into three distinct phases: pre-eruptive tooth movement (phase 1), eruptive tooth movement (phase 2) and post-eruptive tooth movement (phase 3).[6] Pre-eruptive tooth movement is a series of intricate biological events that take place for the preparation of tooth emergence into the oral cavity, which mainly consists of the early stages of tooth development until the onset of tooth root formation.[6] Eruptive tooth movement occurs accompanied by tooth

1 Department of Prosthodontics, Shanghai Ninth People's Hospital, Shanghai Jiao Tong University School of Medicine; College of Stomatology, Shanghai Jiao Tong University; National Center for Stomatology; National Clinical Research Center for Oral Diseases; Shanghai Key Laboratory of Stomatology; Shanghai Research Institute of Stomatology; Shanghai Engineering Research Center of Advanced Dental Technology and Materials, Shanghai, P.R. China.

Corresponding authors: Dr Jia Hui DU and Dr Xin Quan JIANG, Shanghai Ninth People's Hospital, Shanghai Jiao Tong University School of Medicine, 639 Zhizaoju Road, Huangpu District, Shanghai 200011, P.R. China. Tel: 86-21-63135412. Email: jiahuidu2010@126.com; xinquanjiang@aliyun.com.

This work was sponsored by funding from the National Natural Science Foundation of China (82201004 to J.D., 81921002 to X.J., 82130027 to X.J.) and the Young Elite Scientists Sponsorship Programme by CAST (YESS20230102).

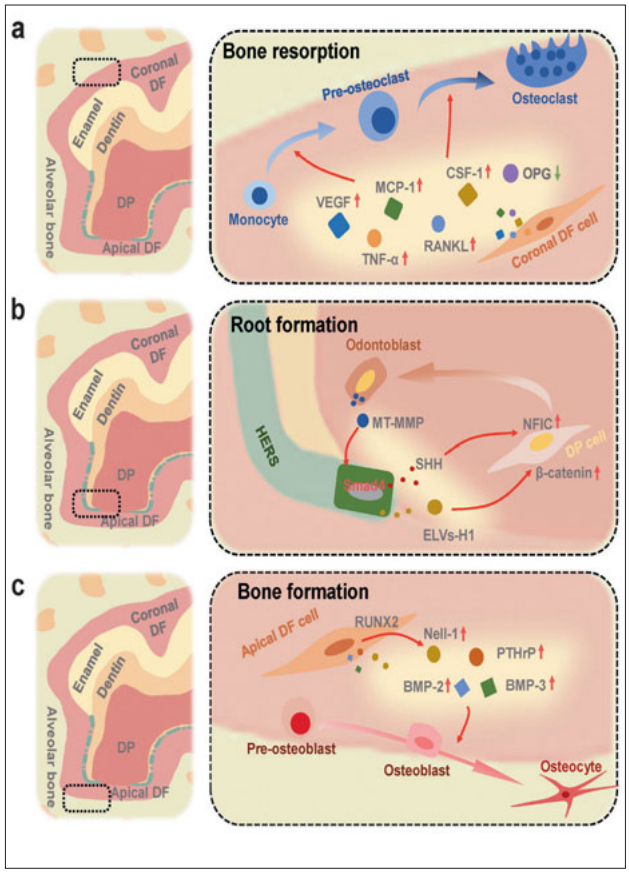

Fig 1a to c Cellular interactions during tooth eruption and tooth root formation. Coronal DF regulates osteoclastic bone resorption during eruptive tooth movement **(a)**. The interaction between HERS and DP participates in tooth root formation **(b)**. Basal DF regulates osteoblastic bone formation during eruptive tooth movement **(c)**.

root formation, and lasts until the tooth crown reaches the occlusal plane. This phase can be divided into two stages: intra- and supraosseous eruptive tooth movement.[6] It involves the formation of Hertwig's epithelial root sheath (HERS), root dentine, the PDL, cementum, alveolar bone in the apical tooth region, and osteoclast-mediated bone resorption of the cortical shell overlaying the tooth crown for eruptive path formation, which jointly facilitate the emergence of the tooth into the oral cavity.[5,7-9] Once the tooth reaches its occlusal position, occlusal force starts to stimulate the continuous maturation of the periodontal attachment apparatus of the tooth.[10] Physiological post-eruptive movement in a vertical direction happens throughout life, which compensates for coronal wear and maintains the position of the tooth within the alveolar bone to achieve proper occlusion.[10] Vertical post-eruptive movement leads to the concerning issue of tooth overeruption after the loss of the opposing occlusion.[6,10,11] Post-eruptive tooth movement in a horizontal direction happens mainly due to adjacent tooth loss or under orthodontic force.[12-14] The potential mechanisms that govern tooth root formation and homeostasis during eruptive and post-eruptive tooth movement remain largely unexplored.

In this review, the present authors summarised the potential mechanisms underlying eruptive and post-eruptive tooth movement (Table 1), specifically highlighting the collaborative intercellular interaction involved in tooth eruption, including HERS, DP and DF (Fig 1). For post-eruptive tooth movement, we focused on the responses of periodontal tissues to vertical mechanical stimuli (Fig 2). Additionally, we described various mouse models used to study occlusal hypofunction or hyperfunction, including molar extraction,[15-22] dietary modifications,[23-25] induction of masticatory muscle atrophy[26,27] and the use of intraoral bite blocks or other devices (Table 2).[16,28-31]

Eruptive tooth movement

Pre-eruptive tooth movement consists of the early stages of tooth development until the onset of tooth root formation. The development of the tooth crown begins from the dental lamina, followed by a series of bud, cap and bell stages. At the interface between the dental epithelium and mesenchyme, odontoblasts and ameloblasts differentiate to form dentine and enamel, respectively.[32]

The process of tooth eruption can be regarded as the result of increments of basal tissue and subtractions of coronal tissue, which are mediated by intricated cellular interactions between HERS, DP, DF and so on (Table 1 and Fig 1).[6,7,11,33-37] The increments mainly include root formation, PDL formation and osteogenesis in the root region, providing motive forces for coronal eruption. Meanwhile, the decrement refers to the formation of the eruption pathway through osteoclastic activities above the tooth crown region. After the bone overlying the erupting tooth is resorbed, the reduced dental epithelium and the oral epithelium fuse, degenerate and form an epithelial canal through which the tooth erupts, thus preventing bleeding during supraosseous tooth eruption. Then the tooth gradually reaches its functional position and achieves occlusal contact with the opposite tooth.[2,3]

HERS

Tooth root initiation and shaping

Once crown formation is completed, epithelial cells of the inner and outer enamel epithelium proliferate

Table 1 Mechanisms of tooth root development and homeostasis during eruptive and post-eruptive movement.

Phase	Cell type	Genotype/model	Mechanism	Phenotype/function
Eruptive tooth movement	HERS	*K14-Cre; Wnt10a*$^{fl/fl}$	Ablation of epithelial *Wnt10a* resulted in the elevation of *Wnt4* and *Axin2* in DP	Loss of *Wnt10a* led to an absence of or apically located root furcation in mouse molars[42]
		K14-Cre; Wnt10a$^{fl/fl}$	Epithelial deletion of *Wnt10a* resulted in decreased *Notch2* and *Jag1* expression in HERS, which might suppress the Notch signalling transduction	Loss of epithelial *Wnt10a* presented enlarged pulp chamber and apical displacement of the root furcation of multi-rooted teeth[43]
		Krt5-rtTA; tetO-Cre; Alk3$^{fl/fl}$	Epithelial *Bmpr1a* knockout promoted Wnt/β-catenin signalling	Cessation of epithelial BMP signalling by *Bmpr1a* depletion during the differentiation stage switched differentiation of crown epithelium into the root lineage and formed ectopic cementum-like structures[49]
		Krt14-rtTA; tetO-Cre; Smad4$^{fl/fl}$*; Shh*$^{fl/fl}$	Loss of *Smad4* resulted in ectopic Shh-Gli1 signalling and maintenance of Sox2+ cells	Loss of *Smad4* in the dental epithelium of developing molars prolonged the maintenance of the cervical loop and molar crown development[50]
		K14-Cre; Smad4$^{fl/fl}$	TGF-b/BMP signalling relied on a Smad-dependent mechanism in regulating *Nfic* expression via Shh signalling to control root development	Loss of *Smad4* in HERS led to abnormal enamel and dentine formation 14 d after kidney capsule transplantation[59]
		Shh-CreER; Ctnnb$^{fl/fl}$*; R26R*	The inactivation of β-catenin in HERS increased EMT of HERS cells and regulated the odontogenic differentiation of DP through inducing the expression of morphogenetic regulators such as *Osx* and *Nfic*	The inactivation of β-catenin in HERS led to failure of odontogenic differentiation of DP cells and interrupted root elongation due to premature disruption of HERS at P10[39]
		Cell culture	ELVs-H1 activated Wnt/β-catenin signalling	ELVs-H1 promoted the migration and proliferation of DP cells and induced odontogenic differentiation[86]
	DP	*Nfic*$^{-/-}$	*Nfic* regulated Hh signalling in dental mesenchyme through upregulation of *Hhip*, contributing to apical DP growth and proper root formation	Loss of *Nfic* led to short and malformed roots and decreased alveolar bone formation[55,59,60]
		Col1-Cre; Osx$^{fl/fl}$	Loss of *Osx* resulted in a decrease in expression of DMP1 and DSPP	Loss of *Osx* led to inhibition in odontoblast differentiation, and short thin root dentine with few dentine tubules at 2 wk[61]
		OC-Cre; Ctnnb1$^{fl/fl}$*; R26R*	Disruption of β-catenin in odontoblasts and cementoblasts diminished expression of Col1α1, OC and DSPP	Inactivation of β-catenin in developing odontoblasts led to normally extended HERS, impaired root odontoblast differentiation and failed root formation from P5-28[62,63]
		Osr2-Cre; Ezh2$^{fl/fl}$	Interplay between EZH2 and ARID1A epigenetically modulated Cdkn2a expression in the dental mesenchyme, influencing root patterning and growth	Mesenchyme lacking *Ezh2* resulted in too few roots, and abnormality in the "bridge" region between the roots; epithelium lacking *Ezh2* led to an incorrect number of roots and lately developed bridges between the roots from P6-28[67]
		Gli1-CreER; Arid1a$^{fl/fl}$	Loss of ARID1A disturbed the differentiation-associated cell cycle arrest of tooth root progenitors through Hh signalling regulation	Loss of ARID1A led to shortened roots and delayed eruption[68]
		Ogn$^{-/-}$	SCAPs secreted OGN to inhibit the Hh pathway to regulate DFSC differentiation and pluripotency	Loss of *Ogn* accelerated root elongation and dentine deposition from P0-30[93]
		Osx-Cre; MT1-MMP$^{fl/fl}$	MT1-MMP mediated matrix remodelling in tooth eruption through effects on bone formation, soft tissue remodelling and organisation of the DF/PDL region	Absence of MT1-MMP in Osx-expressing mesenchymal cells led to altered HERS structure, short roots, impaired dentine formation and mineralisation, and decreased alveolar bone formation at P10, P76-79[96]
		Prx1-Cre; PTH1Rfl/fl	Loss of *PTH1R* in Prx1+ progenitors mutant mice led to reduced alveolar bone formation and decreased expression of key regulators of osteogenesis	Conditional deletion of *PTH1R* using the Prx1 promoter exhibited delayed molar eruption[97]

Table 1 (cont.) Mechanisms of tooth root development and homeostasis during eruptive and post-eruptive movement.

Phase	Cell type	Genotype/model	Mechanism	Phenotype/function
	DF	*PTHrP-CreER; PPR*$^{fl/fl}$; *R26R*$^{tdT/+}$	PPR deficiency induced a cell fate shift of PTHrP+ DF mesenchymal progenitor cells to nonphysiological cementoblast-like cells precociously forming the cellular cementum on the root surface associated with up-regulation of Mef2c and matrix proteins	Loss of PPR in PTHrP+ DF cells resulted in defective formation of the periodontal attachment apparatus, tooth root malformation and failure of tooth eruption in molars from P3-182[69]
		Lepr-Cre; Igf1$^{fl/fl}$; *Slc1a3-CreER; Igf1r*$^{fl/fl}$	Igf1-Igf1r signalling mediated cell-cell interaction between lateral and apical DF domains	Loss of *Igf1* or *Igf1r* led to a larger PDL area at P16.5[58]
		Osr2-Cre; Foxp4$^{fl/fl}$	*Foxp4* partly regulated lineage contribution of the apical DF	Deletion of *Foxp4* in the dental mesenchyme led to an increased PDL area and diminished periostin expression at P16.5[58]
		Runx2 mutation	*Runx2* mutation impaired osteogenesis through inhibiting osteoblast-associated genes, including *Runx2*, *Alpl*, *Osx*, *OC* and *Col1a1*	*Runx2* mutation resulted in cleidocranial dysplasia (CCD) hindered alveolar bone formation and led to eruption failure[74]
		Cell culture	*Runx2* directly interacts with the OSE2 elements to transactivate the human *Nell-1* promoter	Transfection of *Runx2* into rat osteoblasts resulted in the upregulation of *Nell-1* expression, and in Runx2-null calvarial cells, the expression of *Nell-1* was restored[77]
		Harlan Sprague-Dawley rats; cell culture	TNF-α enhances the expression of BMP-2 and BMP-3, with a more pronounced effect on BMP-2	BMP-2, BMP-3 and TNF-α are notably expressed in the basal DF at P3 and P9[72,78]
Post-eruptive tooth movement	Cementoblast	*Rsk2*$^{-/y}$	*Rsk2* was a critical regulator of cementoblast function	Loss of *Rsk2* led to cementum hypoplasia, detachment and disorganisation of the PDL and significant alveolar bone loss with age[102]
		Cell co-culture	*PTHrP* influenced the balance of OPG and RANKL production by cementoblasts	Cementoblasts had the capability to inhibit osteoclast differentiation[105]
		Cell co-culture	Cementoblasts upregulated osteoclastogenesis associated chemokines/cytokines and RANKL through the TLR-2 signaling pathway in response to LPS	Cementoblasts contributed to the recruitment of osteoclastic precursor cells[106]
		Cell culture	Force-loaded cementocytes regulated osteoclastogenesis and osteoclastic root resorption in cell-to-cell communication using the S1P/S1PR1/Rac1 axis during this process	IDG-CM6 cells under compression force regulated osteoclast precursors/osteoclasts[133]
	PDL fibroblast	*Mkx*$^{-/-}$	Mkx upregulated the expression of collagens such as *Col1α1* and *Col1α2*, and inhibited PDL degeneration through the suppression of osteogenic-related gene expression including *Osx*, *Alpl* and Run*x2* in PDL fibroblasts	Loss of Mkx led to changes in PDL properties including expansion of the PDL, collagen fibril degeneration and morphological changes in PDL cells at 6 and 12 mo[113]
		Bgn$^{-/0}$*Fmod*$^{-/-}$	SLRPs regulated TGF-β/BMP signalling, matrix turnover and collagen organisation	Deletion of *Bgn* and *Fmod* resulted in abnormal collagen fibrils in PDL, altered remodelling of alveolar bone and elevated numbers of osteoclasts at 4 to 8 wk[116]
		Cell co-culture	Co-cultures of PBMCs with human primary PDL fibroblasts resulted in a marked increase in ICAM-1 and osteoclastogenesis-related markers (RANKL, RANK, TNF-α)	Cell–cell adhesion between osteoclast precursors and PDL fibroblasts led to a significant rise in osteoclast-like cell numbers[117]
		Unloading model	Unloading led to decreased PLAP-1 in PDL fibroblasts which inhibited *Col1* expression while promoted Osx and OC expression, thus suppressing collagen synthesis and triggering osteogenesis	Unloading resulted in a decrease in collagen disorder in PDL, enhanced osteogenic activity on PDL–bone border, aggravated osteoclast activity in alveolar bone inner part, increase in alveolar bone height, and a gain in the mandibular width[17]

		Unloading model (patient)	Unloading led to a downregulation of BBS7 in PDL of unopposed teeth and occlusal force influenced the expression of BBS7 to mediate Shh signalling activity	Occlusal hypofunction led to a dynamic alternation in PDL, including the cells, fibres, primary cilia and blood vessels[130]
		Unloading model	PDL plays a pivotal role in mechanotransduction by translating physical forces into the intracellular signalling axis Piezo1/Ca^{2+}/HIF-1α/SLIT3, which promotes type H angiogenesis and OSX+ cell-related osteogenesis	Occlusal hypofunction induced periodontal disuse atrophy characterized by a progressive decrease in BV/TV and mineral density, enlargement of the medullary space in the interradicular area, decreased PDL width and increasingly sparse collagen bundles in the furcation areas[20]
		Cell co-culture (vertical force)	Vertical mechanical stress resulted in dose- and time-dependent upregulation of RANKL expression via increased PGE2 production	Vertical mechanical stress led to a notable rise in osteoclast-like cell formation[118]
		Hyper-loading model	Hyper-occlusion predominantly induced CCL2 expression in PDL tissues and promoted chemotaxis and osteoclastogenesis	Mechanical stress-dependent alveolar bone destruction[31]
		CCL2$^{-/-}$ or *CCR2*$^{-/-}$ mice	Hyper-occlusion induced compensatory CCL3 expression and promoted osteoclastogenesis to counterbalance deficient CCL2/CCR2 signalling	Mechanical stress-dependent alveolar bone destruction[30]
	PDLSC	*Gli1-CreER; Ai14* (unloading)	Gli1+ cells in the PDL were MSCs and could contribute to alveolar bone regeneration	Unloading led to a decrease in the activities of PDLSCs, lower alveolar bone height (CEJ-ABC) and lower bone density, which were more dramatic in the furcation and interdental septum regions from 14 to 60 d post[18]
		Lepr-CreER; tdT (unloading and hyper-loading)	Modulation on activation and osteogenic differentiation of Lepr+ PDLSCs under hyper-loading and unloading of occlusal forces depends on Piezo1-mediated mechanosensing	Unloading led to impaired osteogenic differentiation of Lepr+ cells from 1 to 35 d; hyper-loading resulted in osteogenic differentiation of Lepr+ cells from 0 d to 28 d post[16]
		Axin2-CreER; R26R$^{mT-mG/+}$ (hyper-loading)	Wnt-responsive stem/progenitor cells coordinate the functional adaptation of PDL and alveolar bone to hyper-loading	Hyper-loading resulted in increased collagen deposition, a thicker, stiffer PDL, activated bone resorption, the peak of which was followed by a bone formation phase, leading ultimately to an accelerated rate of mineral apposition and an increase in alveolar bone density at hyper-loading 7 to 28 d[19]
	Osteocytes	*Gli1-CreER; Ai14; Sost*$^{-/-}$ (unloading)	Alveolar bone osteocytes negatively regulated Gli1+ PDLSCs activity through Sost in response to unloading	Knockout of Sost eliminated the response of Gli1+ PDLSCs to unloading on 14/30 d post[18]
	Osteoblasts	*Piezo1-CreER; Rosa26-Ai47* (unloading)	PIEZO1 may promote osteoclastic apoptosis through osteoblast-secreted FasL through a PIEZO1-STAT3/ESR1-FasL pathway	Piezo1 activation prevented occlusal force loss-induced alveolar bone loss[22]

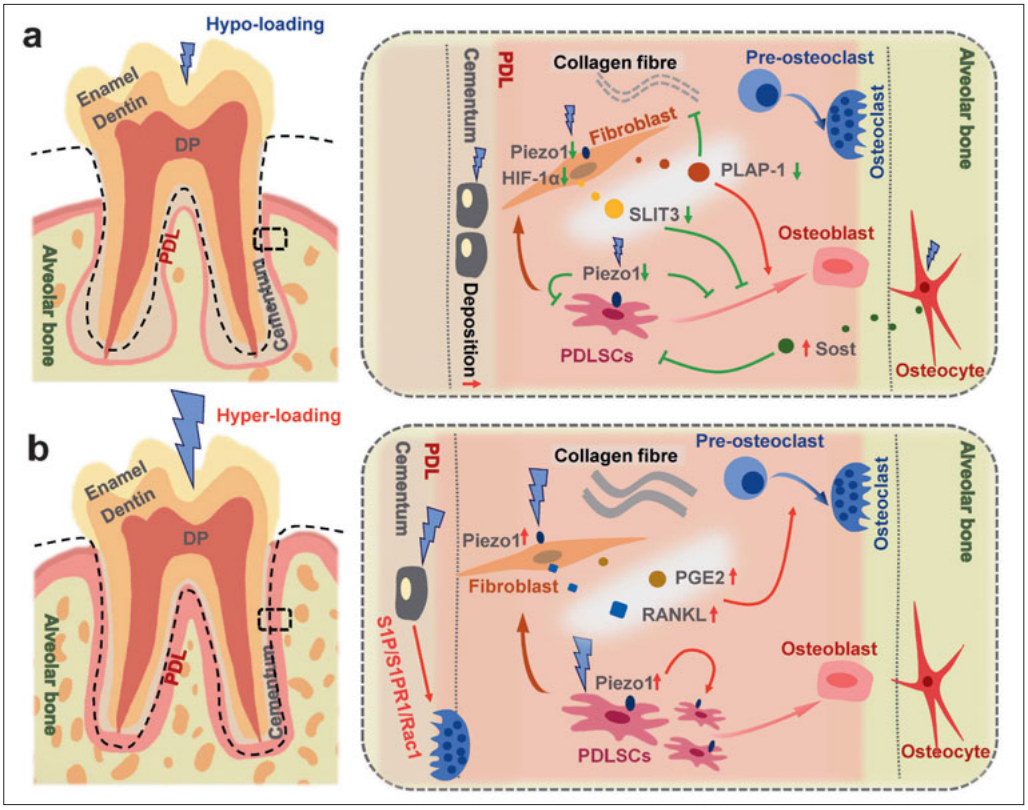

Fig 2a and b Mechanisms of periodontium response to mechanical stimuli. Hypo-loading leads to apical cellular cementum deposition, sparse and disorganised collagen fibres, enhanced osteogenic activity in the PDL-bone border with a gain in alveolar bone height, and aggravated osteoclast activity in alveolar bone marrow with progressive decrease in BV/TV and mineral density **(a)**. Hyper-loading leads to enhanced cementum hardness and resorption, thicker and stiffer collagen fibres and activated bone resorption, followed by a bone formation phase, leading ultimately to increased alveolar bone density **(b)**. The dotted lines represent the normal tooth border.

from the cervical loop of the enamel organ to form a double layer of cells known as HERS.[2,38,39] HERS cells express strong epithelial cell markers Keratin 14 (K14) and E-cadherin.[39,40] HERS elongates apically, acting as a template for root morphology and guiding the emergence of multi-rooted structures in posterior teeth. It invaginates inwards towards the pulp at the location of future root furcation, thus forming multiple roots. Deviations in this process lead to a variety of morphological root variances such as supernumerary roots, pyramidal-shaped roots and taurodontism.[41] For example, researchers found that loss of Wnt10a in the HERS, which is a ligand in canonical Wnt signalling, inhibits cell proliferation and horizontal elongation, leading to taurodontism with the absence of or apically located pulp floor and pulp chamber enlargement.[42,43]

Regulatory mechanism of HERS

The formation and function of HERS are regulated by multiple classical signalling pathways, such as sonic hedgehog (Shh), Wnt/β-catenin and bone morphogenic protein (BMP)/transforming growth factor-beta (TGF-β) signalling pathways.[44] Shh, a member of the vertebrate Hh family and expressed in the apical HERS, is crucial for epithelial-mesenchymal interactions at the root apex. Nakatomi et al[45] identified *Ptc1* as Shh target genes mainly expressed in DP adjacent to the HERS, whose loss leads to inhibited cell proliferation, root elongation and disturbed eruption in homozygous Ptc^{mes} mutants at 4 weeks. β-catenin, expressed in HERS during tooth root formation, is a key mediator of canonical Wnt signalling. Yang et al[39] reported that the inactivation of β-catenin in HERS leads to interrupted root elongation due to premature disruption of HERS. In addition, it has been reported that loss of Wnt ligands results in a breakdown of the epithelial integrity of HERS with aberrant cellular projections.[46] BMP/TGF-β signalling is a key regulator for stem cell fate determination in many epithelial tissues, such as the hair and intestine.[47,48] BMP signalling is actively involved in regulating cell fate decisions during the formation of HERS. Yang et al[49] showed that cessation of the epithelium BMP signalling switches differentiation of crown epithelia into the root lineage, forming ectopic cementum-like structures using a *Krt5-rtTA;tetO-Cre;Alk3*$^{fl/fl}$ mouse model. Li et al[50] found that loss of *Smad4* in the dental epithelium prolongs the maintenance of the cervical loop and molar crown development through BMP-SMAD4-Shh signalling using a *Krt14rtTA;tetO-Cre;Smad4*$^{fl/fl}$*;Shh*$^{fl/fl}$ mouse model.

Table 2 Comparison between different models of occlusal hypofunction/ hyperfunction.

Model	Surgery	Animal	Age	Site/methods	Analysis time	Phenotype
Hypo-loading	Extraction	Swiss Webster mice	35 d	Maxillary molars	6/21 d after surgery	Increased cellular cementum; larger cementocytes[15]
		Gli1-CreER; tdT mice	4 wk	3 maxillary molars	14/30/60 d after surgery	Lower alveolar bone height (CEJ-ABC); lower bone density[18]
		Lepr-CreER; tdT mice	6 wk	Maxillary first molar	14 d after surgery	Impaired osteogenic differentiation of Lepr+ cells[16]
		C57BL/6J mice	4 wk	3 maxillary molars	2/4/6 wk	Decrease in BV/TV and mineral density, bone resorption in the medullary space and PDL atrophy[20]
		C57BL/6J mice	4 wk	3 maxillary molars	1/4/12 wk	Collagen disorder in PDL, enhanced osteogenic activity on the PDL–bone border, aggravated osteoclast activity in alveolar bone inner part, increase in alveolar bone height, gain in mandibular width[17]
		Sprague-Dawley rats	5 wk	Mandibular molars	4 wk after surgery	Active bone formation on the PDL–bone border, expansion in bone marrow and decrease in bone volume[21]
		Sprague-Dawley rats; *Piezo1-CreER; Rosa26-Ai47* mice	6 wk (rats)	3 maxillary/mandibular molars	12 wk after surgery (rats); 3 wk after surgery (mice)	Decreased alveolar bone loss in the Piezo1 activated group[22]
	Diet	*Axin2-CreER; R26Rm*$^{T\text{-}mG/+}$ mice	P15	Soft diet	P15-65	PDL atrophy[23]
		Sprague-Dawley rats	21 wk	Soft diet	27 wk	Higher and wider alveolar process[25]
	Muscle atrophy (single side botulinum toxin [BTX] injection)	Sprague-Dawley rats	18 wk	Masseter and temporal muscles	4 wk after surgery	Masseter and temporal muscle atrophy and alveolar bone loss in injected side[26]
		New Zealand white rabbits	5 mo	Masseter muscle	4/12 wk after surgery	Decreased bone volume in molar regions of both sides[27]
	Devices	Mice	5 wk	Maxilary first molar (flatten cusps)	6 wk after surgery	mx M1: elongation of both the mesial root and its surrounding alveolar bone; mn M1: overeruption of the mesial side of the tooth[28]
		Wistar-strain rats	5 wk	Bite-raising appliance	16 wk	Longer and narrower roots especially the mesial root, a decrease in root area and PDL thickness and area[29]
Hyper-loading	Molar extraction	*Axin2-CreER; R26R*$^{mT\text{-}mG/+}$ mice	5 wk	Maxillary second and third molar	7/14/28/56 d after surgery	Increased collagen deposition, a thicker, stiffer PDL, activated bone resorption followed by bone formation, leading ultimately to mineral apposition and increased alveolar bone density[19]
	Diet	C57BL/6 J mice	3 wk	Hard diet	14 wk	Osteocytes balanced the cytokine expression to enhance jaw bone formation[24]
		Axin2-CreER; R26Rm$^{T\text{-}mG/+}$ mice	P15	Hard diet	P15-65	Mastication-induced strain maintained the PDL fibres[23]
	Devices	*Lepr-CreER; tdT* mice	6 wk	Maxillary first molar(adhere composite resin)	14 d after surgery	Promoted osteogenic differentiation of Lepr+ cells[16]
		Wistar rats/ddY mice	8 wk/ 5 wk	3 mx molars (bond stainless steel wire)	4–7 d after surgery	Upregulated expression of CCL2 in PDL, CCR2 in pre-osteoclasts, and tartrate-resistant acidphosphatase-positive cells in alveolar bone[31]
		CCL2$^{-/-}$ or *CCR2*$^{-/-}$ mice	5 wk	3 maxillary molars	4–7 d after surgery	Increased expression of CCL3 and TRAP-positive cells[30]

P, postnatal day.

DP

Tooth root pulp and dentine formation

At the cap stage, the DP is formed underlying the invaginated dental lamina. Subsequently, DP cells develop into dental pulp cells and odontoblasts.[2,51] It is well documented that stem cells that exist in the apical DP could contribute to tooth root formation.[52] Using lineage tracing mice models, researchers have validated that various markers can be utilised to identify stem cells in the DP in vivo, such as Wnt1,[53] osterix (OSX),[54] Gli1,[55] Axin2[56] and α-smooth muscle actin (α-SMA).[57] Recently, utilising single-cell transcriptome profiling of the mouse molar at postnatal day 3.5 (P3.5), Jing et al[58] revealed that apical DP cells (Aox3+/Tac1+) are progenitor cells with a highly proliferative capacity and give rise to odontoblasts and the dental pulp lineage.

Regulatory mechanism of DP

The development and differentiation of DP are regulated by multiple molecular factors. Nuclear factor I-C (NFIC) is a transcription factor (TF) that binds to DNA through CAATT-boxes. The function of NFIC during postnatal root development has been confirmed using the *Nfic*$^{-/-}$ mouse model, which exhibits short and malformed root morphology but displays normal crowns.[59,60] Besides, Liu et al[55] proved that *Nfic* regulates Hh signalling in the dental mesenchyme by upregulating *Hhip*, an Hh attenuator, thus contributing to apical DP growth and proper root formation. Zhang et al[61] suggested that OSX, a mesenchymal TF involved in osteogenesis and odontogenesis, promotes odontoblast and cementoblast differentiation and root elongation using a *Col1-Cre;Osx*$^{fl/fl}$ mouse model. Beyond its role in HERS, Wnt/β-catenin signalling activity in odontoblast-lineage cells is also indispensable for root formation. Root odontoblast differentiation has been found to be impeded with diminished expression of collagen type I, alpha 1 (Col1α1), osteocalcin (OC) and dentine sialophosphoprotein (DSPP), leading to failed root formation with conditional knockout β-catenin in developing odontoblasts.[62,63]

Epigenetic regulation has also been implicated in the processes of root formation. EZH2, the catalytic subunit of the polycomb repressive complex 2, silences its target genes by generating the lysine 27 trimethylation epigenetic mark on histone H3.[64] ARID1A contains a DNA-binding domain and mediates the chromatin remodelling function of the SWI/SNF complex, playing a role in cell cycle regulation, metabolic reprogramming and epithelial-mesenchymal transition.[65,66] Jing et al[67] revealed that the interplay between EZH2 and ARID1A epigenetically modulates *Cdkn2a* (a cell cycle inhibitor) expression in the dental mesenchyme, influencing root patterning and growth through targeted deletion of EZH2 in the dental mesenchyme using *Osr2-Cre;Ezh2*$^{fl/fl}$ mouse models. Using a *Gli1-CreER;Arid1a*$^{fl/fl}$ mouse model, Du et al[68] showed that loss of ARID1A impairs the differentiation-associated cell cycle arrest of tooth root progenitors through Hh signalling regulation, leading to shortened roots and delayed eruption.

DF

Periodontal tissues and eruption pathway formation

The DF, outside both the enamel organ and DP, contributes to the periodontal attachment apparatus including the cementum, PDL and alveolar bone.[6] It has been demonstrated that distinct cellular domains within the DF function differently during tooth crown and root development.[8,35,58] It has been confirmed that the lateral and apical DF domains contain precursors that can differentiate into PDL fibroblasts, cementoblasts and alveolar bone osteoblasts.[6,58,69] Thus, the removal of the basal half of the DF results in no bone accrual and tooth eruption[11], whereas coronal DF participates in the regulation of osteoclastic bone resorption,[8] and the removal of the coronal DF could result in failed alveolar bone resorption and tooth eruption.[11]

Regulatory mechanism of DF

Parathyroid hormone-related protein (PTHrP)-PTHrP receptor (PPR) autocrine signalling has been found to be critical for root formation and tooth eruption. PPR knockout in PTHrP+ DF cells was shown to cause failed tooth eruption, which may be induced by a lack of motive forces.[7,69-71] In addition, it is reported that Igf1-Igf1r signalling mediates the cell-cell interaction between lateral and apical DF, which is crucial for PDL development, with its absence resulting in an enlarged PDL area but not affecting root length at P16.5 using *Lepr-Cre;Igf1*$^{fl/fl}$ and *Slc1a3-CreER;Igf1r*$^{fl/fl}$ mouse models where *Igf1* and *Igf1r* were specifically knocked out from the lateral and apical DF.[58] In *Osr2-Cre;Foxp4*$^{fl/fl}$ mice, loss of *Foxp4* in DF leads to an increased PDL area and diminished periostin expression, suggesting that the lineage contribution of the apical DF is regulated in part by *Foxp4*.[58]

The cellular expression of factors involved in bone remodelling varies within different DF domains and

stages, reflecting the coordination of osteogenesis and osteoclastogenesis during eruption.[35,72] RUNX2 is a pivotal TF imperative for the differentiation of osteoblasts. RUNX2 mutations result in cleidocranial dysplasia (CCD), which impairs osteogenesis by inhibiting osteoblast-associated genes, including alkaline phosphatase (*Alpl*), *Osx*, *OC* and *Col1α1*, thereby hindering alveolar bone formation, which functions as a motive force for tooth eruption.[73,74] Tang et al[75] identified that Nel-like molecule type 1 (*Nell-1*) protein is restricted to the odontoblasts and endothelial cells of blood vessels during tooth eruption, and it has been revealed that *Runx2* directly regulates the expression of *Nell-1* by binding to osteoblast-specific binding element 2 sites in the *Nell-1* promoter in vitro experiment.[76,77] Thus, the Runx2/Nell-1 axis in the basal DF may act as one of the key regulatory pathways during alveolar bone formation.[8] BMP-2, BMP-3 and tumour necrosis factor-alpha (TNF-α) are notably expressed in the basal DF, correlating with the onset of alveolar bone formation at P3 and accelerated bone growth at P9 in the alveolar bony crypt of the mandibular first molar in rats.[72,78] Yao et al[72] established that TNF-α enhances the expression of BMP-2 and BMP-3, with a more pronounced effect on BMP-2.

Furthermore, the coronal DF plays a prominent role in modulating osteoclast activity through the upregulation of receptor activator of nuclear factor kappa B ligand (RANKL) and downregulation of osteoprotegerin (OPG), thereby creating the eruption pathway.[35,79-81] The crucial modulation of DF on osteoclastogenesis shows two bursts in the rat mandibular molar development model. At P3, it triggers a significant increase in osteoclast formation with the expression of chemotactic protein-1 (MCP-1) and colony-stimulating factor-1 (CSF-1) at peak levels, attracting osteoclast precursors and stimulating their differentiation.[11,35,82] By P9-11, the expression of CSF-1 and MCP-1 dips, while TNF-α and vascular endothelial growth factor (VEGF) peak. VEGF can also recruit osteoclasts and upregulate RANK expression in endothelial cells and osteoclast precursors, suggesting a role in osteoclastogenesis beyond recruiting precursors.[83,84]

Interaction between HERS, DP and DF

HERS, DP and DF interact closely during tooth root development. In addition to its foundational role in root shaping, HERS also plays a vital role during the differentiation of root odontoblasts in DP during root dentine formation.[41] Mullen et al[85] proved that HERS secretes laminin 5 to induce the growth, migration and differentiation of dental mesenchymal cells in the DP. Huang et al[59] demonstrated that tissue-specific knockout of *Smad4* in HERS, the common mediator of BMP/TGF-β signalling, results in abnormal enamel and dentine formation because of the absence of SMAD4-Shh-NFIC signalling. Yang et al[39] indicated that β-catenin plays roles in cell-cell adhesion of HERS to maintain its structural integrity as well as affect epithelial-mesenchymal transition (EMT), and also regulates the odontogenic differentiation of DP through inducing the expression of morphogenetic regulators such as *Osx* and *Nfic*, using *Shh-CreER;Ctnnb*$^{fl/fl}$*;R26R* mice. Zhang et al[86] demonstrated that HERS-derived exosome-like vesicles (ELVs-H1) promote the migration and proliferation of DP cells and also induce odontogenic differentiation and activation of Wnt/β-catenin signalling.

Concurrently, HERS is also essential for the differentiation of DF cells into periodontal tissues.[87] PDL formation starts with the migrated DF cells in contact with the HERS between root dentine and alveolar bone, coinciding with the beginning of HERS perforation.[80,88] Luan et al[89] demonstrated that although HERS itself did not produce cementum, its fenestration was an essential requirement for the onset of cementogenesis. This finding is consistent with Heretier's hypothesis that the absence rather than presence of HERS epithelial cells was critical for cementogenesis, but they did not exclude the possibility of HERS playing an inductive role during the initiation of acellular cementogenesis.[89,90] Recently, some research has shown that HERS cells may have the capability to transform into PDL fibroblasts and cementoblasts in the development of the periodontal tissues.[91,92] Although it is still questionable whether participation is autonomous or non-autonomous, it is undeniable that HERS plays a crucial role in the formation of cementum.

DF development could also be regulated by the adjacent apical DP. Lin et al[93] proved that stem cells from apical DP (SCAPs)-secreted osteoglycin (OGN) inhibits the differentiation and maintains the stemness of DF stem cells (DFSCs) via the OGN-HH pathway during root development by employing a transwell coculture system. Meanwhile, partial SCAP differentiation markers were upregulated after DFSC coculture. They also demonstrated that OGN knockout leads to accelerated root elongation and dentine deposition from P0 to P30 in *Ogn*$^{-/-}$ mice, probably due to upregulated HH signalling in the apical DP and DF.[93]

The precise regulatory mechanism of tooth eruption is widely debated. Tooth eruption and tooth root formation had been considered independent since teeth can emerge into the oral cavity without roots or PDL.[94,95] Xu et al[96] found that the absence of mem-

brane-type matrix metalloproteinase 1 (MT1-MMP) in mesenchyme leads to malformed roots and decreased alveolar bone formation but with teeth erupted into the oral cavity. Cui et al[97] identified deletion of PTH1R in Prx1+-progenitors results in delayed tooth eruption due to reduced alveolar bone formation despite unaffected molar root and PDL development. Controversy remains over the relationship between tooth root formation and tooth eruption, with some other studies supporting the idea that the processes of tooth eruption and root formation are intertwined.[6,70] Tooth eruption is accompanied by root development and periodontal tissue formation, and the direction of crown movement is consistent with that of root growth.[11,70] In addition, in patients with primary failure of eruption (PFE), defective tooth eruption is likely to be caused by a lack of motive forces, as the eruption path is normal.[70]

Post-eruptive tooth movement

Normal homeostasis

The tooth eruption process does not stop upon reaching the occlusal plane but continues throughout life. In humans, mastication involves cyclic loading by forces ranging from tens to occasionally hundreds of Newtons on the teeth. With each chewing cycle, the teeth may move up to several tens of microns.[98] In homeostasis, continuous remodelling and homeostasis of the cementum and PDL of the tooth root, as well as the alveolar bone, are sophisticatedly maintained (Table 1).[6,10,99]

Cementum physiological apposition

Cementum is a mineralised tissue enveloping the roots of teeth, formed by cementoblasts, marked with ALPL, bone sialoprotein (BSP) and OC, and plays a key role in the periodontal attachment apparatus.[2,100] Xie et al[101] identified that Axin2+ PDL cells are primary progenitor cell sources for cementum formation. Koehne et al[102] demonstrated that ribosomal S6 kinase RSK2 is a critical regulator of cementoblast function. They found cementum hypoplasia in Rsk2-deficient mice, which results in detachment and disorganisation of the PDL and is associated with significant alveolar bone loss with age.[102] Cementocytes, the embedded cells within cellular cementum, exhibit mechanoresponsive properties in response to mechanical forces.[103] Cellular cementum primarily exists on the cervical portions of the root, contributing to tooth anchorage. It extends over the apical root dentine and facilitates continuous occlusal adjustment. While similar to bone in composition, cementum is avascular, does not undergo physiological remodelling and grows by continuous apposition throughout life.[103,104] Boabaid et al[105] demonstrated that cementoblasts inhibit osteoclast differentiation by producing and releasing OPG, suggesting that cementoblasts may play a role in maintaining lower levels of osteoclastic activity at the root surface compared to the adjacent alveolar bone in vitro research. Meanwhile, Nemoto et al[106] reported that cementoblasts contribute to the recruitment of osteoclastic precursor cells through the upregulation of osteoclastogenesis associated chemokines/cytokines and RANKL through the TLR-2 signalling pathway in response to Porphyromonas gingivalis lipopolysaccharide in vitro experiments.

Collagen organisation and maintenance in PDL

PDL is made up of collagen fibre bundles located between the cementum and the inner wall of the alveolar bone.[2,107] It functions not only as a cushion against masticatory pressure but also as a transducer that perceives physical signals and converts them into biological responses within the alveolar bone.[20] Stem/progenitor cells within the PDL termed PDLSCs, which can be marked with Axin2+,[19,23] Gli1+[18,108] and Lepr+ cells,[16,109] have robust self-renewal and multilineage differentiation capacities and are critical for the mechanical response of periodontal tissue.[16,18,109-111] PDL fibroblasts are spindle-shaped and elongated connective tissue cells derived from PDLSCs. They can play an essential role in the mechanical response through primary cilia, which are non-motile sensory organelles.[112-115] Koda et al[113] reported that Mohawk homeobox (*Mkx*), a tendon-specific TF, regulates PDL homeostasis by upregulating the expression of collagens such as *Col1α1* and *Col1α2*, and suppressing osteogenic-related gene expression including *Osx*, *Alpl* and *Runx2* in PDL fibroblasts. Small leucine-rich proteoglycans (SLRPs) are extracellular matrix molecules, suggested to regulate collagen organisation and cell signalling. Wang et al[116] demonstrated the importance of SLRPs in maintaining periodontal homeostasis through regulation of TGF-β/BMP signalling, matrix turnover and collagen organisation using a $Bgn^{-/0}Fmod^{-/-}$ mouse model.

The interaction between PDL fibroblasts and osteoclast precursors profoundly influences periodontal homeostasis. Various mechanical forces to PDL fibroblasts could alter their capacity to produce osteoclastogenesis-related molecules.[112,117,118] Bloemen et al[117] reported a marked increase in the expression of intercellular adhesion molecule-1 (ICAM-1) and osteoclas-

togenesis-related markers (RANKL, RANK, TNF-α), as well as a significant rise in osteoclast-like cell numbers in co-cultures of blood mononuclear cells (PBMCs) with human primary PDL fibroblasts, compared to PBMCs cultured alone.

Continuation of remodelling in alveolar bone

Tooth roots are embedded in the alveolar bone by PDL and the alveolar bone continues remodelling in its physiological state through coupled osteoclast-osteoblast actions.[26,119,120] Osteocytes, the most abundant cells in bone, possess mechanosensing appendices stretching through bone canaliculi.[121] These cells regulate local bone remodelling by directing osteoblast and osteoclast activity in response to mechanical stimuli.[104] In addition, when stimulated by occlusal force, osteocytes have the capability to regulate periodontium tissue turnover by activating PDLSCs that surround the neurovascular bundle, contributing to periodontal homeostasis upon mechanical force,[18,110,122-124] for example sclerostin (SOST) from the osteocyte is a negative feedback regulator for Gli1+ PDLSC activity.[18] Yang et al[22] identified Piezo1 as the pivotal mediator of occlusal force in osteoblasts, thereby sustaining alveolar bone homeostasis through the facilitation of osteogenesis and the orchestration of catabolic pathways via Fas ligand (FasL)-mediated osteoclastic apoptosis.

Hypo-loading condition

It is common to employ an unopposed mouse molar model to investigate axial tooth movement. A hypofunctional state leads to augmented area and thickness in apical regions, suggesting that apposition responds to occlusal load changes with neo-cementogenesis adapting to maintain occlusal height.[15,125,126] Significant cementum formation is associated with elevated extracellular matrix gene expression such as *Col1*, *integrin β5* and *osteonectin* gene expression.[15,125,126] The notable changes following the loss of an opposing tooth highlight the significant role of cementum; however, the mechanisms by which cementum responds to alterations in occlusal forces require further investigation.

The collagen fibre density within the PDL decreases with compromised structural integrity under a hypofunctional state.17,23 PDL-associated protein-1 (PLAP-1)/asporin is an extracellular proteoglycan uniquely localized in the PDL. Chen et al17 demonstrated that unloading reduces PLAP-1 levels in PDL fibroblasts significantly, resulting in inhibited Col1 expression while promoting the expression of Osx and OC, thereby suppressing collagen synthesis and inducing osteogenesis. Bardet-Biedl syndrome 7 (BBS7) is an indispensable constituent of a protein complex named the BBSome, and plays a crucial role in ciliogenesis and regulating Shh signalling activity.127-129 Chang et al130 found that the expression of BBS7 is downregulated in PDL of unopposed teeth in vivo and in vitro, and they reported that occlusal force influences the expression of BBS7 to mediate Shh signaling activity, which is vital for cell migration and thus maintaining proper PDL homeostasis. In a recent study, CD31+ Endomucin+ type H endothelium, especially abundant at the root furcation regions, plays a pivotal role in mechanotransduction in PDL through an intracellular Piezo1/Ca2+/HIF-1α/SLIT3 signalling axis.20 Following occlusal unloading, the density of type H vasculature and coupled OSX+ osteoprogenitors decline significantly.20 Gli1+ PDLSCs, predominantly localised within the apical PDL space and surrounding the neurovascular bundle, are responsible for periodontal tissue turnover and damage repair. Men et al18 demonstrated that unloading inhibits Gli1+ PDLSC activation by upregulating SOST secreted by osteocytes in alveolar bone. Zhang et al16 proved that Lepr+ PDLSCs, located in the perivascular niche, are reduced significantly in hypo-loading, resulting in impaired osteogenic differentiation through Piezo1-mediated mechanosensing in the periodontium.

However, opinions differ on the issue of bone mass in unloading models, with some stating that there is an increase and others a decrease. This disagreement may be due to the different detective sites in the alveolar bone and measurement methods. For the resorption or formation of alveolar bone, the PDL–bone border is characterised by enhanced osteogenic activity, whereas the medullary space of the alveolar bone is typical of aggravated osteoclast activity, which contributes to a progressive decrease in volume fraction (bone volume/total volume index, BV/TV) and mineral density.[17,20,21] Regarding alveolar bone height, two kinds of measurements yield divergent outcomes: the distance from the cementoenamel junction to the alveolar bone crest (CEJ-ABC) indicates an increase, suggesting bone loss in the unloading model,[18] while the distance from the mandibular canal level to the alveolar bone beneath the root furcation, defined as mandibular height, also shows an increase, suggesting bone formation in the unloading model.[17] Current studies mainly focus on the effect of osteocytes and PDL on alveolar bone in the presence of disrupted homeostasis. Studies revealing the molecular mechanisms of how these phenotypes are formed remain scarce, especially regarding how osteoclasts accumulate in hypo-loading.

Hyper-loading condition

Trauma from occlusion can be initiated when the magnitude of forces exceeds the adaptive capacity of periodontal supporting tissues (primary trauma) or when the adaptive threshold is compromised, rendering the remaining tissues incapable of withstanding physiological occlusal forces (secondary trauma).[131] Clinically, premature occlusal contacts and lateral displacement of abutment teeth in partial dentures lead to excessive force application on periodontal tissues. Nonaxial forces (lateral or horizontal and torque or rotational) are more likely to damage periodontal tissues compared to axial forces.[131] Consequently, research focuses primarily on orthodontic movement rather than vertical movement. Xu et al[19] developed a finite element (FE) model and an in vivo murine model by extracting the maxillary second molar (mxM2) and maxillary third molar (mxM3), thereby directing the total force onto the mandibular first molar (mnM1). This study aimed to analyse stress distributions within the periodontium under normal and hyper-occlusion conditions. The results indicated that compressive strains are present in all three periodontal tissues, with strain magnitudes increasing fourfold under hyper-loading conditions.[19]

Niver et al1[32] noted that excessive loading significantly enhances cementum hardness while promoting apical cementum resorption. Wang et al[133] demonstrated that force-loaded cementocytes modulate osteoclastogenesis and osteoclastic root resorption through cell-to-cell communication via the Sphingosine-1-phosphate (S1P)/S1PR1/Rac1 pathway.

Hyper-loading leads to increased collagen deposition and a thicker, stiffer PDL.[19,23] Utilising FE modelling, it was illustrated that occlusal hyper-loading could lead to mitotically active Axin2+ PDLSCs in stressed PDL areas, resulting in collagen increase and a stiffer PDL adapted to increased load finally using *Axin2-CreER;R26R*$^{mTmG/+}$ mice.[19,23] Besides, it has also been found that the declined adaptive function of the PDL to masticatory force during aging might be relative to the diminished number of the Axin2+ PDLSCs.[23] Lepr+ PDLSCs are sustained as a quiescent population but can be activated by mechanical stimulation. Zhang et al[16] proved that hyper-loading promotes Lepr+ PDLSCs osteogenic differentiation through Piezo1-mediated mechanosensing in the periodontium.

Hyper-loading activates bone resorption, the peak of which is followed by a bone formation phase partly due to the responses of Wnt-responsive stem/progenitor cells in the alveolar bone, leading ultimately to an accelerated rate of mineral apposition and an increase in alveolar bone density.[19] Kanzaki et al[118] observed that vertical compressive forces on PDL fibroblasts, dose- and time-dependently upregulates RANKL expression via increased prostaglandin E2 (PGE2) production, leading to a notable rise in osteoclast-like cell formation in vitro. Goto et al[30,31] demonstrated that hyper-occlusion elevates C-C chemokine ligand (CCL) 2 expression in PDL, enhancing chemotaxis and osteoclastogenesis and synergistic function of CCL3 and CCL2 in mechanical stress-dependent alveolar bone destruction.

In summary, unloading leads to tooth elongation by apical cellular cementum deposition; sparse and disorganised collagen fibres in the PDL; enhanced osteogenic activity in the PDL-bone border with a gain in alveolar bone height; and aggravated osteoclast activity in alveolar bone marrow with a progressive decrease in BV/TV and mineral density. On the other hand, hyper-loading leads to enhanced cementum hardness and resorption; thicker and stiffer collagen fibres in the PDL; and activated bone resorption, followed by a bone formation phase, leading ultimately to increased alveolar bone density.

Conclusion and prospects

In this review, we systemically summarised the cellular interaction and molecular mechanism that play key roles in regulating tooth root development and homeostasis in the tooth eruption and post-eruption stages mainly based on the mice models. In summary, following the formation of the tooth crown, eruption commences, characterised by axial movement and initiation of root development until the tooth reaches its final position in the oral cavity in contact with the opposing tooth. This process involves cellular interactions within the HERS, DP and DF that govern the development of the tooth crown, root, periodontal tissues and osteogenic and osteoblastic activity, thus contributing to tooth eruption. Even after a tooth attains its functional position, eruptive movement persists due to the remodelling of cementum, PDL and alveolar bone, which are essential for maintaining periodontium homeostasis. Mechanical stimuli, such as occlusal hypofunction, or hyperfunction, can disrupt this homeostasis, and potentially lead to overeruption or occlusal trauma. To understand the cellular mechanism mediating the post-eruptive tooth movement under hypo-loading and hyper-loading conditions, we summarized the advanced findings in recent studies using the transgenic rodent molar models.

Although transgenic rodent molar models are useful tool for studying the mechanisms of tooth eruption, additional large animal models and human subjects are needed to determine the mechanism underlying these phenotypes in the future. For example, the miniature pig model has a diphyodont dentition similar to that of humans. Using a miniature pig model, Wu et al[134,135] validated that tooth eruption could release the accumulated mechanical stress inside the mandible, and the permanent tooth did not develop until the primaryd tooth began to erupt. Using FE analysis models of human teeth, Sarrafpour et al[136,137] proposed that both eruptive and post-eruptive tooth movements result from bone remodelling in the bony crypt and lamina dura, driven by biomechanical forces. These new findings enrich knowledge relating to tooth development and eruption and suggest the significance of interdisciplinary methods, such as biomechanical models, in achieving a more comprehensive understanding of tooth development and maintenance mechanisms.

Eruption disorders are commonly observed in the human population, presenting as either isolated conditions or part of complex syndromes, and invariably lead to impaired mastication, speech, facial aesthetics and social interaction.[4,74] Delayed tooth eruption (DTE), the most frequent deviation from normal eruption timing, occurs when a tooth emerges into the oral cavity at a time that diverges significantly from established norms for various races, ethnicities and sexes.[138] DTE may signal a systemic condition such as cleidocranial dysplasia (CDD) or reflect altered craniofacial physiology, such as physical obstruction due to premature loss of primary teeth.[138,139] Surgical exposure combined with orthodontic intervention is the predominant treatment approach. In orthodontic therapy, the technique of removing impediments and exposing the crown is termed fenestration. By affixing a bracket to the tooth surface at the exposed "window" and employing orthodontic traction, the impacted tooth can gradually return to the normal dental arch, thereby restoring function.[140] Conventional surgery, which involves direct tissue cutting with a surgical blade, often results in bleeding, infection and postoperative trauma. Consequently, the development of early molecular diagnosis and a therapeutic strategy for eruption disorders are crucial and advantageous for affected populations.

Furthermore, it has been reported that up to 31% of adults with occlusal disharmony or bruxism suffer from disrupted periodontal equilibrium due to irregular force loading.[131] When teeth are no longer in occlusal contact, such as after the extraction of an opposing tooth, the balance of forces is disrupted, leading to overeruption, which can cause occlusal interferences and malocclusion, posing challenges for restoration.[141] Lindskog-Stokland et al[14] observed that both unopposed and opposed teeth exhibit overeruption over a 12-year period, with statistically significant greater overeruption in unopposed teeth. Craddock and Youngson[142] noted that 83% of unopposed teeth are prone to overeruption of up to 5.39 mm. Over-erupted teeth necessitate treatment with an orthodontic intrusive force, which is typically generated through the elastic deformation of the archwire.[143] This treatment poses a significant clinical challenge due to its requirement for high technical precision and potential side effects, including root resorption and reactive loading on anchorage teeth.

A detailed understanding of the molecular and cellular mechanisms underlying tooth eruption and overeruption in pathological states is essential not only for elucidating these biological processes but also for guiding potential clinical interventions. Enhancing comprehension of dental tissue development, disease and dental stem cell biology is crucial for establishing a robust foundation for future strategies and clinical therapies in dental medicine.

Conflicts of interest

The authors declare no conflicts of interest related to this study.

Author contribution

Dr En Hui Yao contributed to the literature search, data analysis and manuscript draft; Drs Xin Quan JIANG and Jia Hui DU contributed to the idea for the article. All authors revised the paper critically for intellectual content and approved the final version.

(Received Mar 31, 2024; accepted Aug 09, 2024)

References

1. Friedlander L, Berdal A, Cormier-Daire V, Lyonnet S, Garcelon N. Determinants of dental care use in patients with rare diseases: a qualitative exploration. BMC Oral Health 2023;23:413.
2. Nanci A. Development, Structure, and Function, ed 9. St. Louis: Elsevier, 2018.
3. Nibali L. Development of the gingival sulcus at the time of tooth eruption and the influence of genetic factors. Periodontol 2000 2018;76:35–42.
4. Fleischmannova J, Matalova E, Sharpe PT, Misek I, Radlanski RJ. Formation of the tooth-bone interface. J Dent Res 2010;89:108–115.

5. Marks SC Jr, Schroeder HE. Tooth eruption: Theories and facts. Anat Rec 1996;245:374–393.
6. Nagata M, Ono N, Ono W. Mesenchymal progenitor regulation of tooth eruption: A view from PTHrP. J Dent Res 2020;99:133–142.
7. Richman JM. Shedding new light on the mysteries of tooth eruption. Proc Natl Acad Sci U S A 2019;116:353–355.
8. Zeng L, He H, Sun M, et al. Runx2 and Nell-1 in dental follicle progenitor cells regulate bone remodeling and tooth eruption. Stem Cell Res Ther 2022;13:486.
9. Kjær I. Mechanism of human tooth eruption: review article including a new theory for future studies on the eruption process. Scientifica (Cairo) 2014;2014:341905.
10. Craddock HL, Youngson CC. Eruptive tooth movement--the current state of knowledge. Br Dent J 2004;197:385–391.
11. Wise GE, King GJ. Mechanisms of tooth eruption and orthodontic tooth movement. J Dent Res 2008;87:414–434.
12. Walker CG, Dangaria S, Ito Y, Luan X, Diekwisch TG. Osteopontin is required for unloading-induced osteoclast recruitment and modulation of RANKL expression during tooth drift-associated bone remodeling, but not for super-eruption. Bone 2010;47:1020–1029.
13. Craddock HL, Youngson CC, Manogue M, Blance A. Occlusal changes following posterior tooth loss in adults. Part 2. Clinical parameters associated with movement of teeth adjacent to the site of posterior tooth loss. J Prosthodont 2007;16:495–501.
14. Lindskog-Stokland B, Hansen K, Tomasi C, Hakeberg M, Wennström JL. Changes in molar position associated with missing opposed and/or adjacent tooth: a 12-year study in women. J Oral Rehabil 2012;39:136–143.
15. Lira Dos Santos EJ, Salmon CR, Chavez MB, et al. Cementocyte alterations associated with experimentally induced cellular cementum apposition in Hyp mic. J Periodontol 2021;92:116–127.
16. Zhang D, Lin W, Jiang S, et al. Lepr-expressing PDLSCs contribute to periodontal homeostasis and respond to mechanical force by Piezo1. Adv Sci (Weinh) 2023;10:e2303291.
17. Chen Y, Luo M, Xie Y, Xing L, Han X, Tian Y. Periodontal ligament-associated protein-1 engages in teeth overeruption and periodontal fiber disorder following occlusal hypofunction. J Periodontal Res 2023;58:131–142.
18. Men Y, Wang Y, Yi Y, et al. Gli1+ periodontium dtem cells are regulated by osteocytes and occlusal force. Dev Cell 2020;54:639–654.e6.
19. Xu Q, Yuan X, Zhang X, et al. Mechanoadaptive responses in the periodontium are coordinated by Wnt. J Dent Res 2019;98:689–697.
20. Chen Y, Yin Y, Luo M, et al. Occlusal force maintains alveolar bone homeostasis via Type H sngiogenesis. J Dent Res 2023;102:1356–1365.
21. Ejiri S, Toyooka E, Tanaka M, Anwar RB, Kohno S. Histological and histomorphometrical changes in rat alveolar bone following antagonistic tooth extraction and/or ovariectomy. Arch Oral Biol 2006;51:941–950.
22. Yang Y, Dai Q, Gao X, et al. Occlusal force orchestrates alveolar bone homeostasis via Piezo1 in female mice. J Bone Miner Res 2024;39:580–594.
23. Zhang X, Yuan X, Xu Q, et al. Molecular basis for periodontal ligament adaptation to in vivo loading. J Dent Res 2019;98:331–338.
24. Inoue M, Ono T, Kameo Y, et al. Forceful mastication activates osteocytes and builds a stout jawbone. Sci Rep 2019;9:4404.
25. Mavropoulos A, Odman A, Ammann P, Kiliaridis S. Rehabilitation of masticatory function improves the alveolar bone architecture of the mandible in adult rats. Bone 2010;47:687–692.
26. Kün-Darbois JD, Libouban H, Chappard D. Botulinum toxin in masticatory muscles of the adult rat induces bone loss at the condyle and alveolar regions of the mandible associated with a bone proliferation at a muscle enthesis. Bone 2015;77:75–82.
27. Rafferty KL, Liu ZJ, Ye W, et al. Botulinum toxin in masticatory muscles: Short- and long-term effects on muscle, bone, and craniofacial function in adult rabbits. Bone 2012;50:651–662.
28. Star H, Chandrasekaran D, Miletich I, Tucker AS. Impact of hypofunctional occlusion on upper and lower molars after cessation of root development in adult mice. Eur J Orthod 2017;39:243–250.
29. Motokawa M, Terao A, Karadeniz EI, et al. Effects of long-term occlusal hypofunction and its recovery on the morphogenesis of molar roots and the periodontium in rats. Angle Orthod 2013;83:597–604.
30. Tsutsumi T, Kajiya H, Goto KT, Takahashi Y, Okabe K. Hyperocclusion up-regulates CCL3 expression in CCL2- and CCR2-deficient Mice. J Dent Res 2013;92:65–70.
31. Goto KT, Kajiya H, Nemoto T, et al. Hyperocclusion stimulates osteoclastogenesis via CCL2 expression. J Dent Res 2011;90:793–798.
32. Jernvall J, Thesleff I. Tooth shape formation and tooth renewal: evolving with the same signals. Development 2012;139:3487–3497.
33. He YD, Sui BD, Li M, Huang J, Chen S, Wu LA. Site-specific function and regulation of Osterix in tooth root formation. Int Endod J 2016;49:1124–1131.
34. Thomas HF, Kollar EJ. Differentiation of odontoblasts in grafted recombinants of murine epithelial root sheath and dental mesenchyme. Arch Oral Biol 1989;34:27–35.
35. He M, Wang P, Li B, et al. Rodent incisor and molar dental follicles show distinct characteristics in tooth eruption. Arch Oral Biol 2021;126:105117.
36. Proffit WR, Frazier-Bowers SA. Mechanism and control of tooth eruption: overview and clinical implications. Orthod Craniofac Res 2009;12:59–66.
37. Wise GE. Cellular and molecular basis of tooth eruption. Orthod Craniofac Res 2009;12:67–73.
38. Huang X, Bringas P Jr, Slavkin HC, Chai Y. Fate of HERS during tooth root development. Dev Biol 2009;334:22–30.
39. Yang S, Choi H, Kim TH, et al. Cell dynamics in Hertwig's epithelial root sheath are regulated by β-catenin activity during tooth root development. J Cell Physiol 2021;236:5387–5398.
40. Bi F, Tang H, Zhang Z, et al. Hertwig's epithelial root sheath cells show potential for periodontal complex regeneration. J Periodontol 2023;94:263–276.
41. Wright T. The molecular control of and clinical variations in root formation. Cells Tissues Organs 2007;186:86–93.
42. Yu M, Liu Y, Wang Y, et al. Epithelial Wnt10a is essential for tooth root furcation morphogenesis. J Dent Res 2020;99:311–319.
43. Sun K, Yu M, Wang J, et al. A Wnt10a-Notch signaling axis controls Hertwig's epithelial root sheath cell behaviors during root furcation patterning. Int J Oral Sci 2024;16:25.
44. Li J, Parada C, Chai Y. Cellular and molecular mechanisms of tooth root development. Development 2017;144:374–384.
45. Nakatomi M, Morita I, Eto K, Ota MS. Sonic hedgehog signaling is important in tooth root development. J Dent Res 2006;85:427–431.
46. Lav R, Krivanek J, Anthwal N, Tucker AS. Wnt signaling from Gli1-expressing apical stem/progenitor cells is essential for the coordination of tooth root development. Stem Cell Reports 2023;18:1015–1029.

47. Oshimori N, Fuchs E. Paracrine TGF-β signaling counterbalances BMP-mediated repression in hair follicle stem cell activation. Cell Stem Cell 2012;10:63–75.
48. He XC, Zhang J, Tong WG, et al. BMP signaling inhibits intestinal stem cell self-renewal through suppression of Wnt-beta-catenin signaling. Nat Genet 2004;36:1117–1121.
49. Yang Z, Hai B, Qin L, et al. Cessation of epithelial Bmp signaling switches the differentiation of crown epithelia to the root lineage in a β-catenin-dependent manner. Mol Cell Biol 2013;33:4732–4744.
50. Li J, Feng J, Liu Y, et al. BMP-SHH signaling network controls epithelial stem cell fate via regulation of its niche in the developing tooth. Dev Cell 2015;33:125–135.
51. Nagata M, Ono N, Ono W. Unveiling diversity of stem cells in dental pulp and apical papilla using mouse genetic models: a literature review. Cell Tissue Res 2021;383:603–616.
52. Sonoyama W, Liu Y, Fang D, et al. Mesenchymal stem cell-mediated functional tooth regeneration in swine. PloS One 2006;1:e79.
53. Collignon AM, Castillo-Dali G, Gomez E, et al. Mouse Wnt1-CRE-RosaTomato dental pulp stem cells directly contribute to the calvarial bone regeneration process. Stem Cells 2019;37:701–711.
54. Ono W, Sakagami N, Nishimori S, Ono N, Kronenberg HM. Parathyroid hormone receptor signalling in osterix-expressing mesenchymal progenitors is essential for tooth root formation. Nat Commun 2016;7:11277.
55. Liu Y, Feng J, Li J, Zhao H, Ho TV, Chai Y. An Nfic- hedgehog signaling cascade regulates tooth root development. Development 2015;142:3374–3382.
56. Babb R, Chandrasekaran D, Carvalho Moreno Neves V, Sharpe PT. Axin2-expressing cells differentiate into reparative odontoblasts via autocrine Wnt/β-catenin signaling in response to tooth damage. Sci Rep 2017;7:3102.
57. Vidovic-Zdrilic I, Vining KH, Vijaykumar A, Kalajzic I, Mooney DJ, Mina M. FGF2 enhances odontoblast differentiation by αSMA+ progenitors in vivo. J Dent Res 2018;97:1170–1177.
58. Jing J, Feng J, Yuan Y, et al. Spatiotemporal single-cell regulatory atlas reveals neural crest lineage diversification and cellular function during tooth morphogenesis. Nat Commun 2022;13:4803.
59. Huang X, Xu X, Bringas P Jr, Hung YP, Chai Y. Smad4-Shh-Nfic signaling cascade-mediated epithelial-mesenchymal interaction is crucial in regulating tooth root development. J Bone Miner Res 2010;25:1167–1178.
60. Steele-Perkins G, Butz KG, Lyons GE, et al. Essential role for NFI-C/CTF transcription-replication factor in tooth root development. Mol Cell Biol 2003;23:1075–1084.
61. Zhang H, Jiang Y, Qin C, Liu Y, Ho SP, Feng JQ. Essential role of osterix for tooth root but not crown dentin formation. J Bone Miner Res 2015;30:742–746.
62. Kim TH, Bae CH, Lee JC, et al. β-catenin is required in odontoblasts for tooth root formation. J Dent Res 2013;92:215–221.
63. Zhang R, Yang G, Wu X, Xie J, Yang X, Li T. Disruption of Wnt/β-catenin signaling in odontoblasts and cementoblasts arrests tooth root development in postnatal mouse teeth. Int J Biol Sci 2013;9:228–236.
64. Wu S, Fatkhutdinov N, Fukumoto T, et al. SWI/SNF catalytic subunits' switch drives resistance to EZH2 inhibitors in ARID1A-mutated cells. Nat Commun 2018;9:4116.
65. Jin F, Yang Z, Shao J, et al. ARID1A mutations in lung cancer: biology, prognostic role, and therapeutic implications. Trends Mol Med 2023;29:646–658.
66. Zhou W, Liu H, Yuan Z, et al. Targeting the mevalonate pathway suppresses ARID1A-inactivated cancers by promoting pyroptosis. Cancer Cell 2023;41:740–756.e10.
67. Jing J, Feng J, Li J, et al. Antagonistic interaction between Ezh2 and Arid1a coordinates root patterning and development via Cdkn2a in mouse molars. Elife 2019;8:e46426.
68. Du J, Jing J, Yuan Y, et al. Arid1a-Plagl1-Hh signaling is indispensable for differentiation-associated cell cycle arrest of tooth root progenitors. Cell Rep 2021;35:108964.
69. Takahashi A, Nagata M, Gupta A, et al. Autocrine regulation of mesenchymal progenitor cell fates orchestrates tooth eruption. Proc Natl Acad Sci U S A 2019;116:575–580.
70. Yamaguchi T, Hosomichi K, Shirota T, Miyamoto Y, Ono W, Ono N. Primary failure of tooth eruption: Etiology and management. Jpn Dent Sci Rev 2022;58:258–267.
71. Philbrick WM, Dreyer BE, Nakchbandi IA, Karaplis AC. Parathyroid hormone-related protein is required for tooth eruption. Proc Natl Acad Sci U S A 1998;95:11846–11851.
72. Yao S, Prpic V, Pan F, Wise GE. TNF-alpha upregulates expression of BMP-2 and BMP-3 genes in the rat dental follicle--implications for tooth eruption. Connect Tissue Res 2010;51:59–66.
73. Liu Y, Wang Y, Sun X, et al. RUNX2 mutation reduces osteogenic differentiation of dental follicle cells in cleidocranial dysplasia. Mutagenesis 2018;33:203–214.
74. Ge J, Guo S, Fu Y, et al. Dental follicle cells participate in tooth eruption via the RUNX2-MiR-31-SATB2 loop. J Dent Res 2015;94:936–944.
75. Tang R, Wang Q, Du J, Yang P, Wang X. Expression and localization of Nell-1 during murine molar development. J Mol Histol 2013;44:175–181.
76. Zhang X, Ting K, Bessette CM, et al. Nell-1, a key functional mediator of Runx2, partially rescues calvarial defects in Runx2(+/-) mice. J Bone Miner Res 2011;26:777–791.
77. Truong T, Zhang X, Pathmanathan D, Soo C, Ting K. Craniosynostosis-associated gene nell-1 is regulated by runx2. J Bone Miner Res 2007;22:7–18.
78. Wise GE, Yao S. Regional differences of expression of bone morphogenetic protein-2 and RANKL in the rat dental follicle. Eur J Oral Sci 2006;114:512–516.
79. Ruan X, Zhang Z, Aili M, et al. Activin receptor-like kinase 3: a critical modulator of development and function of mineralized tissues. Front Cell Dev Biol 2023;11:1209817.
80. Zhou T, Pan J, Wu P, et al. Dental follicle cells: Roles in development and beyond. Stem Cells Int 2019;2019:9159605.
81. Ma Y, Xu Y, Zhang Y, Duan X. Molecular mechanisms of craniofacial and dental abnormalities in osteopetrosis. Int J Mol Sci 2023;24:10412.
82. Wise GE, Fan W. Changes in the tartrate-resistant acid phosphatase cell population in dental follicles and bony crypts of rat molars during tooth eruption. J Dent Res 1989;68:150–156.
83. Wise GE, Yao S. Expression of vascular endothelial growth factor in the dental follicle. Crit Rev Eukaryot Gene Expr 2003;13:173–180.
84. Wise GE, Yao S. Expression of tumour necrosis factor-alpha in the rat dental follicle. Arch Oral Biol 2003;48:47–54.
85. Mullen LM, Richards DW, Quaranta V. Evidence that laminin-5 is a component of the tooth surface internal basal lamina, supporting epithelial cell adhesion. J Periodontal Res 1999;34:16–24.
86. Zhang S, Yang Y, Jia S, et al. Exosome-like vesicles derived from Hertwig's epithelial root sheath cells promote the regeneration of dentin-pulp tissue. Theranostics 2020;10:5914–5931.

87. Xiong J, Gronthos S, Bartold PM. Role of the epithelial cell rests of Malassez in the development, maintenance and regeneration of periodontal ligament tissues. Periodontol 2000 2013;63:217–233.
88. Guo Y, Guo W, Chen J, Chen G, Tian W, Bai D. Are Hertwig's epithelial root sheath cells necessary for periodontal formation by dental follicle cells? Arch Oral Biol 2018;94:1–9.
89. Luan X, Ito Y, Diekwisch TG. Evolution and development of Hertwig's epithelial root sheath. Dev Dyn 2006;235:1167–1180.
90. Heritier M. Experimental induction of cementogenesis on the enamel of transplanted mouse tooth germs. Arch Oral Biol 1982;27:87–97.
91. Bertin TJC, Thivichon-Prince B, LeBlanc ARH, Caldwell MW, Viriot L. Current perspectives on tooth implantation, attachment, and replacement in amniota. Front Physiol 2018;9:1630.
92. Nam H, Kim J, Park J, et al. Expression profile of the stem cell markers in human Hertwig's epithelial root sheath/Epithelial rests of Malassez cells. Mol Cells 2011;31:355–360.
93. Lin X, Li Q, Hu L, Jiang C, Wang S, Wu X. Apical papilla regulates dental follicle fate via the OGN-Hh pathway. J Dent Res 2023;102:431–439.
94. Cahill DR, Marks SC Jr. Tooth eruption: evidence for the central role of the dental follicle. J Oral Pathol 1980;9:189–200.
95. Wang XP. Tooth eruption without roots. J Dent Res 2013;92: 212–214.
96. Xu H, Snider TN, Wimer HF, et al. Multiple essential MT1-MMP functions in tooth root formation, dentinogenesis, and tooth eruption. Matrix Biol 2016;52-54:266–283.
97. Cui C, Bi R, Liu W, et al. Role of PTH1R signaling in Prx1+ mesenchymal progenitors during eruption. J Dent Res 2020;99:1296–1305.
98. Naveh GR, Lev-Tov Chattah N, Zaslansky P, Shahar R, Weiner S. Tooth-PDL-bone complex: response to compressive loads encountered during mastication - a review. Arch Oral Biol 2012;57:1575–1584.
99. Luan X, Zhou X, Trombetta-eSilva J, et al. MicroRNAs and periodontal homeostasis. J Dent Res 2017;96:491–500.
100. Komaki M, Iwasaki K, Arzate H, Narayanan AS, Izumi Y, Morita I. Cementum protein 1 (CEMP1) induces a cementoblastic phenotype and reduces osteoblastic differentiation in periodontal ligament cells. J Cell Physiol 2012;227:649–657.
101. Xie X, Wang J, Wang K, et al. Axin2+-mesenchymal PDL cells, instead of K14+ epithelial cells, play a key role in rapid cementum growth. J Dent Res 2019;98:1262–1270.
102. Koehne T, Jeschke A, Petermann F, et al. Rsk2, the kinase mutated in Coffin-Lowry syndrome, controls cementum formation. J Dent Res 2016;95:752–760.
103. Lira Dos Santos EJ, de Almeida AB, Chavez MB, et al. Orthodontic tooth movement alters cementocyte ultrastructure and cellular cementum proteome signature. Bone 2021;153:116139.
104. Zhao N, Foster BL, Bonewald LF. The cementocyte-An osteocyte relative? J Dent Res 2016;95:734–741.
105. Boabaid F, Berry JE, Koh AJ, Somerman MJ, McCcauley LK. The role of parathyroid hormone-related protein in the regulation of osteoclastogenesis by cementoblasts. J Periodontol 2004;75:1247–1254.
106. Nemoto E, Darveau RP, Foster BL, Nogueira-Filho GR, Somerman MJ. Regulation of cementoblast function by P. gingivalis lipopolysaccharide via TLR2. J Dent Res 2006;85:733–738.
107. Seo BM, Miura M, Gronthos S, et al. Investigation of multipotent postnatal stem cells from human periodontal ligament. Lancet 2004;364:149–155.
108. Shalehin N, Seki Y, Takebe H, et al. Gli1+-PDL cells contribute to alveolar bone homeostasis and regeneration. J Dent Res 2022;101:1537–1543.
109. Mizoguchi T. In vivo dynamics of hard tissue-forming cell origins: Insights from Cre/loxP-based cell lineage tracing studies. Jpn Dent Sci Rev 2024;60:109-119.
110. Zhang W, Yelick PC. Tooth repair and regeneration: Potential of dental stem cells. Trends Mol Med 2021;27:501–511.
111. Pakpahan ND, Kyawsoewin M, Manokawinchoke J, et al. Effects of mechanical loading on matrix homeostasis and differentiation potential of periodontal ligament cells: A scoping review [epub ahead of print 12 May 2024]. J Periodontal Res doi: 10.1111/jre.13284.
112. Sokos D, Everts V, de Vries TJ. Role of periodontal ligament fibroblasts in osteoclastogenesis: a review. J Periodontal Res 2015;50:152–159.
113. Koda N, Sato T, Shinohara M, et al. The transcription factor mohawk homeobox regulates homeostasis of the periodontal ligament. Development 2017;144:313–320.
114. Donnelly E, Williams R, Farnum C. The primary cilium of connective tissue cells: Imaging by multiphoton microscopy. Anat Rec (Hoboken) 2008;291:1062–1073.
115. Jeon HH, Teixeira H, Tsai A. Mechanistic insight into orthodontic tooth movement based on animal studies: A critical review. J Clin Med 2021;10:1733.
116. Wang L, Foster BL, Kram V, et al. Fibromodulin and biglycan modulate periodontium through TGFβ/BMP signaling. J Dent Res 2014;93:780–787.
117. Bloemen V, Schoenmaker T, de Vries TJ, Everts V. Direct cell–cell contact between periodontal ligament fibroblasts and osteoclast precursors synergistically increases the expression of genes related to osteoclastogenesis. J Cell Physiol 2010;222:565–573.
118. Kanzaki H, Chiba M, Shimizu Y, Mitani H. Periodontal ligament cells under mechanical stress induce osteoclastogenesis by receptor activator of nuclear factor kappaB ligand up-regulation via prostaglandin E2 synthesis. J Bone Miner Res 2002;17:210–220.
119. Choi H, Yang L, Liu Y, Jeong JK, Cho ES. Npp1 prevents external tooth root resorption by regulation of cervical cementum integrity. Sci Rep 2022;12:21158.
120. Hathaway-Schrader JD, Novince CM. Maintaining homeostatic control of periodontal bone tissue. Periodontol 2000 2021;86:157–187.
121. Galli C, Passeri G, Macaluso GM. Osteocytes and WNT: the mechanical control of bone formation. J Dent Res 2010;89:331–343.
122. Wang K, Xu C, Xie X, et al. Axin2+ PDL cells directly contribute to new alveolar bone formation in response to orthodontic tension force. J Dent Res 2022;101:695–703.
123. Li Y, Zhan Q, Bao M, Yi J, Li Y. Biomechanical and biological responses of periodontium in orthodontic tooth movement: up-date in a new decade. Int J Oral Sci 2021;13:20.
124. Takimoto A, Kawatsu M, Yoshimoto Y, et al. Scleraxis and osterix antagonistically regulate tensile force-responsive remodeling of the periodontal ligament and alveolar bone. Development 2015;142:787–796.
125. Luan X, Ito Y, Holliday S, et al. Extracellular matrix-mediated tissue remodeling following axial movement of teeth. J Histochem Cytochem 2007;55:127–140.
126. Holliday S, Schneider B, Galang MT, Fukui T, Yamane A, Luan X, Diekwisch TG. Bones, teeth, and genes: a genomic homage to Harry Sicher's "Axial Movement of Teeth". World J Orthod 2005;6:61–70.
127. Zaghloul NA, Katsanis N. Mechanistic insights into Bardet-Biedl syndrome, a model ciliopathy. J Clin Invest 2009;119: 428–437.

128. Seo S, Zhang Q, Bugge K, et al. A novel protein LZTFL1 regulates ciliary trafficking of the BBSome and Smoothened. PLoS Genet 2011;7:e1002358.
129. Jin H, White SR, Shida T, et al. The conserved Bardet-Biedl syndrome proteins assemble a coat that traffics membrane proteins to cilia. Cell 2010;141:1208–1219.
130. Chang PE, Li S, Kim HY, Lee DJ, Choi YJ, Jung HS. BBS7-SHH signaling activity regulates primary cilia for periodontal homeostasis. Front Cell Dev Biol 2021;9:796274.
131. Passanezi E, Sant'Ana ACP. Role of occlusion in periodontal disease. Periodontol 2000 2019;79:129–150.
132. Niver EL, Leong N, Greene J, Curtis D, Ryder MI, Ho SP. Reduced functional loads alter the physical characteristics of the bone-periodontal ligament-cementum complex. J Periodontal Res 2011;46:730–741.
133. Wang H, Li T, Jiang Y, et al. Force-loaded cementocytes regulate osteoclastogenesis via S1P/S1PR1/Rac1 axis. J Dent Res 2023;102:1376–1386.
134. Wu X, Hu J, Li G, et al. Biomechanical stress regulates mammalian tooth replacement via the integrin β1-RUNX2-Wnt pathway. EMBO J 2020;39:e102374.
135. Li G, Li Q, Shen Z, et al. Fibulin-1 regulates initiation of successional dental lamina. J Dent Res 2023;102:1220–1230.
136. Sarrafpour B, Rungsiyakull C, Swain M, Li Q, Zoellner H. Finite element analysis suggests functional bone strain accounts for continuous post-eruptive emergence of teeth. Arch Oral Biol 2012;57:1070–1078.
137. Sarrafpour B, El-Bacha C, Li Q, Zoellner H. Roles of functional strain and capsule compression on mandibular cyst expansion and cortication. Arch Oral Biol 2019;98:1–8.
138. Suri L, Gagari E, Vastardis H. Delayed tooth eruption: Pathogenesis, diagnosis, and treatment. A literature review. Am J Orthod Dentofacial Orthop 2004;126:432–445.
139. Yoon H, Kim HJ, Shin HR, et al. Nicotinamide improves delayed tooth eruption in Runx2+/- mice. J Dent Res 2021;100:423–431.
140. Xu D, Wang P, Liu H, Gu M. Efficacy of three surgical methods for gingivectomy of permanent anterior teeth with delayed tooth eruption in children. Head Face Med 2022;18:23.
141. Luan X, Diekwisch TG. Vienna-Chicago: the cultural transformation of the model system of the un-opposed molar. Bioessays 2007;29:819–830.
142. Craddock HL, Youngson CC. A study of the incidence of overeruption and occlusal interferences in unopposed posterior teeth. Br Dent J 2004;196:341–348; discussion 337.
143. Wang D, Turkkahraman H, Chen J, Li B, Liu Y. Quantification of orthodontic loads on teeth in the correction of canine overeruption using different archwire designs. Am J Orthod Dentofacial Orthop 2023;163:e13–e21.

A CALL FOR PERSONALIZED ORAL MEDICINE

NEW

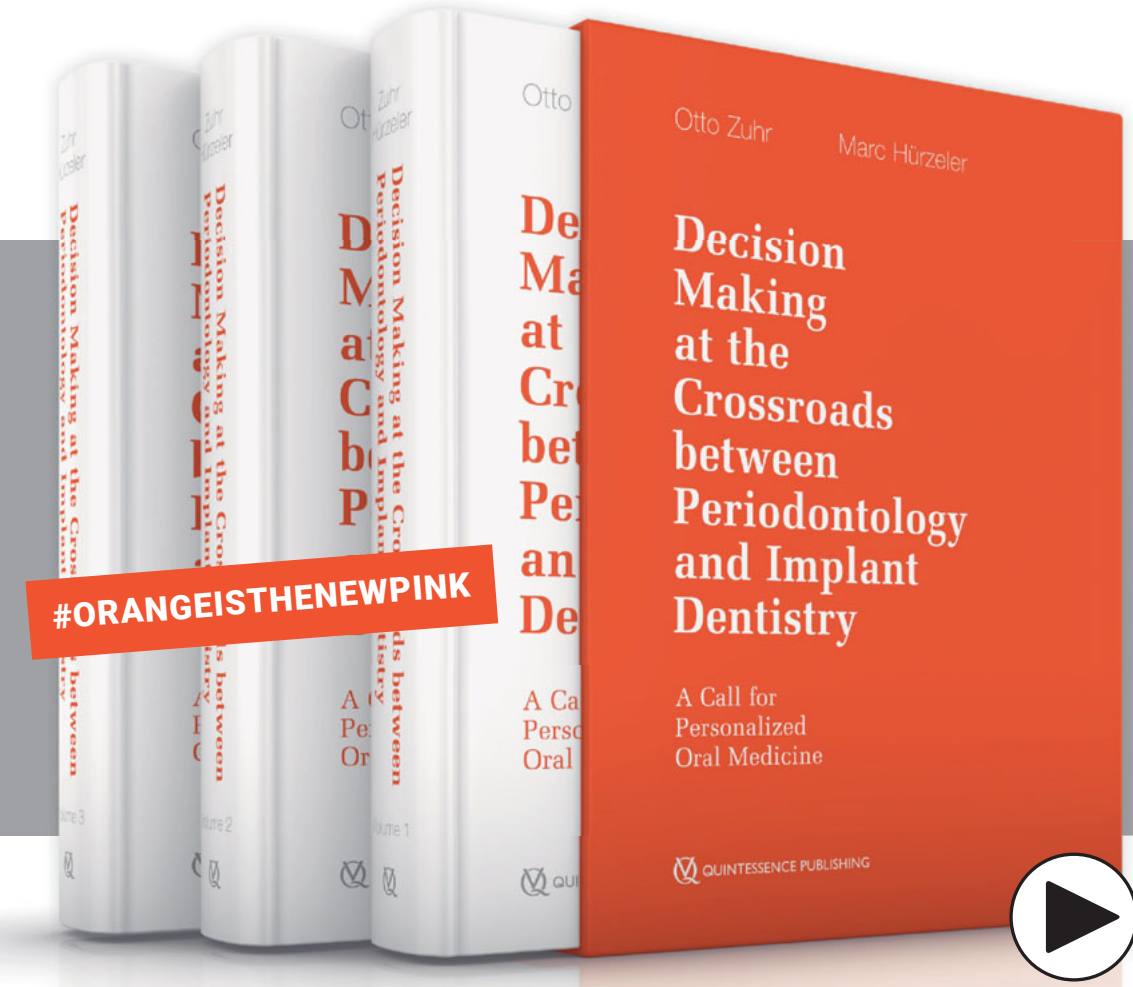

#ORANGEISTHENEWPINK

Otto Zuhr | Marc Hürzeler

Decision Making at the Crossroads between Periodontology and Implant Dentistry

A Call for Personalized Oral Medicine

1st Edition 2025
3 volumes in a hardcover slipcase
1,900 pages, 4,900 illus.
ISBN 978-3-86867-625-9

Preorder price: €398

(valid until publication, thereafter €498)

Available Spring 2025

Including 19 videos with 34 minutes total runtime!

With their book *Plastic-Esthetic Periodontal and Implant Surgery – A Microsurgical Approach*, the two nationally and internationally renowned authors, Dr. Otto Zuhr and Prof. Dr. Marc Hürzeler, have already written one of the most important works on oral surgery. They now present their patient-oriented treatment approach for implantology and periodontal surgery in their new book.

Due to extensive current scientific evidence available in dental medicine, it is no longer appropriate for dentists to be for or against preserving severely damaged teeth or to be for or against implants. The time has come to break away from dogma and combine both worlds – tooth preservation and implant therapy – into a coherent approach for the benefit of patients.

In this groundbreaking three-volume compendium, the authors demonstrate, among other things, how to achieve healthy and stable gingival and peri-implant soft tissue, considering the latest evidence and the individual risk profiles and needs of patients.

The work contains a wealth of information, providing all the necessary biologic and technical principles (Volume 1) as well as the surgical techniques (Volumes 2 and 3) required for practitioners in the fields of implantology, periodontology, and oral surgery. The in-depth work comprises a user-friendly format, including numerous detailed case studies with step-by-step procedures and extensive lists of materials. It is brilliantly illustrated with top-quality photographs and radiographs as well as other illustrative material, and is supplemented by a number of videos. This outstanding work is without doubt a real breakthrough and should be included in every dental library!

www.quint.link/new-pink

books@quintessenz.de

+49 (0)30 761 80 667

QUINTESSENCE PUBLISHING

The Application of Salivary Exosomes in the Diagnosis of Oral Disease

Ming Yang YU[1#], Xing Chi LIU[1#], Zi Li YU[1,2], Jun JIA[1,2]

Oral diseases not only greatly impact patients' daily lives, but also pose a severe threat to their overall health. Due to the constant exposure of saliva to oral diseases, the former plays a vital role in their diagnosis and monitoring. Exosomes, nanosized bilayer lipid encapsulated nanovesicles, are widely present in saliva and can be released by any type of cell. Exosomes inherit features from their mother cells in both physiological and pathological conditions. The molecular characteristics and expression levels of exosomes depend on their cellular origin, and they can directly reflect the physiological state of the body and cells. This makes salivary exosomes a promising source for early detection and monitoring of oral diseases. As a result, researchers have been exploring the potential use of exosomes as biomarkers for diagnosing and predicting various oral diseases. This review provides an overview of the composition, separation and function of salivary exosomes. It also discusses their potential as diagnostic and prognostic markers for several oral diseases, including periodontitis, primary Sjögren's syndrome, oral mucosal diseases, hand-foot-mouth disease and oral squamous cell carcinoma. By studying salivary exosomes, researchers hope to improve the early detection and monitoring of oral diseases, leading to better outcomes for patients.

Keywords: *diagnosis, liquid biopsy, oral disease, prediction, salivary exosomes*
Chin J Dent Res 2024;27(4):291–301; doi: 10.3290/j.cjdr.b5860259

According to the latest Global Burden of Disease (GBD) study, 74.6% of the global population suffer from oral diseases,[1] which means they rank in the top 10 leading causes of years lived with disability globally.[2] Early detection of oral disease greatly increases the likelihood of successful treatment. Conversely, when treatment is delayed or inaccessible, there is a lower chance of survival, the problems associated with treatment become more severe, and the cost of care rises. Therefore, it is crucial to detect and identify pathogens early and adopt effective management to reduce the negative impacts of the disease. Currently, tissue biopsy remains the gold standard for diagnosing various diseases, including oral lesions. However, oral mucosal diseases, especially those with a high incidence rate, are not always homogeneous. This lack of homogeneity poses a serious challenge to the diagnostic accuracy of biopsy specimens due to the limited sample size. For instance, the process of carcinogenesis among different sites of oral leucoplakia (OLC) often varies greatly. During the lengthy carcinogenesis from OLC to oral cancer, it is difficult to decide when the biopsy specimen should be taken, since it is unavoidable and associated with invasion, pain and wounds.[3] In addition, accurately harvesting lesions for biopsy becomes even more frustrating when they are located in deep tissues, such as salivary gland tumours. This difficulty further hampers the early diagnosis of oral diseases. To address this issue, it is crucial to develop detection methods that enable early diagnosis of oral diseases in a convenient, minimally invasive, highly sensitive and selective manner. These methods

1 State Key Laboratory of Oral & Maxillofacial Reconstruction and Regeneration, Key Laboratory of Oral Biomedicine Ministry of Education, Hubei Key Laboratory of Stomatology, School & Hospital of Stomatology, Wuhan University, Wuhan, P.R. China.
2 Department of Oral and Maxillofacial Surgery, School and Hospital of Stomatology, Wuhan University, Wuhan, P.R. China.
# These authors contributed equally to this work as co-first authors.

Corresponding authors: Dr Zi Li YU and Dr Jun JIA, Department of Oral and Maxillofacial Surgery, School and Hospital of Stomatology, Wuhan University, LuoYu Road No. 237, Wuhan 430079, P.R. China. Tel: 86-27-87686215. Email: zili09@whu.edu.cn; junjia@whu.edu.cn.

This work was supported by the Young Elite Scientist Sponsorship Programme (YESS) by China Association for Science and Technology (CAST) (2018QNRC001).

should aim to overcome the limitations of traditional biopsy techniques and provide health care professionals with reliable tools to detect and diagnose oral diseases at an early stage. This, in turn, would improve patient outcomes, reduce the invasiveness of diagnostic procedures and enhance overall convenience for patients.

Taking a liquid biopsy specimen holds great potential in overcoming the limitations of tissue-based biopsy specimens for early lesion identification, disease detection and the prediction of progression in oral mucosal diseases. It offers an alternative method for tumour monitoring without the need for repeated surgical biopsy specimens, minimising the associated risks and invasiveness. Among the various options for liquid biopsy specimens, blood is the most tested in clinical settings, as it contains extensive health-related information. However, in the case of oral diseases, saliva was believed to be superior to blood as a liquid biopsy tool.[4] Saliva is a complex mixture of fluids primarily secreted by the major salivary glands (parotid, submandibular and sublingual) as well as numerous minor salivary glands.[5] Lesions in the oral cavity are constantly immersed in saliva and engage in uninterrupted exchange of substances with it. The saliva contains various bioinformation molecules, including RNA, DNA, proteins and metabolites, which can reflect the relevant stage of oral disease. This characteristic of saliva offers the potential for early diagnosis and monitoring of various oral diseases. The exchange of bioinformation molecules between lesions and saliva allows for the detection of specific molecules or biomarkers that are indicative of the presence and progression of oral diseases. By analysing these molecules in saliva, researchers can gain valuable insights into the molecular changes associated with different stages of oral diseases. The availability of these biomarkers in saliva opens possibilities for the early diagnosis, monitoring and management of oral diseases. It offers a non-invasive and convenient approach, eliminating the need for invasive biopsy specimens in many cases. This can lead to earlier detection and intervention and personalised treatment strategies for individuals with oral diseases.[6]

Exosomes are nanosized bilayer lipid-coated nanovesicles that are released by all types of cells and widely present in saliva.[7] It is widely accepted that exosomes carry various bioactive molecules that are detected in their parental cell.[8] Most importantly, the molecular profiles of exosomes vary with cellular and tissue origins. Thus, the molecular profiles of exosomes can well recapitulate their parental cells. This is also the theoretical basis of exosome-based liquid biopsy specimens. In recent years, interest has increased among research scholars regarding exploration of the potential of exosomes as biomarkers for the diagnosis and prediction of oral diseases. Previous studies have shown promising results regarding the use of salivary exosomes as biomarkers in oral cancer patients. Zhong et al[9] observed that the levels of salivary exosomes are significantly increased in individuals with oral cancer compared to healthy individuals. Furthermore, the elevated levels of salivary exosomes have been found to correlate with the prognosis, staging and clinical outcomes of oral cancer patients.[9] The present authors have also designed a wedge-shaped and high magnetic field gradient-mediated chip to realise the one-step detection of multiple salivary exosome–based biomarkers to differentiate oral cancer from oral ulcers.[10] The aforementioned studies have provided compelling evidence for the significant potential of salivary exosomes as diagnostic and prognostic biomarkers in various oral diseases.

In this comprehensive review, the authors summarise recent studies focusing on salivary exosomes, including their composition, separation techniques and functional roles. They also explore and discuss the application potential of salivary exosomes as diagnostic and prognostic markers in a range of oral diseases, including periodontitis, primary Sjögren's syndrome, oral mucosal disease, foot, and mouth disease, and oral squamous cell carcinoma (Fig 1). In summary, the comprehensive review of these studies confirms the substantial application potential of salivary exosomes as diagnostic and prognostic markers in various oral diseases. The characterisation of exosomal cargo and their correlation with disease status may lead to improved diagnostic accuracy, personalised treatment approaches and better patient outcomes. Further research in this field is warranted to fully exploit the clinical potential of salivary exosomes in oral disease management.

Overview of salivary exosomes

Characteristics of salivary exosomes

Salivary exosomes are usually defined as nanovesicles that are secreted by oral epithelial cells. Many studies have identified their size range of 30 to 150 nm and cup-shape morphology though advanced microscopy techniques such as field emission scanning electron microscopy (FESEM) and atomic force microscopy (AFM).[11-13] As in other exosomes from body fluids, salivary exosomes are also enriched in components, including proteins, RNA, microRNAs (miRNAs), enzymes and

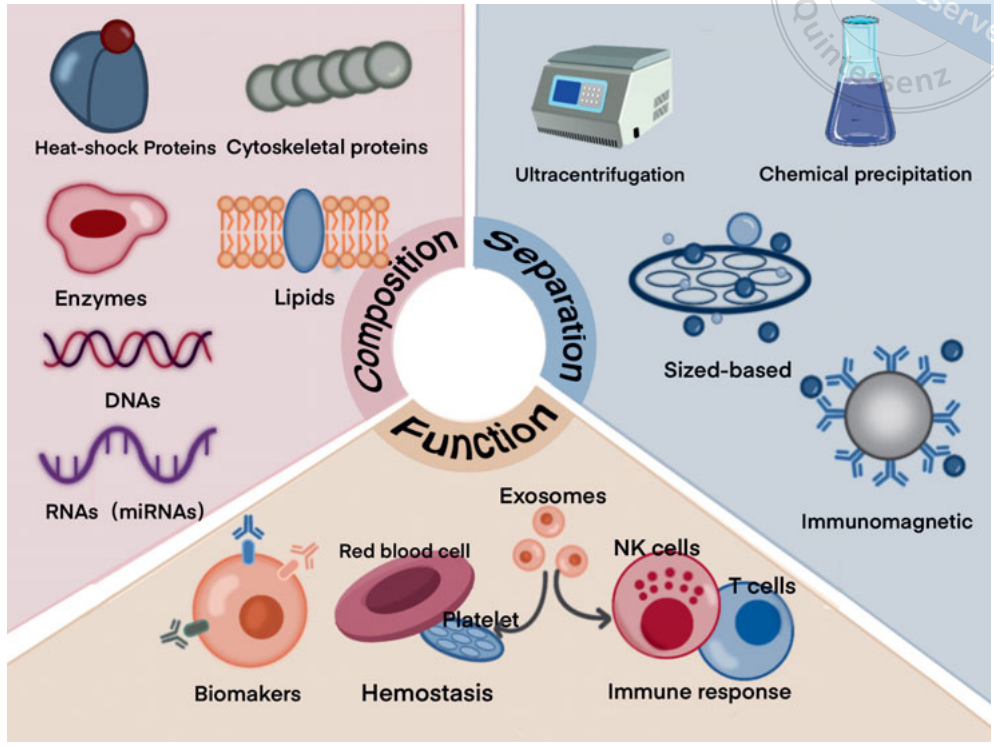

Fig 1 Exosomes as a new target for liquid biopsy. Exosomes are rich in body fluids and are closely related to disease occurrence, progression and metastasis. They are also rich in components, various proteins, enzymes, lipids and genetic factors. Traditional and advanced techniques have been used to isolate exosomes from a variety of body fluids and detect exosomes. Exosomes play an active role in coagulation and immune response, and can be used as biomarkers to provide novel strategies for disease inference, prediction of progression and prognostic monitoring.

lipids.[14] The differential expression of these proteins can help distinguish salivary exosomes from other types of exosomes. Salivary exosomes can be categorised into two types according to their size and protein features.[15] Salivary exosome I is slightly larger than exosome II. Until now, 101 proteins for exosomes have been detected in salivary exosome I, whereas 154 have been found in exosome II. The most common proteins are Alix, TSG101, HSP70, CD81, CD63, IgA and pIgR. Approximately 40% of them belong to a family of secretory proteins. Notably, unlike exosomes derived from other sources such as plasma or tissues, CD81 is accepted as more representative marker for salivary exosomes than CD63. In addition, aquaporin-5, associated with salivary secretion, has been identified to exist in salivary exosomes. The differential expression of the above proteins can distinguish salivary exosomes from other exosomes.[15,16]

Many different proteins, thought to be involved in intracellular communication, have been identified in exosomes. Tetraspanins are a family of membrane proteins that play a crucial role in various cellular processes. They are involved in cellular migration, adhesion, proliferation and immune response.[14] Tetraspanins, such as CD9 CD63 and CD81, are particularly rich in exosomes and have been found to be important for the formation and function of some exosomes.[17] These proteins help in the organisation and biogenesis of exosomes, as well as in sorting specific cargo molecules into exosomes. In terms of cellular migration, tetraspanins have been involved in processes such as cell adhesion, migration and invasion. In addition, tetraspanins are involved in cellular proliferation. They can regulate cell cycle progression, cell growth and cell survival through various signalling pathways.[18] The abundance of tetraspanins in exosomes indicates their active role in mediating intercellular communication through exosomes.[19] Some scholars have studied human saliva and identified exosomes according to their size and protein characteristics. So far, the most common proteins identified are Alix, TSG101 and HSP.[15] The presence of these proteins suggests that salivary exosomes originate from circulating lymphocytes and intravascular fluids.[14] Additionally, exosomes carry different types of RNA, which can be used to identify mutations associated with malignancy in related cells. A study successfully isolated miRNAs (e.g., miR-125a, miR-200a, miR-31 and miR-17-92) from salivary exosomes, confirming that the composition of the exosome is a reflection of the physiological state.[20] As mentioned earlier, exosomes can be regarded as biomarkers for diagnosing and predicting different diseases, thereby greatly facilitating the advancement of disease diagnosis and therapeutic strategies through improved accuracy and efficiency.

Separation of salivary exosomes

Salivary exosomes can be isolated in various ways, according to their physical and chemical properties. Both glandular and whole saliva can be used as excellent sources for separating salivary exosomes. The possible influence on classification by contamination of normal cells must be considered in whole saliva; glandular saliva is obviously more suitable for exosome isolation.[21] At present, there are two commonly used methods of isolating the salivary exosomes: ultracentrifugation and chemical precipitation.[22] Different forms of separation have their own unique limitations. Ultracentrifugation is time-consuming and yields low recovery, whereas chemical precipitation operation is simple but yields a low purity; these methods are limited by specific conditions.[23] It is important to consider these limitations when choosing a separation method and to explore alternative techniques based on the specific requirements of the experiment or application in question. Therefore, separation technologies that require higher accuracy, lower loss, lower cost and less time spent must be explored. In a particular study, salivary exosomes were separated using differential centrifugation.[24] The researchers then measured the mid-infrared absorbance spectra of these exosomes and machine learning technology was utilised to establish a discriminant model based on the absorbance data.[25] By training the machine learning model on known patterns and characteristics of protein, lipid and nucleic acid changes in exosomes, it was able to accurately classify and detect these changes in the salivary exosomes being analysed. This highlights the potential for using such methods in studying disease biomarkers, diagnostics, and monitoring changes in biological samples. Beyond that, the researchers also used density gradient centrifugation,[26] immunoaffinity capture,[27] size exclusion chromatography[28] and polymer-based precipitation[29] to try to isolate salivary exosomes precisely. Researchers are continuing their efforts to find efficient and precise methods for isolating salivary exosomes.

Function of salivary exosomes

Given the role of other exosomes in diagnosing and treating diseases, salivary exosomes may have similar diagnostic and therapeutic potential.[4] Exosomes can cross epithelial barriers,[29] and blood and saliva are exchanged for DNA, RNA, proteins, metabolites and microbiota. These can be used as diagnostic evidence of disease. Particularly in the diagnosis and treatment of malignant tumours, salivary exosomes may serve as biomarkers.[30] They also have various functions. Salivary exosomes have been shown to shorten coagulation time and achieve haemostasis through the participation of tissue factors in the initial stage of blood coagulation.[31] They could also modulate and participate in the body's humoral immune response.[22] Minor variations in salivary exosomes can also be used to diagnose various oral diseases, including periodontitis,[32] oral lichen planus,[33] oral squamous cell carcinoma and some oral precancerous lesions.[34]

Exosomes in oral disease

Potential role of exosomes in periodontitis

Periodontitis is a chronic inflammatory disease characterised by an imbalance of the periodontal biofilm caused by plaque buildup.[35] Patients usually present local or total oral irreversible periodontal membrane damage, periodontal pocket deepening, alveolar bone absorption and other symptoms, which eventually lead to tooth loosening and loss, masticatory dysfunction and even arch defects.[36] Early detection and appropriate management are crucial to prevent the progression of periodontitis and mitigate its consequences. Thus, given the irreversible nature of periodontitis, the development of reliable tests for early detection of both periodontitis and periimplantitis is subject to significant focus in current research.[37] Salivary exosomes have been shown to be biomarkers for early detection and timely prevention of periodontitis. The disease was shown to lead to a significant increase in the secretion of certain components of exosomes by comparing the protein profiles of exosomes from healthy donors and patients with periodontitis and gingivitis.[38] In addition, the high specificity and sensitivity of global 5mC hypermethylation in salivary exosomes can differentiate periodontitis patients from healthy control subjects.[38] Researchers successfully isolated exosomal mRNA from the saliva samples of 61 patients and 30 controls for comparison. The results revealed that compared to the control group, the expression of PD-L1 was significantly elevated in patients with periodontitis, and there were significant differences in salivary exosomal PD-L1 mRNA levels among different stages of periodontitis.[39] In one study, researchers discovered that out of the ten mature miRNAs found in saliva, only three (hsa-miR-140-5p, hsa-miR-146a-5p and hsa-miR-628-5p) exhibited a significant increase within the exosomes of individuals with periodontitis when compared to the healthy control group.[33] These miRNAs have demonstrated con-

siderable potential in accurately identifying periodontitis and can be employed for diagnostic purposes.[40] Salivary exosomes miR-25-3p were significantly enriched in periodontitis patients with type 2 diabetes.[41] Interestingly, in patients with periodontitis, a notable reduction in the levels of CD9 and CD18 exosome-related tetraspanins was observed. These decreases exhibited a negative correlation with clinical measurements.[42,43]

Potential role of exosomes in primary Sjögren's syndrome

Primary Sjögren's syndrome (pSS) is an autoimmune disease that primarily affects female patients. It is considered one of the three most prevalent autoimmune disorders. Patients with this condition often experience symptoms such as dry mouth and dry eyes, which result from the focal infiltration of lymphocytes into the exocrine glands.[44,45] While the exact principles and mechanisms of action are yet to be fully understood, experimental studies have shown that exosomes play a role in both regulating and dysregulating the immune system.[46] Autoimmune responses targeting Ro/SSA and La/SSB antigens are significant in pSS. Salivary gland epithelial cells (SGECs) are crucial in initiating and facilitating the local immune response.[47,48] SGECs can also mediate the exposure of Ro/SSA and La/SSB autoantigens to the immune system, increase the apoptosis of apoptotic bodies, regulate the release of autoantigens and promote the secretion of exosomes containing autoantigens (Fig 2). Studies have reported the isolation and detection of APMAP, GNA13 and WDR1 in saliva-derived exosomes, as well as APEX1, PRDX3 and CPNE1 in tear-derived exosomes from patients with pSS.[49-51] These proteins are the components that exhibit the greatest deviation in biological replicates when compared to the control group. These exosomal components hold promise as potential biomarkers for early diagnosis and subsequent treatment of pSS, thereby enhancing diagnostic accuracy.[49]

The Epstein-Barr virus (EBV) has been found to be another critical factor in the pathogenesis of pSS, with a strong salivary gland homogeneity and the ability to infect B cells preferentially.[52] EBV-miR-BART13-3p, a specific microRNA derived from the EBV, has been found to be present in both EBV-infected B cells and epithelial cells in saliva. The levels of this microRNA were significantly higher in individuals infected with EBV compared to those who were not.[53] This exosome directly targets the mechanism that interacts with molecule 1 (STM1) to regulate and influence Ca^{2+} entry into SOCE channels, leading to SOCE loss and Ca^{2+}-dependent NFAT activation, ultimately affecting the salivary function of pSS.[44]

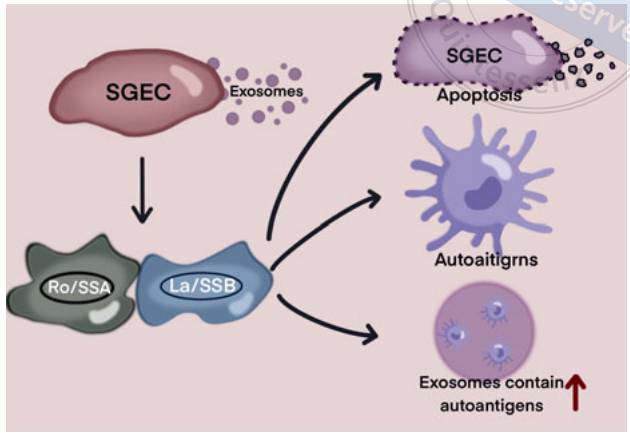

Fig 2 Schematic representation of the development and regulation of local autoimmune responses in pSS. In inflamed salivary tissues, exposure to danger signals or apoptosis-inducing factors prompts salivary gland epithelial cells (SGECs) to present Ro/SSA and La/SSB to the immune system, and these antigens are released into the microenvironment via exosomes or apoptotic bodies. This progress increases the apoptosis of apoptotic bodies, regulates the release of autoantigens and promotes the secretion of exosomes containing autoantigens.

Potential role of exosomes in oral mucosal disease

The oral mucosa is in prolonged contact with saliva in the mouth. It is reasonable to assume that the development of oral mucosal diseases can impact the secretion and composition of salivary exosomes. Salivary exosomes hold potential as biomarkers for various types of oral mucosal diseases and can contribute to their diagnosis and subsequent treatment.

Exosomes in leucoplakia

According to the World Health Organisation's definition, "white plaque of questionable risk having excluded (other) known diseases or disorders that carry no increased risk for cancer" is known as leucoplakia.[54] Leucoplakia is a typical precancerous lesion of the mouth. Risk factors include smoking, heavy alcohol consumption and areca chewing. There is no significant sex difference with regard to its incidence.[55-57] Experimental studies in oral medicine and research are continuously conducted to enhance the convenience and accuracy of diagnostic methods used in clinical practice.[58-61] These studies aim to develop and refine techniques that can detect the early stages of malignant transformation in oral leucoplakia, as well as identify potential indica-

tors of early oral malignancies.[58-61] One study referred to the OncAlert oral cancer rapid test, where saliva was collected and tested to compare pan-CD44 and total protein expression in patients with oral leucoplakia and an average healthy population.[62] Elevated levels of SolCD44 and complete protein have been observed in the saliva of patients diagnosed with oral leucoplakia, and these levels tend to increase with the severity of the clinical pattern of leucoplakia. These findings indicate that SolCD44 and complete protein could potentially serve as biomarkers for leucoplakia, as they show statistical differences in their expression between individuals with the disease and healthy individuals.[49] It is important to note that further research and validation studies are required to confirm the specificity and sensitivity of SolCD44 and complete protein as biomarkers for leucoplakia. Some findings suggest that the delivery of microRNAs through exosomes can modulate the inflammatory response, inhibit cell proliferation, suppress angiogenesis and induce apoptosis.[63] This approach holds promise as a potential novel treatment for precancerous lesions such as oral leucoplakia. By targeting specific pathways and mechanisms, exosomal-delivered microRNAs have the potential to offer new therapeutic options for managing precancerous conditions.

Exosomes in oral lichen planus

Oral lichen planus (OLP) is an idiopathic inflammatory mucosal form of autoimmune disease.[64] Its exact pathogenesis is not known. OLP lesions often involve the oral mucosa, tongue and gums, and the intraoral lesions always show a bilateral symmetrical distribution. Clinically, six types of OLP, namely reticular, papular, plaque-like, atrophic/erosive, ulcerative and bullous, can be identified.[65] Recent studies have indicated that microRNAs present in salivary exosomes may play a role in the development and progression of OLP.[33,66] One study found that salivary exosomes obtained from OLP patients exhibited significantly higher levels of miR-4484 compared to healthy individuals.[33] Another study found that salivary exosomes from OLP patients showed notably higher levels of miR-21 and substantially lower levels of miR-125a.[67] Additionally, an increase in miR-31 levels was observed in saliva from OLP patients with developmental abnormalities, but this pattern was not observed in patients with non-developmental abnormalities in OLP. These findings indicate that salivary exosomes have the potential to serve as biomarkers for diagnosing OLP, predicting prognostic outcomes and more.[67] Further research is needed to fully understand the diagnostic and prognostic implications of these specific microRNAs in OLP. MicroRNAs have been shown to be closely associated with cytokines in a variety of inflammation-related diseases, suggesting that in OLP, these specific microRNAs have the potential to contribute to the pathogenesis of OLP and may also participate in the regulation of inflammatory processes within the body.

Exosomes in hand, foot and mouth disease

Hand, foot and mouth disease (HFMD) is an acute viral infection, and the two most common pathogens are human enterovirus 71 (EV71) and coxsackievirus A16 (CVA16), which account for more than 70% of outbreaks.[68,69] It has also been reported that coxsackievirus A10 can lead to the occurrence of HFMD infection, which needs to be taken seriously.[70] Jia et al[71] verified that miRNAs (miR-671-5p, miR-16-5p and miR-150-3p) were significantly abnormally expressed in the serum exosomes of patients by testing the blood of children with HFMD compared to healthy children, suggesting that exosomes could be used as potential biomarkers for HFMD. Similar exosomal changes in saliva need to be confirmed by further experiments; miR-16-5p expression in exosomes was found to be especially higher, and miR-671-5p and miR-150-3p levels in exosomes were particularly lower than those in healthy children.[71] In their study, Jia et al[71] demonstrated significant dysregulation of specific microRNAs (miR-671-5p, miR-16-5p and miR-150-3p) in serum exosomes of patients with HFMD when compared to healthy children. These observations highlight the potential diagnostic value of these microRNAs in HFMD; however, further experiments are required to validate whether similar exosomal changes occur in saliva.

Potential role of exosomes in oral squamous cell carcinoma

Head and neck tumours are the sixth most common malignancy globally, with more than 500,000 patients diagnosed each year. Approximately 30% of head and neck cancers are oral cancers.[72] Lip and oral cancers accounted for around 354,000 new cases and over 177,000 deaths in 2018 alone.[73] Saliva plays a crucial role as the first line of defence against oral cancer due to its composition of various enzymes, proteins and immunoglobulins. Studies have confirmed that saliva contains high levels of immunoglobulins that are involved in the immune regulation of the body and exhibit promising anti-inflammatory effects.[15,50] Immunoglobulins, also known as antibodies, are produced by immune cells in response to foreign substances and play a significant role in the immune response. In the case of oral cancer,

the presence of high levels of immunoglobulins in saliva suggests that they may contribute to the immune surveillance and defence mechanisms against cancer cells in the oral cavity. The anti-inflammatory effects of saliva have been observed and acknowledged. Inflammation is closely linked to the development and progression of cancer. By having a good anti-inflammatory effect, saliva may help prevent or reduce the inflammatory processes that can contribute to the initiation or growth of oral cancer cells.[15] By comparing the morphological and molecular characteristics of salivary exosomes in oral cancer patients and healthy subjects, a group of researchers found significant differences between the two, confirming that salivary exosomes also possess the potential to become biomarkers in oral cancer patients involved in diagnosis and later treatment.[74]

By processing the corresponding saliva samples using ultracentrifugation, it was observed that exosomes isolated from saliva samples of head and neck cancer patients carried more PD-L1, FasL and TGF-β compared to those isolated from healthy patients.[75] Furthermore, the levels of these components were associated with tumour staging.[75] miRNA-365 has been noticed and studied as a potential biomarker for oral squamous cell carcinoma (OSCC). miRNA-365 can be detected as significantly elevated in different oral cancer cell lines in culture, and the expression level varies among cell lines. This implies that miRNA-365 has the potential for differential diagnosis of oral cancer and its phenotype.[34,76] OSCC accounts for over 95% of oral cancer cases. A study conducted on head and neck squamous cell carcinoma (HNSCC) discovered that using circulating tumour DNA (ctDNA) extracted from oral saliva as a biomarker resulted in a 100% positive rate for early tumour diagnosis, and this diagnostic rate was significantly higher compared to blood tests.[77] A group of researchers compared salivary exosomes from oral cancer patients and healthy controls by quantitative real-time polymerase chain reaction (qRT-PCR) and found that increased miR-31 expression could promote exosome-mediated miR-29a-3p expression by regulating the macrophage SOCS1/STA T6 signalling pathway. miR-125a and miR-200a expression decreased, and miRNA expression was reduced after tumour resection.[78] This experimental result demonstrated that salivary exosomes may be used not only for early diagnosis of oral cancer, but also for prognostic monitoring of tumours.

In a study comparing oral saliva samples from patients with OSCC and healthy individuals, researchers found that the size and concentration of OSCC-derived exosomes were significantly higher than those

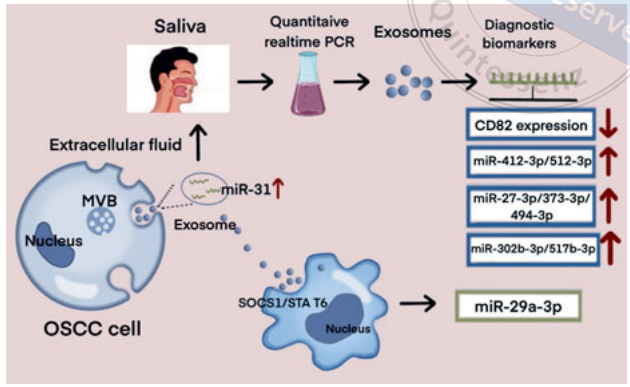

Fig 3 Schematic diagram of the proposed mechanism. Through the separation and detection of salivary exosomes, a significant decrease in CD82 expression[29] and upregulation of miR-412-3p, miR512-3p, miR-27a-3p, miR-373-3p and miR-494-3p occurred in OSCC patients. Salivary exosomal miR-31 is a potential novel diagnostic biomarker for OSCC. Exosomal miR-31 promotes exosome-mediated miR-29a-3p expression by regulating the macrophage SOCS1/STA T6 signalling pathway.

in the healthy group.[79] Additionally, there was a notable decrease in the expression of a molecule called CD82 in OSCC patients, and several miRNAs including miR-412-3p, miR-512-3p, miR-27a-3p, miR-373-3p and miR-494-3p were upregulated in OSCC patients compared to the healthy group.[79] Interestingly, OSCC patients exhibited the specific expression of miR-302b-3p and miR-517b-3p, which was not observed in the healthy group (Fig 3). The role of biomarkers in salivary exosomes in oral disease diagnosis is summarised in Table 1.

Recent advancements in saliva biopsy techniques have led to the development of innovative methods such as Fourier-transform infrared-based salivary exosome spectroscopy.[80] This technique has shown promising potential in distinguishing OSCC from healthy individuals. With a sensitivity of 100% and a specificity of 89%, it effectively detects the specific mid-infrared spectral features of OSCC salivary exosomes. Changes in salivary exosomal proteins, lipids and nucleic acids in OSCC patients contribute to these discernible differences. Furthermore, researchers have explored combining exosome technology with nanoplatforms, such as microfluidics, flow cytometry and electrochemical analysis, to add a new dimension to cancer diagnosis.[81]

Conclusion

In recent years, research has focused on studying the role of salivary exosomes in oral diseases like periodontitis, oral lichen planus and oral precancerous lesions. Salivary exosomes have shown potential as biomarkers

Table 1 The role of RNA, DNA, and protein in salivary exosomes in the diagnosis of oral disease.

Class	Exosome biomarker	Type of disease	Description	References
RNA	PD-L1 mRNA	Periodontitis	Significantly elevated in patients with periodontitis and expression levels vary when different stages of periodontitis are classified	39
	PD-L1 mRNA	Head and neck cancer	PD-L1 is highly expressed in saliva samples from patients, and the levels of these components were associated with tumour staging	75
	hsa-miR-140-5p, hsa-miR-146a-5p, hsa-miR-628-5p	Periodontitis	Exhibited a significant increase within the exosomes of individuals with periodontitis	40
	miR-25-3p	Periodontitis	Significantly enriched in periodontitis patients with type 2 diabetes	41
	EBV-miR-BART13-3p	Sjögren's syndrome	Higher in individuals infected with EBV compared to those who were not	53
	mRNA	Leucoplakia	The delivery of microRNAs through exosomes can modulate the inflammatory response, inhibit cell proliferation, suppress angiogenesis, and induce apoptosis	63
	miR-4484	OLP	Salivary exosomes obtained from OLP patients exhibited significantly higher levels of miR-4484 compared to healthy individuals	33
	miR-21	OLP	Notably higher levels of miR-21 from OLP patients	67
	miR-125a	OLP	Substantially lower levels of miR-125a from OLP patients	67
	miRNA-365	OSCC	Can be detected as significantly elevated in different oral cancer cell lines in culture, and the expression level varies among cell lines	34,75
	miR-125a, miR-200a	OSCC	miR-125a, miR-200a expression decreased, and miRNA expression was reduced after tumour resection	34,82
	miR-412-3p, miR-512-3p, miR-27a-3p, miR-373-3p, miR-494-3p	OSCC	Upregulated in OSCC patients compared to the healthy group	79
	miR-302b-3p, miR-517b-3p	OSCC	Specific expression in patients' salivary exosomes	79
DNA	ctDNA	OSCC	Using circulating tumour DNA (ctDNA) extracted from oral saliva as a biomarker resulted in a 100% positive rate for early tumour diagnosis which was significantly higher compared to blood tests	77
Protein	CD82	OSCC	Notable decrease in the expression of a molecule called CD82 in OSCC patients	79
	CD9\CD18	Periodontitis	A notable reduction in the levels of CD9 and CD18 exosome-related tetraspanins was observed	42,43

for noninvasive disease diagnosis and predicting therapeutic response. Salivary exosomes can also be used to monitor disease progression and treatment response. However, more research is needed to understand their regulation and specific roles in recipient cells. Despite the enormous diagnostic and therapeutic potential of salivary exosomes in oral diseases, there are still numerous limitations in their actual clinical application.

Conflicts of interest

The authors declare no conflicts of interest related to this study.

Author contribution

Drs Ming Yang YU and Xing Chen LIU drafted the manuscript and made the figures; Drs Ming Yang YU and Zi Li YU discussed and revised the manuscript; Drs Zi Li YU and Jun JIA designed the study. All authors read and approved the final manuscript.

(Received Nov 22, 2023; accepted April 23, 2024)

References

1. Shoaee S, Ghasemi E, Sofi-Mahmudi A, et al. Global, regional, and national burden and quality of care index (QCI) of oral disorders: a systematic analysis of the global burden of disease study 1990-2017. BMC Oral Health 2024;24:116.
2. The Lancet. GBD 2015: from big data to meaningful change. Lancet 2016;388:1447.
3. Shi S, Yu ZL, Jia J. The roles of exosomes in the diagnose, development and therapeutic resistance of oral squamous cell carcinoma. Int J Mol Sci 2023;24:1968.
4. Han Y, Jia L, Zheng Y, Li W. Salivary exosomes: Emerging roles in systemic disease. Int J Biol Sci 2018;14:633–643.
5. Pedersen AML, Sørensen CE, Proctor GB, Carpenter GH, Ekström J. Salivary secretion in health and disease. J Oral Rehabil 2018;45:730–746.
6. Nonaka T, Wong DTW. Saliva diagnostics. Annu Rev Anal Chem (Palo Alto Calif) 2022;15:107–121.
7. Raab-Traub N, Dittmer DP. Viral effects on the content and function of extracellular vesicles. Nat Rev Microbiol 2017;15:559–572.
8. Latifkar A, Cerione RA, Antonyak MA. Probing the mechanisms of extracellular vesicle biogenesis and function in cancer. Biochem Soc Trans 2018;46:1137–1146.
9. Zhong WQ, Ren JG, Xiong XP, et al. Increased salivary microvesicles are associated with the prognosis of patients with oral squamous cell carcinoma. J Cell Mol Med 2019;23:4054–4062.
10. Hong SL, Yu ZL, Bao ZH, et al. One-step detection of oral ulcers and oral cancer derived exosomes on wedge-shaped and high magnetic field gradient mediated chip. Sensors and Actuators B: Chemical 2022;357:131403.
11. Hyun KA, Gwak H, Lee J, Kwak B, Jung HI. Salivary exosome and cell-free DNA for cancer detection. Micromachines (Basel) 2018;9:340.
12. Sharma S, Rasool HI, Palanisamy V, et al. Structural-mechanical characterization of nanoparticle exosomes in human saliva, using correlative AFM, FESEM, and force spectroscopy. ACS Nano 2010;4:1921–1926.
13. Palanisamy V, Sharma S, Deshpande A, Zhou H, Gimzewski J, Wong DT. Nanostructural and transcriptomic analyses of human saliva derived exosomes. PLoS One 2010;5:e8577.
14. Cheshmi B, Cheshomi H. Salivary exosomes: properties, medical applications, and isolation methods. Mol Biol Rep 2020;47:6295–6307.
15. Ogawa Y, Miura Y, Harazono A, et al. Proteomic analysis of two types of exosomes in human whole saliva. Biol Pharm Bull 2011;34:13–23.
16. Ogawa Y, Kanai-Azuma M, Akimoto Y, Kawakami H, Yanoshita R. Exosome-like vesicles with dipeptidyl peptidase IV in human saliva. Biol Pharm Bull 2008;31:1059–1062.
17. Farooqi AA, Desai NN, Qureshi MZ, et al. Exosome biogenesis, bioactivities and functions as new delivery systems of natural compounds. Biotechnol Adv 2018;36:328–334.
18. Vences-Catalán F, Levy S. Immune targeting of tetraspanins Involved in cell invasion and metastasis. Front Immunol 2018;9:1277.
19. Belting M, Wittrup A. Nanotubes, exosomes, and nucleic acid-binding peptides provide novel mechanisms of intercellular communication in eukaryotic cells: implications in health and disease. J Cell Biol 2008;183:1187–1191
20. Michael A, Bajracharya SD, Yuen P, et al. Exosomes from human saliva as a source of microRNA biomarkers. Oral Dis 2010;16:34–38.
21. Zlotogorski-Hurvitz A, Dayan D, Chaushu G, et al. Human saliva-derived exosomes: Comparing methods of isolation. J Histochem Cytochem 2015;63:181–189
22. Li P, Melisa K, Han LS, Yao J, Gao Z. Progress in exosome isolation techniques. Theranostics 2017;7:789–804.
23. Zhang Y, Bi J, Huang J, et al. Exosome: A review of its classification, isolation techniques, storage, diagnostic and targeted therapy applications. Int J Nanomedicine 2020;15:6917–6934.
24. Skog J, Würdinger T, van Rijn S, et al. Glioblastoma microvesicles transport RNA and proteins that promote tumour growth and provide diagnostic biomarkers. Nat Cell Biol 2008;10:1470–1476.
25. Iwai K, Minamisawa T, Suga K, Yajima Y, Shiba K. Isolation of human salivary extracellular vesicles by iodixanol density gradient ultracentrifugation and their characterizations. J Extracell Vesicles 2016;5:30829.
26. Rupp AK, Rupp C, Keller S, et al. Loss of EpCAM expression in breast cancer derived serum exosomes: Role of proteolytic cleavage. Gynecol Oncol 2011;122:437–446.
27. Gyorgy B, Modos K, Pallinger E, et al. Detection and isolation of cell-derived microparticles are compromised by protein complexes resulting from shared biophysical parameters. Blood 2011;117:e39–e48.
28. Deregibus MC, Figliolini F, D'Antico S, et al. Charge-based precipitation of extracellular vesicles. Int J Mol Med 2016;38:1359–1366.
29. Schneider A, Simons M. Exosomes: vesicular carriers for intercellular communication in neurodegenerative disorders. Cell Tissue Res 2013;352:33–47.
30. Yu D, Li Y, Wang M, et al. Exosomes as a new frontier of cancer liquid biopsy. Mol Cancer 2022;21:56.
31. Kim H, Lee JW, Han G, Kim K, Yang Y, Sun HK. Extracellular vesicles as potential theranostic platforms for skin diseases and aging. Pharmaceutics 2021;13:760.
32. Nik Mohamed Kamal NNS, Shahidan WNS. Salivary exosomes: From waste to promising periodontitis treatment. Front Physiol 2022;12:798682.
33. Byun JS, Hong SH, Choi JK, Jung JK, Lee HJ. Diagnostic profiling of salivary exosomal microRNAs in oral lichen planus patients. Oral Dis 2015;21:987–993.
34. Krishnan A, Bhattacharya B, Mandal D, Dhar R, Muthu S. Salivary exosomes: A theranostics secret of oral cancer - Correspondence. Int J Surg 2022;108:106990.
35. Hajishengallis G. Periodontitis: from microbial immune subversion to systemic inflammation. Nat Rev Immunol 2015;15:30–44.
36. Tonetti MS, Henry G, Kornman KS. Staging and grading of periodontitis: Framework and proposal of a new classification and case definition. J Periodontol. 2018; 89(suppl 1): S159–S172.
37. Slots J. Periodontology: Past, present, perspectives. Periodontol 2000 2013;62:7–19.
38. Han P, Bartold PM, Salomon C, Ivanovski S. Salivary outer membrane vesicles and DNA methylation of small extracellular vesicles as biomarkers for periodontal status: A pilot study. Int J Mol Sci 2021;22:2423.
39. Yu J, Lin Y, Xiong X, et al. Detection of exosomal PD-L1 RNA in saliva of patients with periodontitis. Front Genet 2019;10:202.
40. Han P, Bartold PM, Salomon C, Ivanovski S. Salivary small extracellular vesicles associated miRNAs in periodontal status-A pilot study. Int J Mol Sci 2020;21:2809.
41. Byun JS, Lee HY, Tian J, et al. Effect of salivary exosomal miR-25-3p on periodontitis with insulin resistance. Front Immunol 2022;12:775046.

42. Zheng Y, Dong C, Yang J, et al. Exosomal microRNA-155-5p from PDLSCs regulated Th17/Treg balance by targeting sirtuin-1 in chronic periodontitis. J Cell Physiol 2019;234:20662–20674.
43. Tobón-Arroyave SI, Celis-Mejía N, Córdoba-Hidalgo MP, Isaza-Guzmán DM. Decreased salivary concentration of CD9 and CD81 exosome-related tetraspanins may be associated with the periodontal clinical status. J Clin Periodontol 2019;46:470–480.
44. Fox RI. Sjögren's syndrome. Lancet 2005;366:321–331.
45. Kroese FGM, Haacke EA, Bombardieri M. The role of salivary gland histopathology in primary Sjögren's syndrome: Promises and pitfalls. Clin Exp Rheumatol 2018;36(suppl 112):222–233.
46. Rui K, Hong Y, Zhu Q, et al. Olfactory ecto-mesenchymal stem cell-derived exosomes ameliorate murine Sjogren's syndrome by modulating the function of myeloid-derived suppressor cells. Cell Mol Immunol 2021;18:440–451.
47. Kyriakidis NC, Kapsogeorgou EK, Tzioufas AG. A comprehensive review of autoantibodies in primary Sjogren's syndrome: Clinical phenotypes and regulatory mechanisms. J Autoimmun 2014;51:67–74.
48. Martín-Nares E, Hernández-Molina G. Novel autoantibodies in Sjögren's syndrome: A comprehensive review. Autoimmun Rev 2019;18:192–198.
49. Aqrawi LA, Galtung HK, Vestad B, et al. Identification of potential saliva and tear biomarkers in primary Sjögren's syndrome, utilising the extraction of extracellular vesicles and proteomics analysis. Arthritis Res Ther 2017;19:14.
50. Tomosugi N, Kitagawa K, Takahashi N, Sugai S, Ishikawa I. Diagnostic potential of tear proteomic patterns in Sjögren's syndrome. J Proteome Res 2005;4:820–825.
51. Li B, Sheng M, Li J, et al. Tear proteomic analysis of Sjögren syndrome patients with dry eye syndrome by two-dimensional-nano-liquid chromatography coupled with tandem mass spectrometry. Sci Rep 2014;4:5772.
52. Lucchesi D, Pitzalis C, Bombardieri M. EBV and other viruses as triggers of tertiary lymphoid structures in primary Sjögren's syndrome. Expert Rev Clin Immunol 2014;10:445–455.
53. Gallo A, Jang SI, Ong HL, et al. Targeting the Ca(2+) sensor STIM1 by exosomal transfer of Ebv-miR-BART13-3p is associated with Sjögren's syndrome. EBioMedicine 2016;10:216–226.
54. Warnakulasuriya S, Johnson NW, van der Waal I. Nomenclature and classification of potentially malignant disorders of the oral mucosa. J Oral Pathol Med 2007;36:575–580.
55. Petti S. Pooled estimate of world leukoplakia prevalence: A systematic review. Oral Oncol 2003;39:770–780.
56. Petti S, Scully C. Association between different alcoholic beverages and leukoplakia among non- to moderate-drinking adults: A matched case-control study. Eur J Cancer 2006;42:521–527.
57. Arduino PG, Bagan J, El-Naggar AK, Carrozzo M. Urban legends series: oral leukoplakia. Oral Dis 2013;19:642–659.
58. Kannan S, Chandran GJ, Pillai KR, et al. Expression of p53 in leukoplakia and squamous cell carcinoma of the oral mucosa: Correlation with expression of Ki67. Clin Mol Pathol 1996;49:M170–M175.
59. Pitiyage G, Tilakaratne WM, Tavassoli M, Warnakulasuriya S. Molecular markers in oral epithelial dysplasia: review. J Oral Pathol Med 2009;38:737–752.
60. Nasser W, Flechtenmacher C, Holzinger D, Hofele C, Bosch FX. Aberrant expression of p53, p16INK4a and Ki-67 as basic biomarker for malignant progression of oral leukoplakias. J Oral Pathol Med 2011;40:629–635.
61. Monteiro L, Mello FW, Warnakulasuriya S. Tissue biomarkers for predicting the risk of oral cancer in patients diagnosed with oral leukoplakia: A systematic review. Oral Dis 2021;27:1977–1992.
62. Čēma I, Dzudzilo M, Kleina R, Franckevica I, Svirskis Š. Correlation of soluble CD44 expression in saliva and CD44 protein in oral leukoplakia tissues. Cancers (Basel) 2021;13:5739.
63. Wang L, Yin P, Wang J, et al. Delivery of mesenchymal stem cells-derived extracellular vesicles with enriched miR-185 inhibits progression of OPMD. Artif Cells Nanomed Biotechnol 2019;47:2481–2491.
64. Nogueira PA, Carneiro S, Ramos-E-Silva M. Oral lichen planus: An update on its pathogenesis. Int J Dermatol 2015;54:1005–1010.
65. Chiang CP, Yu-Fong Chang J, Wang YP, et al. Oral lichen planus –Differential diagnoses, serum autoantibodies, hematinic deficiencies, and management. J Formos Med Assoc 2018;117:756–765.
66. Ma H, Wu Y, Yang H, et al. MicroRNAs in oral lichen planus and potential miRNA-mRNA pathogenesis with essential cytokines: A review. Oral Surg Oral Med Oral Pathol Oral Radiol 2016;122:164–173.
67. Mehdipour M, Shahidi M, Manifar S, et al. Diagnostic and prognostic relevance of salivary microRNA-21, -125a, -31 and -200a levels in patients with oral lichen planus - A short report. Cell Oncol (Dordr) 2018;41:329–334.
68. Yan JJ, Su IJ, Chen PF, Liu CC, Yu CK, Wang JR. Complete genome analysis of enterovirus 71 isolated from an outbreak in Taiwan and rapid identification of enterovirus 71 and coxsackievirus A16 by RT-PCR. J Med Virol 2001;65:331–339.
69. Aswathyraj S, Arunkumar G, Alidjinou EK, Hober D. Hand, foot and mouth disease (HFMD): Emerging epidemiology and the need for a vaccine strategy. Med Microbiol Immunol 2016;205:397–407.
70. Bian L, Gao F, Mao Q, et al. Hand, foot, and mouth disease associated with coxsackievirus A10: more serious than it seems. Expert Rev Anti Infect Ther 2019;17:233–242.
71. Jia HL, He CH, Wang ZY, et al. MicroRNA expression profile in exosome discriminates extremely severe infections from mild infections for hand, foot and mouth disease. BMC Infect Dis 2014;14:506.
72. Delman KA. Introducing the "Virtual Tumor Board" series in CA: A Cancer Journal for Clinicians. CA Cancer J Clin 2020;70:77.
73. Bray F, Ferlay J, Soerjomataram I, Siegel RL, Torre LA, Jemal A. Global cancer statistics 2018: GLOBOCAN estimates of incidence and mortality worldwide for 36 cancers in 185 countries. CA Cancer J Clin 2018;68:394–424.
74. Zlotogorski-Hurvitz A, Dayan D, Chaushu G, Salo T, Vered M. Morphological and molecular features of oral fluid-derived exosomes: Oral cancer patients versus healthy individuals. J Cancer Res Clin Oncol 2016;142:101–110.
75. Tengler L, Tiedtke M, Schütz J, et al. Optimization of extracellular vesicles preparation from saliva of head and neck cancer patients. Sci Rep 2024;14:946.
76. Coon J, Kingsley K, Howard KM. miR-365 (microRNA): Potential biomarker in oral squamous cell carcinoma exosomes and extracellular vesicles. Int J Mol Sci 2020;21:5317.
77. Wang Y, Springer S, Mulvey CL, et al. Detection of somatic mutations and HPV in the saliva and plasma of patients with head and neck squamous cell carcinomas. Sci Transl Med 2015;7:293ra104.

78. Cai J, Qiao B, Gao N, Lin N, He W. Oral squamous cell carcinoma-derived exosomes promote M2 subtype macrophage polarization mediated by exosome-enclosed miR-29a-3p. Am J Physiol Cell Physiol 2019;316:C731–C740.
79. Gai C, Camussi F, Broccoletti R, et al. Salivary extracellular vesicle-associated miRNAs as potential biomarkers in oral squamous cell carcinoma. BMC Cancer 2018;18:439.
80. Zlotogorski-Hurvitz A, Dekel BZ, Malonek D, Yahalom R, Vered M. FTIR-based spectrum of salivary exosomes coupled with computational-aided discriminating analysis in the diagnosis of oral cancer. J Cancer Res Clin Oncol 2019;145:685–694.
81. Shao H, Im H, Castro CM, Breakefield X, Weissleder R, Lee H. New technologies for analysis of extracellular vesicles. Chem Rev 2018;118:1917–1950.
82. Liu CJ, Lin SC, Yang CC, Cheng HW, Chang KW. Exploiting salivary miR-31 as a clinical biomarker of oral squamous cell carcinoma. Head Neck 2012;34:219–224.

PRESERVE HEALTHY TOOTH STRUCTURE

NEW

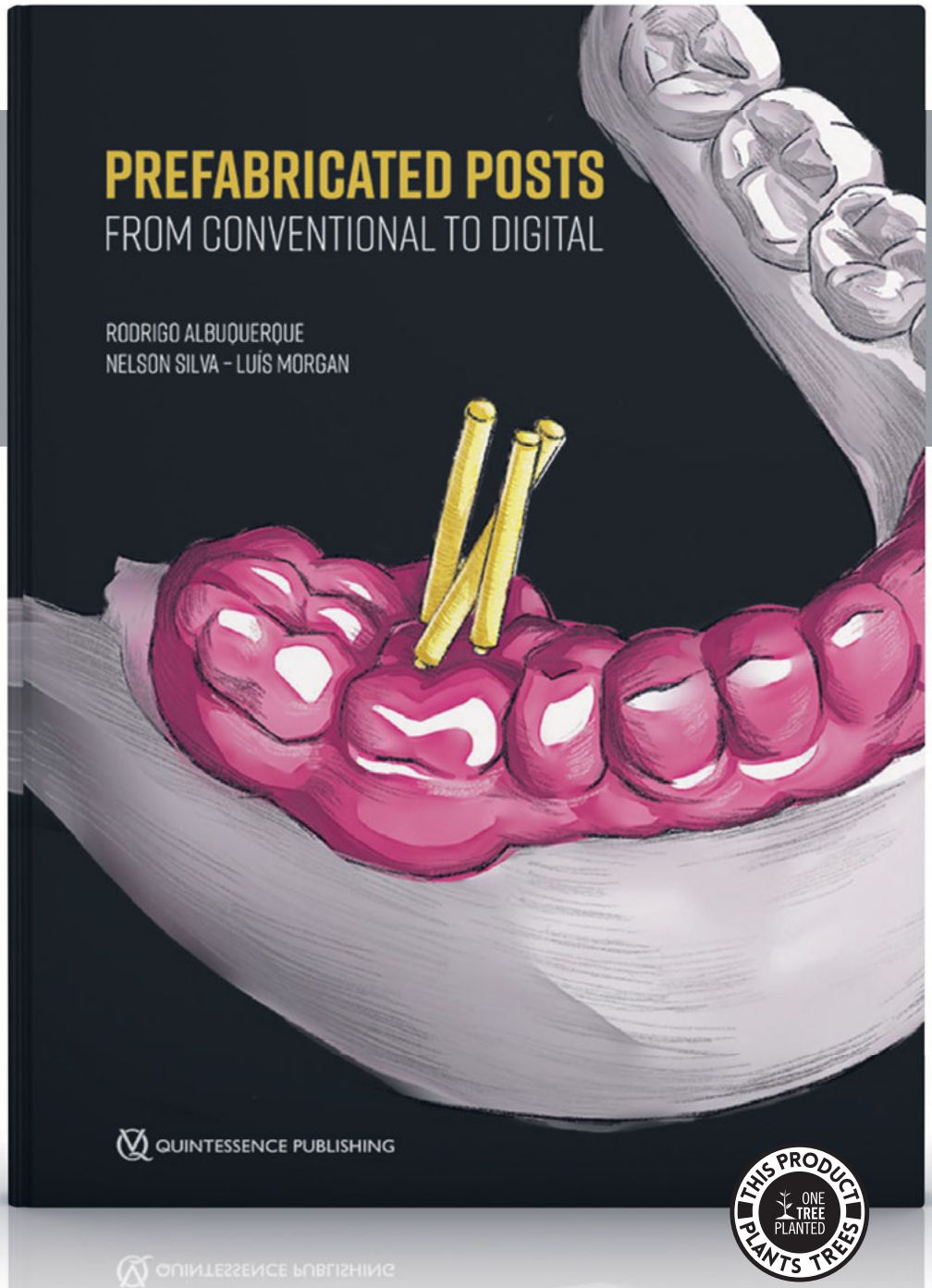

Rodrigo Albuquerque | Nelson Silva
Luís Morgan

Prefabricated Posts

From Conventional to Digital

280 pages, 1,023 illus.
ISBN 978-1-78698-144-8
€138

Restoring endodontically treated teeth is undoubtedly a complex procedure. A sound knowledge of biomechanical and clinical principles, careful planning, and the selection of appropriate materials and restorative techniques is essential to achieve the best functional and esthetic outcomes. This concise and exquisitely illustrated book, based on the philosophy and clinical experience of its authors and on sound scientific evidence, is divided into 10 chapters in a didactic sequence to make it easier for dentists to apply the techniques in everyday practice. The focus is on preserving the heathy tooth structure as much as possible using both conventional and digital methodologies.

www.quint.link/posts
books@quintessenz.de
+49 (0)30 761 80 667
QUINTESSENCE PUBLISHING

SIRT2 Mediated Microtubule Acetylation in Osteogenic Differentiation

Xin Ru ZHOU[1], Can ZHANG[1], Chen Rong XU[1], Xin Er TAN[1], Qian Qian HAN[1], Xi YANG[1], Tian Yu SUN[1], Long Quan SHAO[1], Jia LIU[1]

Objective: *To assess the role of microtubule acetylation in the transportation of amorphous calcium phosphate (ACP)-containing vesicles that mediate the osteogenic differentiation process of rat bone mesenchymal stem cells (BMSCs).*

Methods: *Rat BMSCs were cultured and transfected with sirtuin 2 (SIRT2) overexpression plasmids for an in vitro model. The microtubule acetylation-related protein levels were detected by western blots. The microtubule acetylation and the secretion rate of extracellular ACP-containing vesicles were observed with immunofluorescence and live cell fluorescence imaging. The secretion of ACP was observed by transmission electron microscopy. The mineralised nodule formation was stained with Alizarin Red S staining and observed by microscopy.*

Results: *Microtubule acetylation was increased during osteogenic differentiation of BMSCs, and microtubule transport efficiency was enhanced. Mechanically, microtubule acetylation is the key reason for the increased transportation rate of ACP-containing vesicles and enhanced osteogenic differentiation, as both were blocked after SIRT2-mediated microtubule acetylation inhibition.*

Conclusion: *Microtubule acetylation mainly promotes the transportation and secretion of ACP vesicles, and ultimately promotes the osteogenic differentiation process.*

Keywords: *biomineralization, intracellular transport, microtubule acetylation, osteogenic differentiation*

Chin J Dent Res 2024;27(4):303–310; doi: 10.3290/j.cjdr.b5860280

During bone tissue healing, mineralisation is a highly prevalent and tightly regulated process. Abnormalities in this process can result in severe pathological conditions such as osteoporosis, osteoarthritis, osteogenesis imperfecta and Paget's disease.[1] Currently, bone healing is classified into two categories: intramembranous ossification and endochondral ossification. Unlike endochondral ossification, which involves stages such as fibrous callus formation, bony callus formation and bony callus remodelling and restructuring to promote bone tissue regeneration, intramembranous ossification involves direct ossification of the bone gap and reconstruction of the Haversian system, enabling the direct connection of the two ends of the fractured bone and thereby restoring the mechanical continuity of the skeleton.[2,3]

For most of the bone healing process, one of the most important events is the recruitment of osteoprogenitor cells to the injury site to then differentiate into osteoblasts; these newly formed osteoblasts then secrete calcium phosphate salts to facilitate bone regeneration.[4] More specifically, the earliest form of calcium phosphate salt is an amorphous precursor called amorphous calcium phosphate (ACP), which is conveyed to the cell membrane before being released into the extracellular matrix via exocytosis.[4-6] Once delivered into the collagen matrix outside the cell, ACP can further convert into octacalcium phosphate and

1 Stomatological Hospital, School of Stomatology, Southern Medical University, Guangzhou, P.R. China.

Corresponding authors: Dr Long Quan SHAO and Dr Jia LIU, Stomatological Hospital, School of Stomatology, Southern Medical University, S366 Jiangnan Boulevard, Haizhu District, Guangzhou 510280, P.R. China. Tel: 86-20-84413940. Emails: liujia1988@smu.edu.cn; shaolongquan@smu.edu.cn

This Project is funded by the National Natural Science Foundation of China (82001077), Science and Technology Programme of Guangzhou (2024A04J3527), and the Young Elite Scientist Support Programme by CSA (2020PYRC001, 2022PYRC002).

subsequently undergo hydrolysis to form hydroxyapatite, the primary mineral component found in mature bone,[7] ultimately facilitating collagen fibre mineralisation. While mechanisms for mineralisation of collagen fibres have been established, numerous unanswered questions persist regarding the generation and transportation of ACP precursors to extracellular sites for mineralisation that require urgent clarification.

A substantial body of research has revealed the presence of mineral particles within intracellular vesicles of osteoblasts (also named matrix vesicles). These particles are synthesised within the cells and subsequently discharged into the extracellular environment via exocytosis.[8-10] The aforementioned studies suggest that after the intracellular synthesis of mineral precursor ACP, it is primarily localised to organelles such as mitochondria and autophagosomes, and is then transported to the extracellular matrix (ECM) utilising a microtubule-mediated transport system to trigger collagen mineralisation.[5,8] As a major constituent of the cellular cytoskeleton, microtubules participate in types of biological process, which exhibit a dynamic nature that enables constant switching between growth and shrinkage, facilitating exploration and sensing of intracellular space. The stringent modulation of their dynamics is vital for microtubule structure and function. Notably, it has been demonstrated that alterations in the structural stability of the microtubule system have a direct impact on bone formation.[11-13]

Tubulin post-translational modifications (PTMs) regulate microtubule properties and functions, attracting increased attention as the discovery of many more enzymes has enabled the functions of these rarely studied modifications to be determined.[10,14] While most known PTMs function on the outer surface of assembled microtubules, acetylation of a-tubulin's lysine 40 (K40) has been identified as a modification occurring on the inner surface, within the lumen of the microtubule.[15] Recent studies have pointed out that acetylation, as a type of post-translational modification in the microtubule system, plays an important role in regulating microtubule function.[16] More importantly, some studies illustrate that microtubule acetylation has various effects on biomineralisation depending on the tissue type. For example, Li et al[17] reported that promoting alpha-tubulin acetylation may contribute to interstitial mineral deposition for renal tubular epithelial; however, for the odontogenesis process, Zhan et al[18] did not find evidence of microtubule acetylation involvement in the differentiation of odontoblasts. In this study, the authors focused on biomineralisation related to osteogenic differentiation and paid closer attention to the level of microtubule acetylation within this process. The results showed that microtubule acetylation plays a role in the early stages of osteogenic differentiation in bone mesenchymal stem cells (BMSCs), whereas its significance diminishes in the later stages.

Therefore, this study constructed a BMSC osteogenic differentiation model and aimed to investigate the role of microtubule acetylation in biomineralisation and elucidate its internal mechanism in depth, and the results provide ideas for the development of new therapeutic strategies for regulating osteogenesis in the future.

Materials and methods

Chemicals

Foetal bovine serum and Dulbecco's modified Eagle medium were purchased from Gibco (Thermo Fisher Scientific, Waltham, MA, USA). Anti-α-tub (mouse mAb) was purchased from Abclonal (Woburn, MA, USA). Anti-α-tub (rabbit mAb) and -acet-α-tub antibodies were purchased from Proteintech (Chicago, IL, USA). Fluo-3 AM and Hoechst 33342 were purchased from Invitrogen (Thermo Fisher Scientific).

Cell culture

Rat BMSCs were purchased from Cyagen (Guangzhou, China), and then cultured in Dulbecco's modified Eagle medium supplemented with 10% foetal bovine serum. The culture medium was changed every 3 days. In vitro osteogenic differentiation was performed using the prepared osteoblast-inducing conditional media.

Plasmid construction and transfection

The SIRT2 overexpression plasmids were constructed from Vigenebio (Rockville, MD, USA) and prepared in growth medium and transfected utilising Lipofectamine 2000 (Thermo Fisher Scientific) according to the manufacturer's protocol.

Cell fluorescence imaging for microtubule acetylation

After treatment of nontransfected or SIRT2 overexpressing plasmid-transfected BMSCs, the cells were incubated with antibodies against acet-α-tub (dilution 1:1000) and/or α-tub (dilution 1:200) overnight and the corresponding secondary antibody (dilution 1:100). Cellular fluorescence was observed using confocal microscopy (Leica,

Wetzlar, Germany) and analysed in Image-Pro Plus 6.0 software (Media Cybernetics, Rockville, MD, USA).

Western blot analysis

Cells were extracted and lysed, and the total proteins were collected. Then, the samples were heated at 100°C for 5 minutes for protein denaturation. 10 μg protein was separated by electrophoresis on a 10% sodium dodecyl sulphate (SDS) polyacrylamide gel. The separated proteins were transferred to a polyvinylidene fluoride (PVDF) membrane. The membranes were blocked and incubated with a specific antibody and corresponding secondary antibody. The protein band was obtained using enhanced chemiluminescence (ECL) reagent (Meilunbio, Dalian, China) and analysed in ImageJ (National Institutes of Health, Bethesda, MD, USA).

RT-qPCR

Cells were extracted and lysed, and the total RNA were obtained. Then, cDNA was acquired from total RNA using Evo M-MLV RT Master Mix (Accurate Biology, Changsha, China). The target genes, SIRT2, were detected and analysed through real-time fluorescence quantitative polymerase chain reaction (RT-qPCR) (LightCycler 96 Instrument, Roche, Basel, Switzerland). The mRNA expression levels of SIRT2 were normalized to those of GAPDH. The SIRT2 primer sequences were as follows: Forward Primer: CACGGCACCTTCTACACATCAC, Reverse Primer: CACGGCACCTTCTACACATCAC. GAPDH primer sequence: Forward Primer: GACATGCCGCCTGGAGAAAC, Reverse Primer: AGCCCAGGATGCCCTTTAGT.

Alizarin red S staining

After 4 weeks of osteogenic differentiation using osteogenic induction medium, the BMSCs were fixed with 4% paraformaldehyde for 30 to 45 minutes, then treated with alizarin red S solutions (KeyGEN, Nanjing, China). The osteogenic differentiation status was observed through microscopy (Zeiss, Stereo Lumar V12, Oberkochen, Germany), and the alizarin red was further extracted with cetylpyridinium chloride and detected using a spectrophotometer at an absorbance value of 562 nm.

Alkaline phosphatase (ALP) enzyme assay

The ALP activity was detected using an Alkaline Phosphatase Assay Kit (Beyotime, Shanghai, China), and the experiments were carried out in accordance with the manufacturer's protocol.

Live cell fluorescence imaging for evaluating the transportation speed of Ca^{2+} containing vesicles

The cells were seeded in 24-well plates. After treatment with or without the SIRT2 overexpression plasmid, the cells were washed gently three times and stained with Fluo-3 AM (100 nM) (Thermo Fisher Scientific) at 37°C for 30 minutes. Cellular fluorescence was observed and captured in real time by confocal microscopy (Leica) and analysed using Image-Pro Plus 6.0 software.

Transmission electron microscopy (TEM)

Before TEM to observe the secretion of ACP, the cells were washed twice. The collected cells were fixed with 2.5% glutaraldehyde, dehydrated with graded ethanol solutions and acetone, and finally embedded. Ultrathin sections were prepared and observed via an H-7500 TEM instrument (Hitachi, Tokyo, Japan).

Statistical analysis

Data were presented as mean ± standard deviation (SD). Each experiment was repeated at least three times. A one-way analysis of variance was performed, combined with a Fisher least significant difference multiple comparison post-hoc test to measure statistical significance for three or more groups. For comparison between two groups, a Student *t* test was applied. $P < 0.05$ was considered statistically significant. SPSS 21.0 (IBM, Armonk, NY, USA) was used for statistical analysis.

Results

Microtubule acetylation during osteogenic differentiation of BMSCs

Some studies have confirmed that microtubule acetylation can effectively maintain the stability of microtubule structure, while reducing the microtubule acetylation level with overexpression deacetylase could have a significant inhibitory effect on cell morphology and function.[19] We therefore asked whether the microtubule acetylation level changed during the osteogenic differentiation process for BMSCs. The immunofluorescence experiment in this study showed that the acetylation level of the microtubule system in BMSCs was significantly increased during osteogenic differentiation

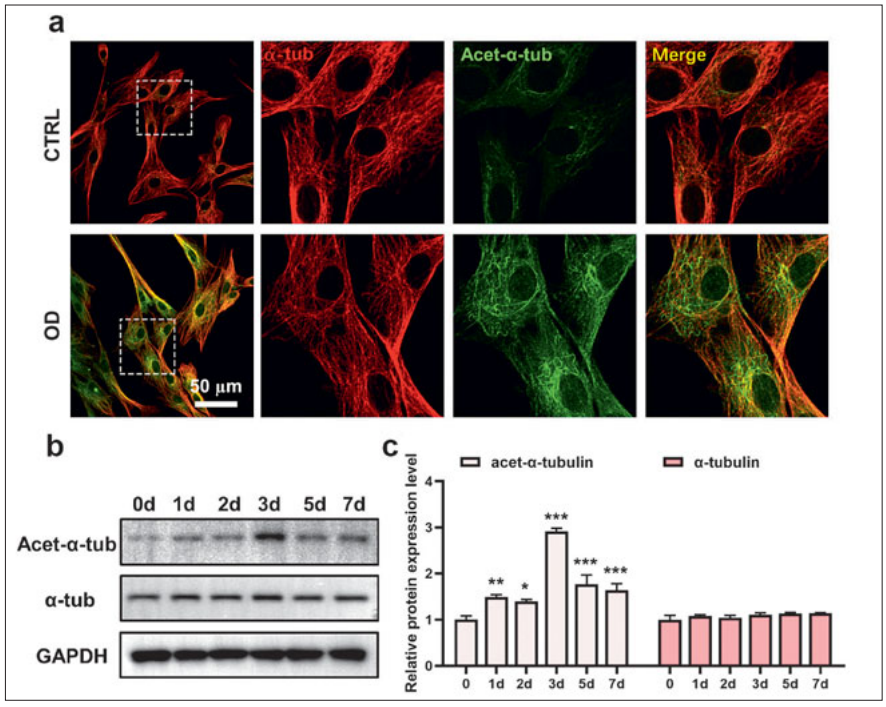

Fig 1a to c Acetylation of α-tubulin is involved in osteogenic differentiation of BMSCs. Representative fluorescence images of BMSCs immunostained for acet-α-tubulin (green) and α-tubulin (red) after osteogenic induction (OD) for 3 days **(a)**. Western blotting of acet-α-tubulin and α-tubulin expression in BMSCs treated with osteogenic induction for various durations. Changes in protein expression were quantified after normalisation to GAPDH **(b and c)**. **P* < 0.05, ***P* < 0.01, ****P* < 0.001 compared to the control group.

(Fig 1a). Similar results were obtained for the microtubule acetylation protein level: the protein levels of acetylated α-tubulin increased and peaked after 3 days of osteogenic differentiation and then declined until 7 days, but were still significantly higher than the base level (Fig 1b and c). The above data indicate that microtubule acetylation is likely to be an important biological phenomenon during osteogenic differentiation, but its exact role is still unknown.

Microtubule transportation efficiency of BMSCs was enhanced during osteogenic differentiation

Microtubules act as the main material transportation channel in cells and play a key role in ACP transportation and secretion. By using calcium ion marker Fluo-3 to label intracellular calcium ions, the transport rate of calcium ions was dynamically observed under a confocal microscope in living cells. The results showed that the transport rate of intracellular calcium during the osteogenic differentiation process for BMSCs was accelerated significantly (Fig 2a and b). Meanwhile, TEM data showed that the amount of extracellular ACP increased significantly after 7 days of osteogenic differentiation compared with the control group, indicating that ACP secretion occurred (Fig 2c). The above results suggest that microtubule transport efficiency is indeed significantly accelerated in the osteogenic differentiation process of BMSCs.

Microtubule acetylation is the key reason for the enhancement of transportation efficiency

Microtubule acetylation modification can improve microtubule work efficiency.[20,21] For example, acetylated microtubules can enhance microtubule transport efficiency and ultimately promote intracellular material secretion.[22,23] Thus, microtubule acetylation may be an important factor for regulating transport efficiency during the osteogenic differentiation process of BMSCs. To further clarify the crucial role of microtubule acetylation in osteogenic differentiation, the present authors constructed an overexpression plasmid for deacetylase SIRT2.[24] Existing studies have demonstrated that SIRT2 can interact with microtubule proteins through Co-Immunoprecipitation experiments.[25,26] Firstly, our data showed that the SIRT2 expression level was declined at 2 and 3 days and then increased to baseline at 7 days during BMSCs osteogenic differentiation, which indicated an opposite tendency compared to microtubule acetylation levels (Fig 3a). After overexpression of SIRT2, RT-qPCR detection showed that the gene expression of SIRT2 increased in BMSCs treated with osteogenic induction medium (Fig 3b). Importantly, immunofluorescence experiments showed the increase of acetylated α-tubulin protein expression level that occurred during BMSCs osteogenic differentiation was inhibited significantly after overexpression of SIRT2 (Fig 3c). Meanwhile, western blotting results also showed simi-

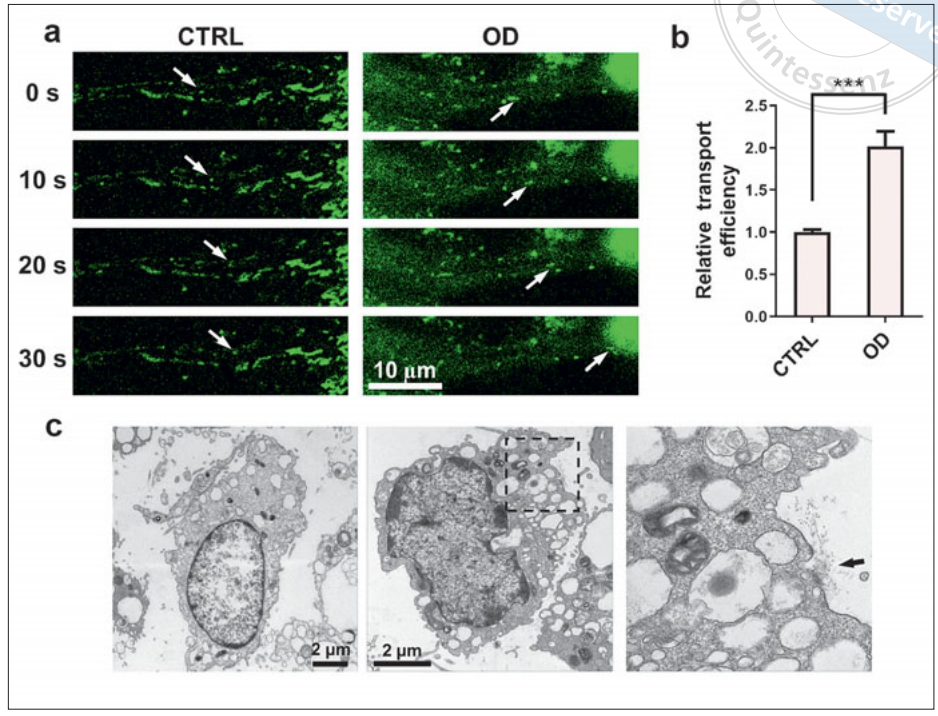

Fig 2a to c Microtubule-mediated intracellular transport increase during osteogenic differentiation of BMSCs. Live fluorescence images of calcium transportation (arrows) in BMSCs after osteogenic induction for 3 days. The translocation rate of calcium was quantified **(a and b)**. Representative TEM images showing releasement of ACP (arrows) after BMSCs were treated without or with osteogenesis induction medium for 7 days **(c)**. ***P < 0.001 compared to the control group.

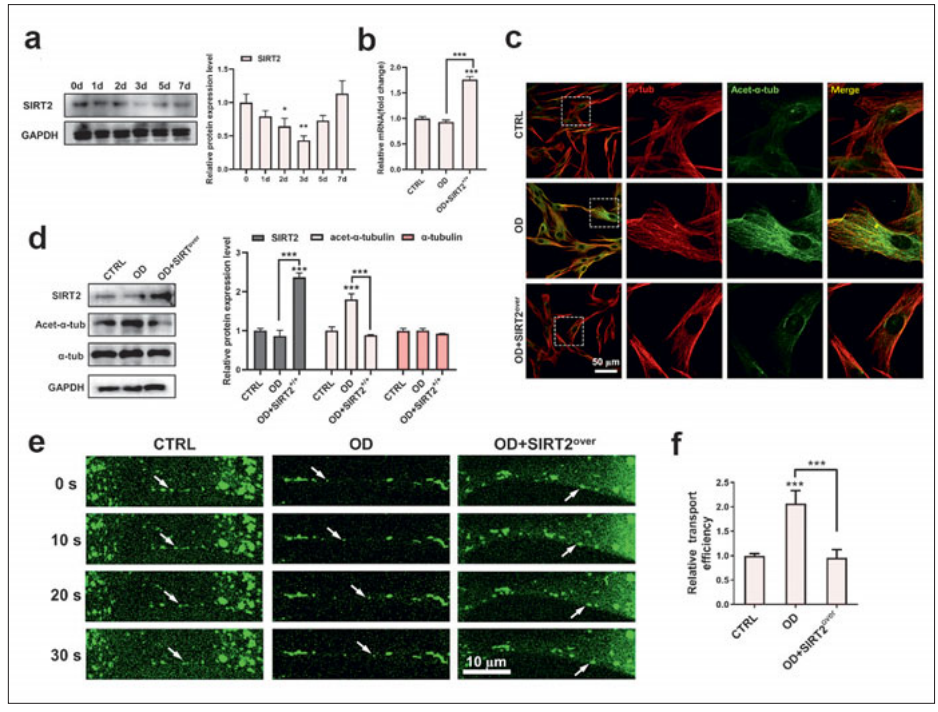

Fig 3a to f SIRT2 overexpression reduces the transportation efficiency via microtubule acetylation inhibition. Western blotting of SIRT2 expression in BMSCs treated with osteogenic induction for various durations. Changes in protein expression of SIRT2 were quantified after normalisation to GAPDH **(a)**. RT-qPCR detection of SIRT2 mRNA level in BMSCs after osteogenic induction for 3 days with or without SIRT2 overexpression. Changes in gene expression of SIRT2 were quantified after normalisation to GAPDH **(b)**. BMSCs were transfected with SIRT2 overexpression plasmid, then immunostained with antibodies against acet-α-tubulin (green) and α-tubulin (red), respectively **(c)**. Western blotting of SIRT2, acet-α-tubulin and α-tubulin expression in BMSCs after osteogenic induction for 3 days with or without SIRT2 overexpression. Changes in protein expression were quantified after normalization to GAPDH **(d)**. Live fluorescence images of calcium transportation (arrows) in BMSCs after osteogenic induction for 3 days with or without SIRT2 overexpression. The translocation rate of calcium was quantified **(e and f)**. *P < 0.05, **P < 0.01, ***P < 0.001 compared to the control group or the OD group as indicated.

lar results (Fig 3d). These data indicate that SIRT2 is an important enzyme that regulates microtubule acetylation, and its overexpression can indeed regulate the level of microtubule acetylation during osteogenic differentiation.

Secondly, after constructing a deacetylase SIRT2 overexpression plasmid to inhibit intracellular microtubule acetylation level, we evaluated the transport rate of calcium ion vesicles (such as ACP). The results showed that overexpressing SIRT2 can effectively inhib-

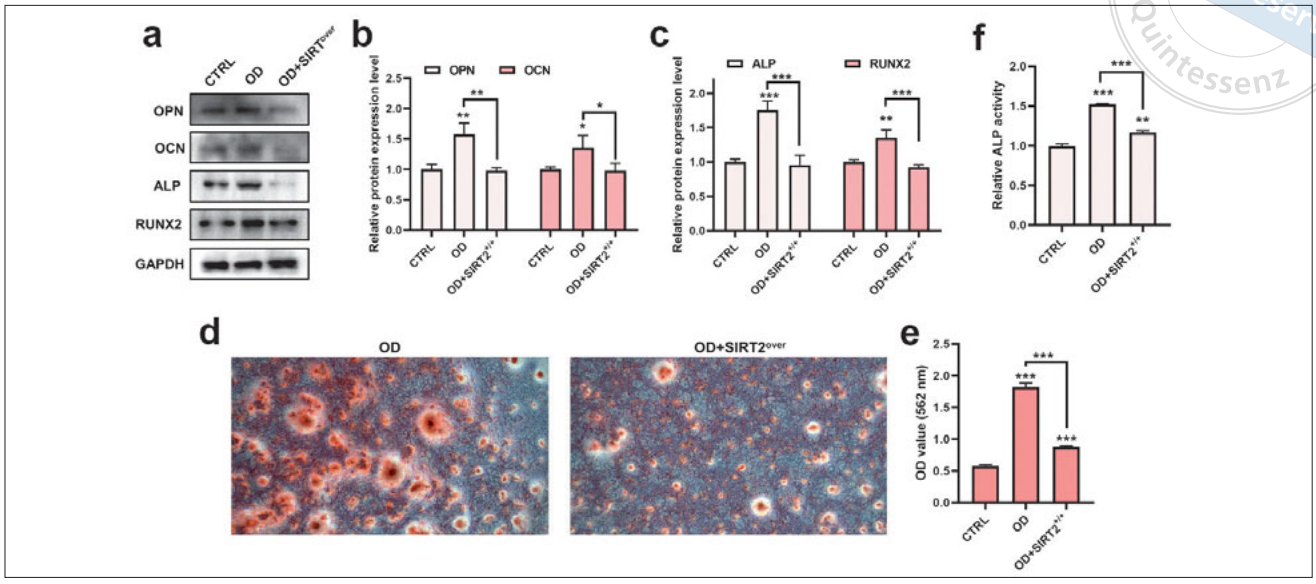

Fig 4a to f Reduced α-tubulin acetylation further hinders the osteogenic differentiation process. BMSCs were transfected with SIRT2 overexpression plasmid, then western blotting of matrix proteins and proteins related to osteogenic differentiation in BMSCs treated with osteogenic induction for 7 days. Changes in protein expression were quantified after normalisation to GAPDH **(a to c)**. Representative images of Alizarin red staining in BMSCs treated with osteogenic induction for 28 days (×50 magnification) **(d)**. Quantitative analyses of Alizarin red staining as treatment in **(d) (e)**. Quantitative analyses of ALP activities in BMSCs treated with osteogenic induction for 7 days **(f)**. **P* < 0.05, ***P* < 0.01, ****P* < 0.001 compared to the control group or the OD group as indicated.

it the transport rate of intracellular calcium ion vesicles (Fig 3e and f). Thus, we indicate that microtubule acetylation is one crucial factor for enhancing cellular transport efficiency during osteogenic differentiation.

Inhibition of microtubule acetylation blocks the osteogenic differentiation process

It is important to examine whether microtubule acetylation enhanced transportation efficiency will further affect the osteogenic differentiation effect and ultimately impact the biomineralisation process. The present authors detected the changes in the expression level of key osteogenic differentiation proteins in BMSCs under the condition of SIRT2 overexpression. The results showed that key osteogenic differentiation proteins and matrix proteins, such as ALP, Runt-related transcription factor 2 (RUNX2), osteocalcin (OCN) and osteopontin (OPN), increased during osteogenic differentiation, but they were all significantly inhibited under SIRT2 overexpression for reducing the intracellular microtubule acetylation level (Fig 4a to c). In addition, by using Alizarin red to detect the level of mineralised nodule formation, the results showed that osteogenic differentiation of BMSCs can achieve a good mineralisation induction effect that mainly manifests as a significant increase in the level of mineralised nodule formation. However, by overexpressing SIRT2 to reduce intracellular microtubule acetylation, the abovementioned mineralised nodule formation effect was significantly blocked (Fig 4d and e). We also detected ALP activity with or without overexpressing SIRT2 during osteogenic differentiation of BMSCs, and similar results were obtained to show that increased ALP levels were observed under osteogenic differentiation, but inhibited after overexpressing SIRT2 (Fig 4f). These data all suggest that the osteogenic differentiation process is indeed regulated by microtubule acetylation, where enhanced transportation efficiency is one main influential factor.

Discussion

The cytoskeleton is known to function in mechanical sensing and mechanical transduction. Interactions between cytoskeletal proteins, integrins and mechanical forces can affect the cell shape, proliferation and even differentiation.[27,28] Because of this, there has been increasing interest in the interplay between the cytoskeleton and stem cell differentiation. Interestingly, microtubules have been shown to play an indistinct role

in osteogenic differentiation, as it was observed that the morphology and structure of microtubules did not change significantly during the differentiation of mesenchymal stem cells.[28] However, during biomineralisation, osteoblasts must transport substantial amounts of mineral matrix out of the cell into the extracellular matrix. The microtubule system is a key component of the cytoskeleton involved in regulating this material transport. Thus, understanding how the biological function of microtubules evolves during biomineralisation is a compelling issue that warrants further investigation.

PTMs on microtubules are a key controller of microtubule properties and functions.[29] Among these, microtubule acetylation is recognised as the most stable modification, primarily regulated by the recruitment of the αTAT1 protein to the microtubule lumen, making it less susceptible to interference from other biological enzymes.[19,30,31] More intriguingly, a previous study by the present authors also reported that enhancing microtubule acetylation is beneficial for alleviating lysosomal autophagy blockades resulting from microtubule disruption, where the enhanced microtubule acetylation helps maintain microtubule structure, significantly promoting vesicle transport and fusion, and thereby sustaining normal metabolic functions.[32] Thus, in this study, exploring how microtubule acetylation mediates mineral transport could provide new insights into the biomineralisation process.

The present data demonstrate that microtubule acetylation plays a critical role in ACP-containing vesicle transportation during osteogenic differentiation, which is needed for biomineralisation.[33,34] However, other important factors also can influence ACP formation and biomineralisation, such as lysosome mediated biogenesis of matrix vesicles.[35] Some articles have indicated that matrix vesicles are vesicular structures rich in calcium and phosphate, contaiing organic materials such as acidic proteins. Lysosomes are thought to be one type of early matrix vesicle, capable of enriching calcium and phosphate and subsequently transporting ACP without crystallisation.[34,36] As we reported previously, lysosome transportation could also be mediated via microtubule acetylation.32 Given this, it is essential to investigate whether microtubule acetylation also participate in the lysosomal transportation and secretion, and then influence the biogenesis of matrix vesicles and ACP formation during biomineralisation. Exploring these issues could yield more valuable insights into the regulatory mechanisms of microtubule acetylation underlying biomineralisation.

Furthermore, osteogenesis is not limited to osteoblasts but also involves biological functions among various cell types within the bone microenvironment, including osteocytes, endothelial cells and immune cells. Given the wide range of cell types that participate in bone formation,[37] it is conceivable that modulation of microtubule acetylation during osteogenesis should have a widespread effect on a variety of cells. For instance, microtubule dynamics are known to influence the behaviour of osteoclasts during bone resorption and could impact the balance between bone formation and degradation.[12] As such, more research should be funded to investigate how the modulation of microtubule acetylation affects the biological process of other crucial cells within the bone microenvironment, which not only help to achieve a comprehensive understanding of the function of the microtubule system in bone formation, but also may pave the way for the development of novel therapeutic strategies that target the osteogenic microenvironment as a whole. Therefore, while the role of microtubule acetylation in osteogenic differentiation is becoming clearer, much remains to be explored regarding its function in other biological processes and cell types participating in bone formation. Future research should aim to expand understanding of the osteogenic microenvironment and the potential role of microtubule modifications across different cell types in bone formation.

Conclusion

In summary, microtubule acetylation is one of the key biological phenomena in the osteogenic differentiation of BMSCs, where increased microtubule acetylation could promote the transportation and secretion of ACP vesicles, and ultimately the osteogenic differentiation process.

Conflicts of interest

The authors declare no conflicts of interest related to this study.

Author contribution

Dr Xin Ru ZHOU contributed to the experiments and manuscript draft and editing; Drs Can ZHANG, Chen Rong XU, Xin Er TAN, Qian Qian HAN, Xi YANG and Tian Yu SUN contributed to the data collection or methodology; Dr Long Quan SHAO contributed to study supervision; Dr Jia LIU contributed to study conceptualisation, supervision and critical revision of the manuscript.

(Received Dec 11, 2023; accepted May 16, 2024)

References

1. Chai YC, Carlier A, Bolander J, et al. Current views on calcium phosphate osteogenicity and the translation into effective bone regeneration strategies. Acta Biomater 2012;8:3876–3887.
2. Ye X, He J, Wang S, et al. A hierarchical vascularized engineered bone inspired by intramembranous ossification for mandibular regeneration. Int J Oral Sci 2022;14:31.
3. Zhao F, Qiu Y, Liu W, et al. Biomimetic hydrogels as the inductive endochondral ossification template for promoting bone regeneration. Adv Healthc Mater 2024;13:e2303532.
4. Tsukasaki M, Takayanagi H. Osteoimmunology: evolving concepts in bone–immune interactions in health and disease. Nat Rev Immunol 2019;19:626–642.
5. Pei DD, Sun JL, Zhu CH, et al. Contribution of mitophagy to cell-mediated mineralization: Revisiting a 50-year-old conundrum. Adv Sci (Weinh) 2018;5:1800873.
6. Kovacs CS, Chaussain C, Osdoby P, Brandi ML, Clarke B, Thakker RV. The role of biomineralization in disorders of skeletal development and tooth formation. Nat Rev Endocrinol 2021;17:336–349.
7. Qiu N, Fang WJ, Li HS, He ZM, Xiao ZS, Xiong Y. Impairment of primary cilia contributes to visceral adiposity of high fat diet-fed mice. J Cell Biochem 2018;119:1313–1325.
8. Nollet M, Santucci-Darmanin S, Breuil V, et al. Autophagy in osteoblasts is involved in mineralization and bone homeostasis. Autophagy 2014;10:1965–1977.
9. Bertolotti F, Carmona FJ, Dal Sasso G, et al. On the amorphous layer in bone mineral and biomimetic apatite: A combined small- and wide-angle X-ray scattering analysis. Acta Biomater 2021;120:167–180.
10. Müller WEG, Ackermann M, Al-Nawas B, et al. Amplified morphogenetic and bone forming activity of amorphous versus crystalline calcium phosphate/polyphosphate. Acta Biomater 2020;118:233–247.
11. Dejaeger M, Böhm AM, Dirckx N, et al. Integrin-linked kinase regulates bone formation by controlling cytoskeletal organization and modulating BMP and Wnt signaling in osteoprogenitors. J Bone Miner Res 2017;32:2087–2102.
12. Liu H, Zhang R, Ko SY, et al. Microtubule assembly affects bone mass by regulating both osteoblast and osteoclast functions: stathmin deficiency produces an osteopenic phenotype in mice. J Bone Miner Res 2011;26:2052–2067.
13. Lee K, Kim H, Jeong D. Microtubule stabilization attenuates vascular calcification through the inhibition of osteogenic signaling and matrix vesicle release. Biochem Biophys Res Commun 2014;451:436–441.
14. Nicot S, Gillard G, Impheng H, et al. A family of carboxypeptidases catalyzing α- and β-tubulin tail processing and deglutamylation. Sci Adv 2023;9:eadi7838.
15. Prokop A. Microtubule regulation: Transcending the tenet of K40 acetylation. Curr Biol 2022;32:R126–R128.
16. Naren P, Samim KS, Tryphena KP, et al. Microtubule acetylation dyshomeostasis in Parkinson's disease. Transl Neurodegener 2023;12:20.
17. Li S, Wu W, Yang B, et al. Histone deacetylase 6 suppression of renal tubular epithelial cell promotes interstitial mineral deposition via alpha-tubulin acetylation. Cell Signal 2024;116:111057.
18. Zhan Y, Wang H, Zhang L, Pei F, Chen Z. HDAC6 regulates the fusion of autophagosome and lysosome to involve in odontoblast differentiation. Front Cell Dev Biol 2020;8:605609.
19. Xu Z, Schaedel L, Portran D, et al. Microtubules acquire resistance from mechanical breakage through intralumenal acetylation. Science 2017;356:328–332.
20. Wippich F, Vaishali, Hennrich ML, Ephrussi A. Nutritional stress-induced regulation of microtubule organization and mRNP transport by HDAC1 controlled α-tubulin acetylation. Commun Biol 2023;6:776.
21. Janke C, Montagnac G. Causes and consequences of microtubule acetylation. Curr Biol 2017;27:R1287–R1292.
22. Monteiro P, Yeon B, Wallis SS, Godinho SA. Centrosome amplification fine tunes tubulin acetylation to differentially control intracellular organization. EMBO J 2023;42:e112812.
23. Yang Y, Chen X, Feng Z, et al. MEC17-induced α-tubulin acetylation restores mitochondrial transport function and alleviates axonal injury after intracerebral hemorrhage in mice. J Neurochem 2022;160:51–63.
24. Zhang L, Hou X, Ma R, Moley K, Schedl T, Wang Q. Sirt2 functions in spindle organization and chromosome alignment in mouse oocyte meiosis. FASEB J 2014;28:1435–1445.
25. Zhao Y, Xie L, Shen C, et al. SIRT2-knockdown rescues GARS-induced Charcot-Marie-Tooth neuropathy. Aging Cell 2021;20:e13391.
26. Skoge RH, Ziegler M. SIRT2 inactivation reveals a subset of hyperacetylated perinuclear microtubules inaccessible to HDAC6. J Cell Sci 2016;129:2972–2982.
27. Caporizzo MA, Prosser BL. The microtubule cytoskeleton in cardiac mechanics and heart failure. Nat Rev Cardiol 2022;19:364–378.
28. Saidova AA, Vorobjev IA. Lineage commitment, signaling pathways, and the cytoskeleton systems in mesenchymal stem cells. Tissue Eng Part B Rev 2020;26:13–25.
29. Janke C, Magiera MM. The tubulin code and its role in controlling microtubule properties and functions. Nat Rev Mol Cell Biol 2020;21:307–326.
30. Szyk A, Deaconescu AM, Spector J, et al. Molecular basis for age-dependent microtubule acetylation by tubulin acetyltransferase. Cell 2014;157:1405–1415.
31. Portran D, Schaedel L, Xu Z, Théry M, Nachury MV. Tubulin acetylation protects long-lived microtubules against mechanical ageing. Nat Cell Biol 2017;19:391–398.
32. Liu J, Kang Y, Yin S, et al. Key role of microtubule and its acetylation in a zinc oxide nanoparticle-mediated lysosome-autophagy system. Small 2019;15:e1901073.
33. Cruz MAE, Ferreira CR, Tovani CB, et al. Phosphatidylserine controls calcium phosphate nucleation and growth on lipid monolayers: A physicochemical understanding of matrix vesicle-driven biomineralization. J Struct Biol 2020;212:107607.
34. Iwayama T, Bhongsatiern P, Takedachi M, Murakami S. Matrix vesicle-mediated mineralization and potential applications. J Dent Res 2022;101:1554–1562.
35. Otsuru S, Desbourdes L, Guess AJ, et al. Extracellular vesicles released from mesenchymal stromal cells stimulate bone growth in osteogenesis imperfecta. Cytotherapy 2018;20:62–73.
36. Iwayama T, Okada T, Ueda T, et al. Osteoblastic lysosome plays a central role in mineralization. Sci Adv 2019;5:eaax0672.
37. Chen Y, Wang H, Yang Q, et al. Single-cell RNA landscape of the osteoimmunology microenvironment in periodontitis. Theranostics 2022;12:1074–1096.

Localisation of the Infraorbital and Mental Foramen in Orthognathic Surgery: a CBCT Study

Xin CHEN[1,#], Cheng TAO[2,#], Tie Mei WANG[2]

Objective: *To establish precise positional references for orthognathic surgery by examining the relative positioning of the infraorbital foramen (IOF) in relation to the anterior nasal spine (ANS) and the mental foramen (MF) in relation to the pogonion (Pog).*
Methods: *A cohort of 115 patients with CBCT images was randomly selected for analysis. Distances and positional relationships between the IOF and ANS, as well as the MF and Pog, were measured using 3D reconstruction images.*
Results: *On average, the ANS was situated 21.40 mm below the IOF, with a horizontal distance of 26.42 mm. The horizontal and vertical distances between the MF and Pog were 23.57 and 9.71 mm, respectively. Scatter plots centred on the ANS indicated that 83% (191/230) of the IOF were distributed in a 30- to 45-degree fan shape, the radius of which ranged from 30 to 40 mm. Similarly, 98% (226/230) of the MF occupied a 45-degree fan shape within a 20 to 30 mm radius in the bilateral superior quadrant centred on the Pog.*
Conclusion*: During maxillary osteotomy, there is a potential risk of damaging the infraorbital neurovascular bundle located 21.40 mm above the ANS. To mitigate the risk of IOF injury, caution is advised, particularly when retracting the flap below a 30-degree fan shape within a 30 to 40 mm radius centred on the ANS and a 45-degree fan shape within a 20 to 30 mm radius centred on the Pog. Special attention is warranted during flap elevation in this specified area.*
Keywords: *CBCT, infraorbital foramen, mental foramen, orthognathic surgery*
Chin J Dent Res 2024;27(4):311–317; doi: 10.3290/j.cjdr.b5860286

Orthognathic surgery is commonly performed for the correction of dentofacial deformities and malocclusion.[1] Neurosensory impairment is a virtually universal outcome following osteotomy procedures, attributed not only to accidental nerve section but also to stretching or avulsion during surgery.[2]

The lower two-thirds of the skin in the craniofacial region is predominantly innervated by infraorbital and mental nerves. The infraorbital foramen (IOF) and mental foramen (MF), the respective foramina for these nerves, are frequently encountered in various orthognathic procedures.[2,3] While IOF is primarily at risk during maxillary osteotomy due to soft tissue retraction, permanent nerve damage is rare.[2] Conversely, the dissection and dissociation of MF pose a greater challenge, as the mental nerve may undergo retraction or even resection, leading to sensory dysfunction in the chin and lower lip.[4] Thus, the identification and preservation of both foramina are critical aspects of orthognathic surgery.

Although some studies have explored the relationship between these foramina and adjacent dental or bony landmarks,[5,6] dental structures can be displaced by preoperative orthodontics or third molar eruption. Common bony landmarks, such as the infraorbital rim, upper margin of the nasal aperture and jugale, may offer clinical information for maxillofacial fracture repair or local anesthesia.[7,8] However, these bony landmarks might remain elusive and seem invisible during orthognathic surgery. The anterior nasal spine

1 Department of Oral and Maxillofacial Surgery, Jiangyin People's Hospital Affiliated to Nantong University, Wuxi, Jiangsu Province, P.R. China.
2 Nanjing Stomatological Hospital, Affiliated Hospital of Medica School, Research Institute of Stomatology, Nanjing University, Nanjing, Jiangsu Province, P.R. China.
# These two authors contributed equally to this work.

Corresponding author: Dr Tie Mei WANG, Nanjing Stomatological Hospital, Affiliated Hospital of Medica School, Research Institute of Stomatology, Nanjing University, Nanjing 210008, Jiangsu Province, P.R. China. Tel: 86-25-83620351. Email: Tiemeiwang106@163.com

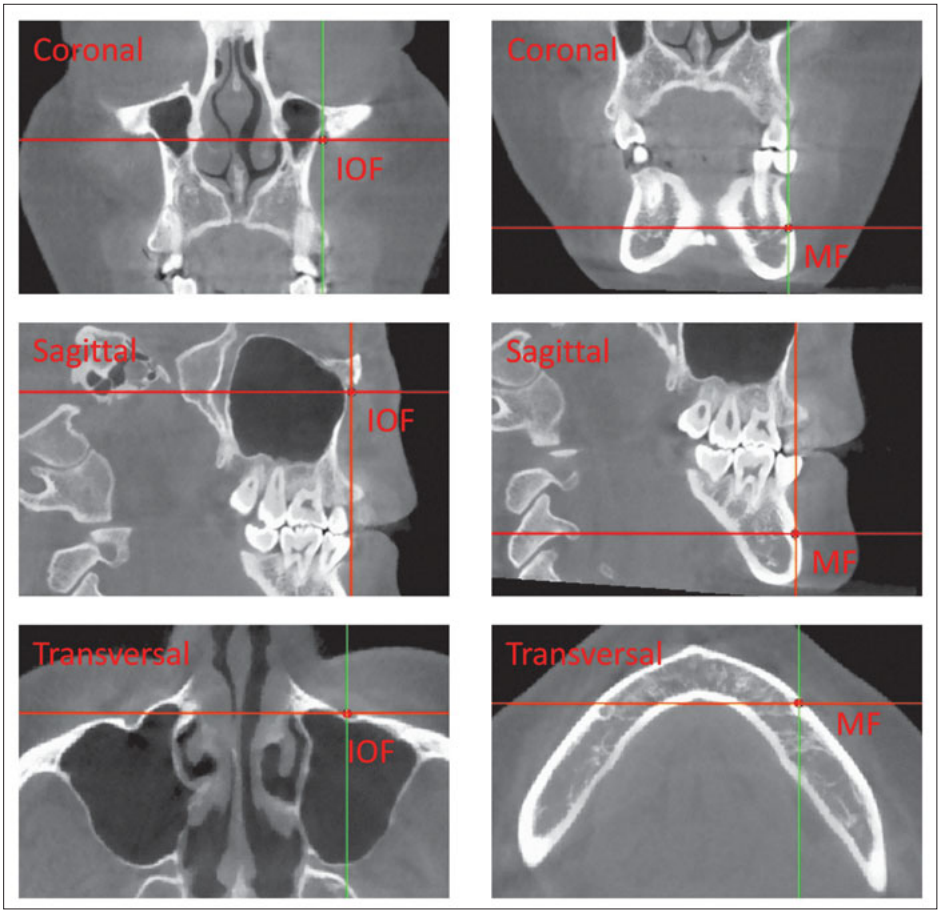

Fig 1 Location of the IOF and MF.

(ANS) and pogonion (Pog) stand out as more prominent bony landmarks, consistently exposed and preserved throughout these procedures.[5,9]

The present study aims to establish the position of the IOF relative to the ANS and MF relative to Pog, providing a more accessible reference for the precise location of both foramina in orthognathic surgery.

Materials and methods

CBCT images from 115 patients were collected between October 2019 and October 2020. The patients were randomly selected from all those who attended Nanjing Stomatological Hospital. The inclusion criteria encompassed complete written records, CBCT images without metal artifacts and motion artifacts, absence of facial trauma, maxillofacial surgery, significant periodontal disease, open bite or craniomaxillofacial dysplasia, and an age range from 20 to 25 years. Participants were informed of the inclusion of their demographic and imaging data in the study, and all provided approval. All procedures performed in studies involving human participants were in accordance with the ethical standards of the institutional and/or national research committee and with the 1964 Helsinki declaration and its later amendments or comparable ethical standards. This study was approved by the local ethics committee of Nanjing Stomatological Hospital (No: JX-2020NL-06). CBCT examinations were conducted by the same professional imaging specialist following a standardised protocol on a NewTom VGi machine (NewTom, Imola, Italy) with uniform parameter settings (tube voltage 110 kV, tube current 9.47 to 15.90 mA, field of view 5 × 5 cm, exposure time 4.3 seconds, voxel size 0.1 mm). Mimics 15.0 software (Materialisen, Leuven, Belgium) in the oral radiology department of our hospital was used for image measurements.

Reference planes were established as previously described.[10] Briefly, the axial plane was aligned parallel to the Frankfort horizontal plane (FH plane), while the sagittal and coronal planes were perpendicular to each other and to the FH plane. The IOF was identified as the most superolateral point on the exterior end of the infraorbital canal, and the MF was the most anterior

point of the opening transmitting the inferior alveolar nerve on the mandibular surface (Fig 1). Horizontal distances from the frontal projection point of the IOF to ANS and the MF to Pog were denoted as "w1" and "w2", representing the width of both points, while vertical distances were recorded as "h1" and "h2", indicating the height of both points (Fig 2). In addition, the 3D distance from MF to Pog was measured. All distances were first determined by locating the corresponding points on the 2D image, and then calculated based on the coordinates of these points. We classified the patients into three categories according to the Angle classification method by analysing the positional relationship of the maxillary and mandibular first molars on sagittal images. We then marked the FH and mandibular plane (MP) on sagittal images and measured the Frankfort-mandibular plane angle (FMA). Patients were classified as high-angle if the FMA was greater than 32 degrees, low-angle if it was less than 22 degrees, and average-angle if it was between 22 and 32 degrees.

Two independent oral radiologists with a minimum of 3 years' experience in CBCT image interpretation performed measurements individually. Intraobserver reliability was assessed by repeating measurements of 30% randomly selected samples after a 1-month interval. Another 30% subjects were randomly chosen for re-evaluations to assess inter-observer variability using intraclass correlation coefficient (ICC).

Data were collected for both sides, and side differences were analysed using a paired *t* test. The paired *t* test was also employed to analyse width differences between the IOF and MF. Sex differences were evaluated using an independent samples *t* test. A one-way between-subjects analysis of variance (ANOVA) was conducted to compare the differences in distances among different Angle classifications. Differences in distances among different facial types were also analysed using a one-way ANOVA. Statistical analyses were conducted using SPSS (version 19.0), and results with $P < 0.05$ were deemed statistically significant.

Results

This study included a total of 115 CBCT examinations from 58 men and 57 women, with a mean age of 22 years. This resulted in a sample of 230 sides for the analysis of the location of the IOF and MF.

Both intra- (ICC ≥ 0.918, $P < 0.001$) and interobserver reproducibility (ICC ≥ 0.906, $P < 0.001$) were excellent (Table S1 and S2, provided on request). The mean of the independent measurements taken by the two operators was adopted.

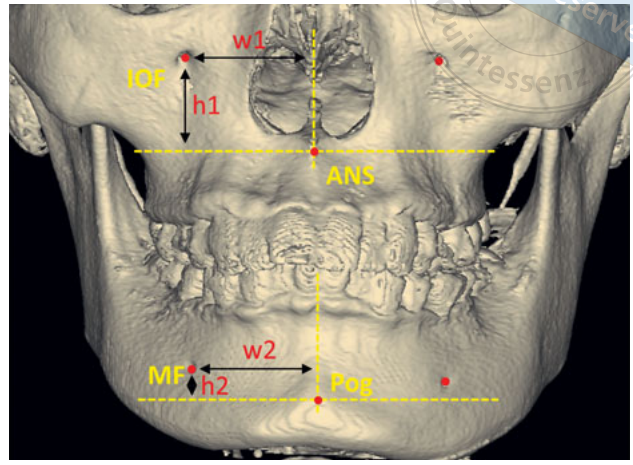

Fig 2 Measurement diagram: the width (w1) and height (h1) of the IOF to the ANS on the frontal projection, and the width (w2) and height (h2) of the MF to the Pog on the frontal projection.

On average, the ANS was positioned 21.40 mm below the IOF, with a horizontal distance of 26.42 mm. The horizontal, vertical and 3D distances between MF and Pog was 23.57, 9.71 and 29.87 mm, respectively. Men exhibited a 1.60 mm broader width of the IOF (95% confidence interval [CI] 1.06 to 2.14 mm, $P = 0.000$) and a 2.45 mm larger height of the IOF (95% CI 1.77 to 3.13 mm, $P = 0.000$) compared to women. Moreover, the 3D distance between Pog and MF was found to be 0.9 mm longer in men compared to women (95% CI 0.37 to 1.49 mm, $P = 0.000$), while no significant sex-based differences were observed for the MF in width and height (Table 1). The width of the IOF was 2.85 mm larger than that of the MF (95% CI 2.55 to 3.14 mm, $P = 0.000$) (Table 2). There were no significant differences in the distance between both sides ($P > 0.05$).

There was a significant difference in the width and the 3D distance from MF to Pog at the $P < 0.05$ level across the three Angle classifications ($P = 0.000$). Post hoc analysis with a Bonferroni correction revealed that patients with a distal molar relationship had an MF-Pog width that was 0.73 mm greater compared to those with a mesial molar relationship ($P = 0.014$) and 0.80 mm greater compared to those with a neutral molar relationship ($P = 0.000$). Additionally, the MF-Pog 3D distance in patients with a distal molar relationship was 2.16 mm longer compared to those with a mesial molar relationship ($P = 0.000$) and 1.70 mm longer compared to those with a neutral molar relationship ($P = 0.000$) (Table 3). A significant difference in the height of the MF was also observed at the $P < 0.05$ level among the three different facial types. The post-hoc Bonferroni correction indicated that patients with a low-angle

Table 1 Width and height of the IOF relative to the ANS and the MF relative to the Pog in men and women.

		Men	Women	Mean difference	95% CI	*P* value
IOF	w1 (mm)	27.21 ± 2.12	25.61 ± 2.03	1.60	1.06, 2.14	0.000
	h1 (mm)	22.61 ± 2.57	20.16 ± 2.66	2.45	1.77, 3.13	0.000
MF	w2 (mm)	23.89 ± 1.57	23.24 ± 1.40	0.65	−0.26, 1.04	0.375
	h2 (mm)	9.85 ± 2.85	9.57 ± 3.00	0.27	−0.49, 1.03	0.478
	3D (mm)	30.32 ± 2.16	29.40 ± 2.15	0.93	0.37, 1.49	0.001

Width (w1) and height (h1) of the IOF to the ANS on the frontal projection; width (w2), height (h2) and 3D distance (3D) of the MF to the Pog on the frontal projection. The width, height and 3D distance of both points were presented as mean ± standard deviation (SD) and an independent samples *t* test was applied for sex comparison.

Table 2 Width of the IOF relative to the ANS and MF relative to the Pog.

	IOF	MF	Mean difference	95% CI	*P* value
Width (mm)	26.42 ± 2.22	23.57 ± 1.52	2.85	2.55, 3.14	0.000

The width and height of both points were presented as mean ± standard deviation (SD). A paired *t* test was also adopted to analyse the width difference.

Table 3 Width and 3D distance of the MF relative to Pog in different Angle classifications.

	Class I	Class II	Class III	*P* value	P_{IandII}	$P_{IandIII}$	$P_{IIandIII}$
w2 (mm)	23.23 ± 1.55	23.30 ± 1.35	24.03 ± 1.48	0.000	1.000	0.001	0.014
3D (mm)	29.28 ± 2.00	28.81 ± 1.76	30.98 ± 2.11	0.000	0.561	0.000	0.000

The width and 3D distance of MF were presented as mean ± standard deviation (SD). A one-way between-subjects ANOVA was adopted to analyse the width and distance difference. A Bonferroni correction was used for post-hoc comparisons.

Table 4 Height of the MF relative to the Pog in different facial types.

	Group L	Group A	Group H	*P* value	P_{LandA}	P_{LandH}	P_{AandH}
h2 (mm)	8.20 ± 2.40	11.34 ± 2.47	12.30 ± 2.19	0.000	0.000	0.000	0.424

Group L, low-angle group; group A, average-angle group; group H, high-angle group. The height of the MF was presented as mean ± standard deviation (SD). A one-way between-subjects ANOVA was adopted to analyse the height. A Bonferroni correction was used for post-hoc comparisons.

facial type had an MF-Pog height that was 0.33 mm greater compared to those with an average-angle facial type ($P = 0.000$) and 0.64 mm greater compared to those with a high-angle facial type ($P = 0.000$) (Table 4).

Scatter plots centred on the ANS and Pog revealed that both the IOF and MF were distributed in a 45-degree fan shape in the superior quadrant (Fig 3 and 4). Specifically, 83% (191/230) of the IOF appeared in a 30- to 45-degree fan shape with a radius from 30 to 40 mm, and 98% (226/230) of the MF occupied a 45°-degree fan shape with a radius from 20 to 30 mm.

Discussion

Among the critical anatomical considerations in orthognathic surgery are the neurovascular bundles associated with the IOF and MF. While numerous anatomical studies have explored aspects such as the shape, extra openings and positions of these foramina relative to adjacent dental roots, these landmarks are not always visible during orthognathic procedures. Therefore, utilising readily available structures like ANS and Pog becomes pivotal for guiding orthognathic procedures.

In our study, the width of the IOF measured 26.4 mm, aligning with measurements from Indian (28.5 mm)[3] and Spanish (27.0 mm)[11] populations but slightly higher than the 24.7 mm reported in Lebanese subjects[7] using CBCT. Variations could possibly be due to racial differences and the measurement methods, as the authors obtained the relative value in an undefined coronal plane.[7] The mucoperiosteal flap on the labial buccal side of the anterior maxilla needs to be elevated to expose the inferior margin of the piriform aperture and the region 5 mm above the dental roots during Lefort I osteotomy.[5] It is important to highlight the potential risk of direct injury to infraorbital neurovascular

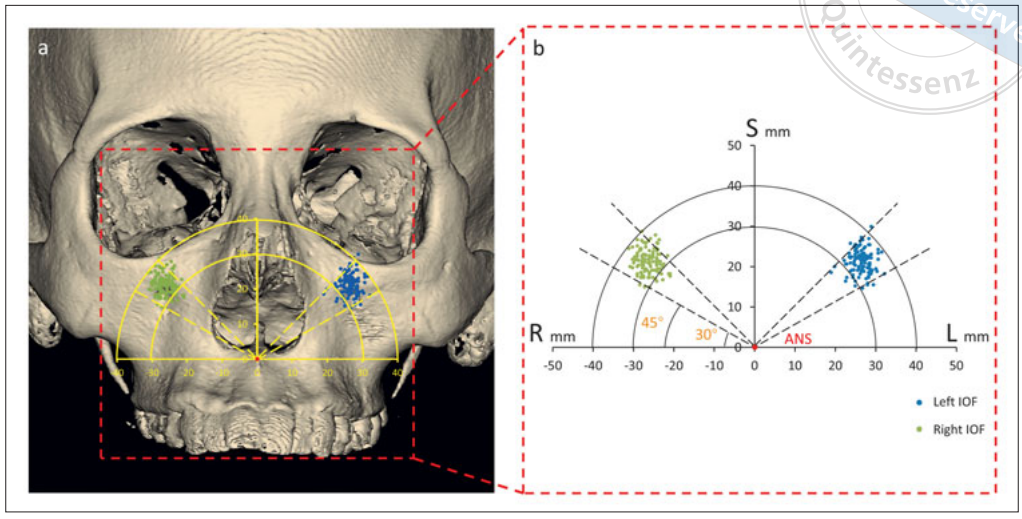

Fig 3a and b Positional relationship between the IOF and ANS. Scatter plot of the IOF relative to the ANS on the frontal projection.

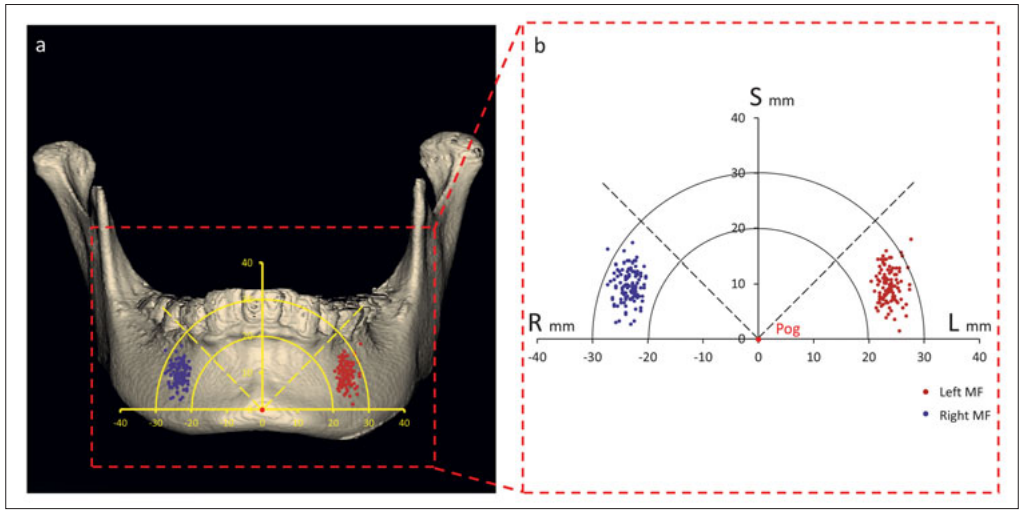

Fig 4a and b Positional relationship between the MF and the Pog. Scatter plot of the MF relative to the Pog on the frontal projection.

bundles 21.4 mm above the ANS during higher osteotomies or fixation placement, particularly in Lefort I osteotomy. Additionally, infraorbital nerve injuries, including upper lip paraesthesia, may result from traction.[2,12] Researchers have utilised the lateral marginal of the piriform aperture and the inferior rim of the orbit to locate the IOF during fracture operations.[7,8,13] A similar study, based on 518 adult crania, found that the IOF was located midway between the nasospinale and jugale[14]; however, these nearby bony landmarks might escape exposure during Lefort I osteotomy. To establish an ideal location for the IOF, we created a scatter plot diagram centred on the ANS, the most prominent identifiable hard structure in the surgical field.[15] The majority of the IOF appeared in a 30- to 45-degree fan shape in the bilateral superior quadrant, indicating that the line between the retractor and ANS should exceed 45 degrees in the mesial region and should not surpass 30 degrees in the distal region. It is advisable to follow the principle of safety when lowering the retractor, especially on the maxillary surface below the 30-degree fan shape within a 30- to 40-mm radius centred on the ANS.

The occurrence of a long-term neurosensory deficit in the lower lip has been reported to be as high as 20% after isolated genioplasty.[4] A critical intraoperative consideration is the prevention of injury, including stretching, sectioning and avulsion, to the inferior alveolar nerve adjacent to the MF. Evidence suggests that the MF is often located below the apex of the second premolar[16,17]; however, this method might not be effective in orthognathic surgery, where premolars might undergo extraction during preoperative orthodontics. In anterior mandibular orthognathic surgeries, the Pog is consistently kept exposed and intact. Hence, the present authors chose the prominent Pog as the land-

mark for MF location. In our study, the width of the MF measured 23.6 mm, aligning with cadaveric measurements ranging from 22.0 to 25.8 mm.[3,11] Understanding the width of the MF is crucial in defining safe areas in anterior mandibular subapical osteotomy. Additionally, the MF distribute in a 45-degree fan shape, with a radius ranging from 20 to 30 mm centred on the Pog, indicates the danger zone for elevating a mucoperiosteal flap. Minimising iatrogenic nerve injury caused by retractors and saws is feasible, as the MF can be well visualised and protected with atraumatic retraction after dissociation and exposure.[4]

Gupta[3] conducted a study measuring horizontal distances between the facial foramina and midline in 79 adult skulls, and found no sex difference in MF width (22.5 mm in men, 20.5 mm in women). The present study yielded a similar result, indicating that the width and height of the MF relative to Pog showed no sex difference; however, the 3D distance is approximately 0.9 mm longer in men than in women. This suggests that the hazardous area for flap elevation shows slight differences in the sagittal direction. Interestingly, the IOF tended to be located in a more inferior and medial position in women compared to men. Recognising sex differences in IOF width and height is crucial, as total disassociation of the IOF is necessary in certain surgeries, such as Le Fort II osteotomy. Additionally, the horizontal and vertical positional relationships of MF to Pog can be estimated separately based on different molar relationships and facial types, which holds significant clinical relevance. Nevertheless, the majority of IOF appeared in a 30- to 45-degree fan shape centred on ANS. Safe zones for retraction can be employed universally in adults undergoing anterior maxillary osteotomy or Le Fort I osteotomy.

The longitudinal axis passing through the IOF and MF tends to incline outwards as the horizontal distance from the IOF to ANS was 2.9 mm longer than that from the MF to Pog. The result obtained in the present study was contrary to the popular belief that the IOF and MF were situated on the same vertical plane.[3,18] This discrepancy may arise from considering the individual diameters of both foramina and obtaining values relative to the same midline.[3] In the present study, the foramina were positioned relative to adjacent prominent landmarks such as ANS and Pog, offering more valuable anatomical information, especially for individuals diagnosed with asymmetric dentomaxillofacial deformities.

Accessory foramina may exist, and injury to any branch could result in sensory defects.[6,8,19] The frequency and location of accessory foramina warrant thorough analysis and classification. Additionally, it is important to note that the present study was based on apparently normal samples. Patients with dentomaxillofacial deformities are pertinent candidates for orthognathic surgery, and these individuals might exhibit variants in bony structures.

Conclusion

During maxillary osteotomy, there is a potential risk of injuring infraorbital neurovascular bundles, specifically in procedures situated 21.40 mm above the ANS. To prevent injury to the IOF, it is crucial to minimise excessive flap retraction, especially beneath the 30-degree fan-shaped region within a radius of 30 to 40 mm centred on the ANS. The MF predominantly resides in the superior part relative to the Pog within a 45-degree fan-shaped area with a radius of 20 to 30 mm. Special attention should be paid to flap elevation in this particular region to ensure the safety of the procedure.

Conflicts of interest

The authors declare no conflicts of interest related to this study.

Author contribution

Drs Xin CHEN and Cheng TAO contributed to the data collection, analysis, manuscript draft and revision; Dr Tie Mei WANG contributed to the study design, supervision and manuscript revision.

(Received Mar 26, 2024; accepted Sep 05, 2024)

References

1. Zaroni FM, Cavalcante RC, João da Costa D, Kluppel LE, Scariot R, Rebellato NLB. Complications associated with orthognathic surgery: A retrospective study of 485 cases. J Craniomaxillofac Surg 2019;47:1855–1860.
2. McLeod NM, Bowe DC. Nerve injury associated with orthognathic surgery. Part 3: Lingual, infraorbital, and optic nerves. Br J Oral Maxillofac Surg 2016;54:372–375.
3. Gupta T. Localization of important facial foramina encountered in maxillo-facial surgery. Clin Anat 2008;21:633–640.
4. Lin HH, Denadai R, Sato N, Hung YT, Pai BCJ, Lo LJ. Avoiding inferior alveolar nerve injury during osseous genioplasty: A guide for the safe zone by three-dimensional virtual imaging. Plast Reconstr Surg 2020;146:847–858.
5. Bendrihem R, Vacher C, Fohlen A, Pelage JP. Anatomic basis of Le Fort 1 impaction osteotomy: A radiological study. Surg Radiol Anat 2017;39:1209–1214.

6. Vieira CL, Veloso SDAR, Lopes FF. Location of the course of the mandibular canal, anterior loop and accessory mental foramen through cone-beam computed tomography. Surg Radiol Anat 2018;40:1411–1417.
7. Sokhn S, Challita R, Challita A, Challita R. The infraorbital foramen in a sample of the Lebanese population: A radiographic study. Cureus 2019;11:e6381.
8. Polo CL, Abdelkarim AZ, von Arx T, Lozanoff S. The morphology of the infraorbital nerve and foramen in the presence of an accessory infraorbital foramen. J Craniofac Surg 2019;30:244–253.
9. Han YS, Lee H. The influential bony factors and vectors for predicting soft tissue responses after orthognathic surgery in mandibular prognathism. J Oral Maxillofac Surg 2018;76:1095.e1-1095.e14.
10. Chen X, Zhu J, Guo S, Hu Y, Jiang H. CBCT study on the positional relationship between marginal points of pterygomaxillary junction and anterior nasal spine. Surg Radiol Anat 2021;43:219–224.
11. Cutright B, Quillopa N, Schubert W. An anthropometric analysis of the key foramina for maxillofacial surgery. J Oral Maxillofac Surg 2003;61:354–357.
12. Karas ND, Boyd SB, Sinn DP. Recovery of neurosensory function following orthognathic surgery. J Oral Maxillofac Surg 1990;48:124–134.
13. Aziz SR, Marchena JM, Puran A. Anatomic characteristics of the infraorbital foramen: a cadaver study. J Oral Maxillofac Surg 2000;58:992–996.
14. Zdilla MJ, Koons AW, Russell ML, Mangus KR, Bliss KN. The infraorbital foramen is located midway between the nasospinale and jugale: Considerations for infraorbital nerve block and maxillofacial durgery. J Craniofac Surg 2018;29:523–527.
15. Gulses A, Oren C, Altug HA, et al. A new preoperative radiological assessment in LeFort I surgery: anterior nasal spine-sphenoidal rostrum. Oral Maxillofac Surg 2014;18:197–200.
16. Khorshidi H, Raoofi S, Ghapanchi J, Shahidi S, Paknahad M. Cone beam computed tomographic analysis of the course and position of mandibular canal. J Maxillofac Oral Surg 2017;16:306–311.
17. Goyushov S, Tözüm MD, Tözüm TF. Assessment of morphological and anatomical characteristics of mental foramen using cone beam computed tomography. Surg Radiol Anat 2018;40:1133–1139.
18. Chung MS, Kim HJ, Kang HS, Chung IH. Locational relationship of the supraorbital notch or foramen and infraorbital and mental foramina in Koreans. Acta Anat (Basel) 1995;154:162–166.
19. Ali IK, Sansare K, Karjodkar FR, Salve P. Cone beam computed tomography assessment of accessory infraorbital foramen and determination of Infraorbital Foramen Position. J Craniofac Surg 2018;29:e124–e126.

EXPERT "RECIPE MANUAL"

NEW

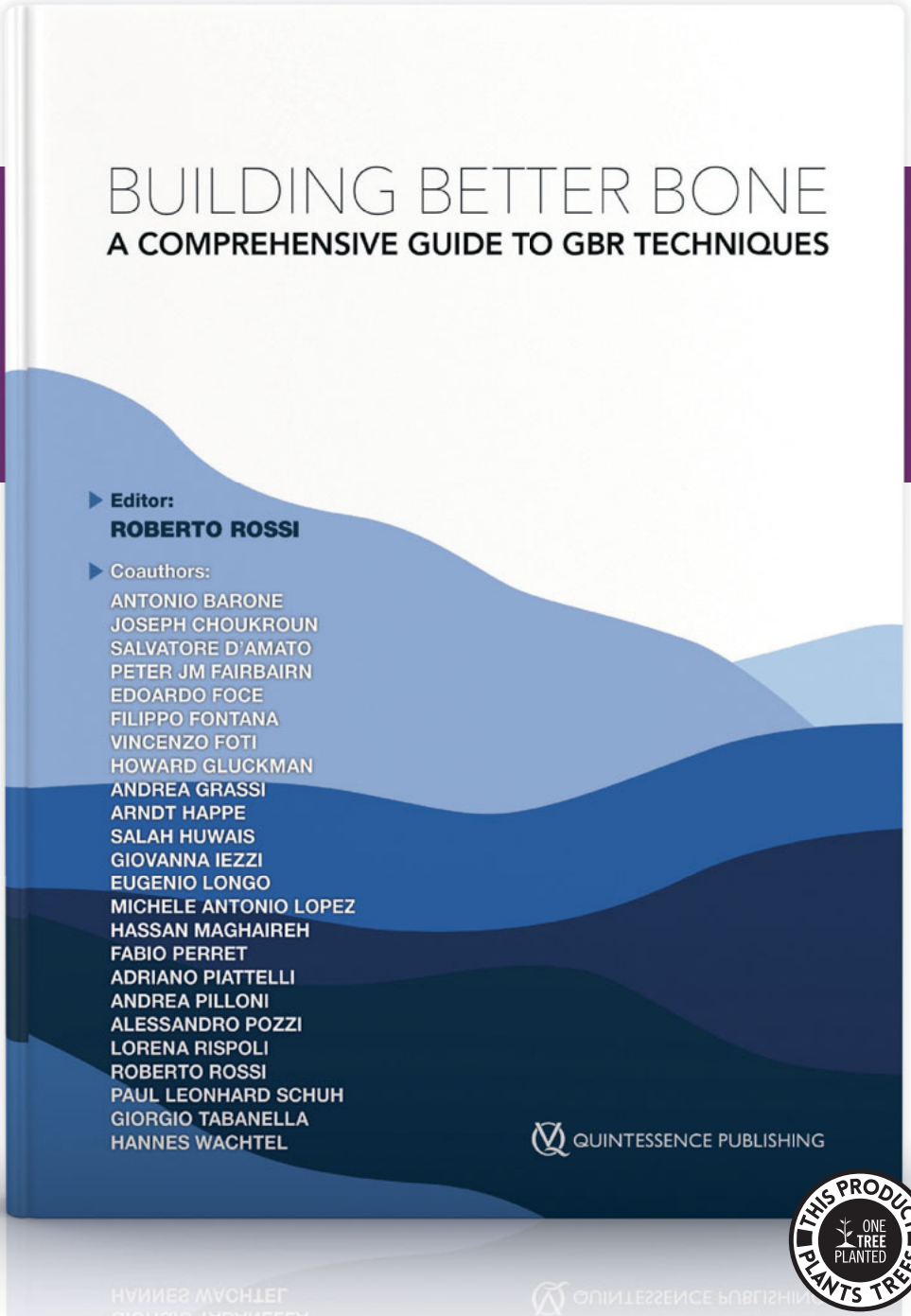

Roberto Rossi (Ed)

Building Better Bone

A Comprehensive Guide to GBR techniques

1st Edition 2024
Hardcover; incl 14 Videos, 408 pages, 1,360 illus.
ISBN 978-88-7492-096-9
€218

This book analyzes all aspects of a common problem in implant dentistry: the loss of one or more teeth, and the subsequent physiologic resorption of both hard and soft tissue. Defects resulting from tooth loss can be treated in several different ways, with similar but different surgical techniques, materials, and methods. GBR is a well-established approach with both advantages and disadvantages. Understanding how to select the optimal GBR technique ensures reduced risks for patients and clinicians alike. This book is intended to be a "recipe manual" for how to help build better bone, and includes varied protocols representing the state of the art in modern dentistry, without commercial bias. The book is also enriched by 14 videos that provide detailed explanations of the techniques adopted, and each chapter illustrates expert recommendations for optimizing the techniques presented.

www.quint.link/better-bone
books@quintessenz.de
+49 (0)30 761 80 667
QUINTESSENCE PUBLISHING

Comparison of Low-speed Drilling and Conventional Drilling in Implant Surgery: an Experimental Study

Teng Da LIU[1], Jing Jing CHEN[2], Shu Ya LI[3], Shu Hong WANG[4]

Objective: *To compare accuracy, duration of drilling and accumulation of bone chips between low-speed drilling and conventional drilling in freehand implant placement surgery.*
Methods: *The implant surgery procedures were performed using identical drill bits on pig ribs in the low-speed drilling group and the conventional drilling group. CBCT images of the preoperative implant design and postoperative implant positions were compared by using the space vector formula to calculate the angular deviation of the implants between the two groups, as well as the horizontal and vertical deviations of the implant necks and roots. The duration of the procedure was recorded, and the bone chips were collected and compared using a screening method and scanning electron microscopy.*
Results: *There were no significant differences in any of the four primary outcome variables relating to accuracy between the low-speed and conventional drilling methods. However, the results revealed that the length of the procedure differed significantly between the two groups and more large bone fragments could be collected when performing low-speed drilling.*
Conclusion: *Low-speed drilling does not affect the accuracy of implant nest preparation, but it can harvest large bone chips which may have better osteogenic activity. Low-speed drilling could be an alternative to conventional drilling.*
Keywords: *bone graft, dental implant, low-speed drilling, surgical procedure*
Chin J Dent Res 2024;27(4):319–326; doi: 10.3290/j.cjdr.b5860294

Oral implants have been proven to be more comfortable and efficient compared to other prostheses as they do not cause damage to adjacent teeth, and have become the preferred treatment option for restoring the morphology and function of missing teeth. The stability of oral implants is based on osseointegration, which is influenced by many biological and mechanical factors[1,2] and is related to primary stability.[3] Primary stability occurs immediately following placement and is a direct result of the mechanical engagement between the implant and surrounding bone,[3,4] which is influenced by several factors, including implant design, bone condition and surgical procedures.[4] During implantation, clinicians usually choose an appropriate procedure, such as simplified drilling or single bur drilling, to reduce damage while ensuring high initial stability. Conventional drilling initiated with a small-diameter drill before moving on to larger-diameter drills is the most common method, for which the drilling speed is approximately 1000 rpm,[5] depending on the implant system. The procedure must be carried out with irrigation throughout the implant bed preparation.

A novel technique referred to as low-speed drilling, and also known as biological drilling (50 to 100 rpm) without irrigation, has recently been proposed as an alternative to conventional drilling. It has been confirmed that this procedure will not make the temperature rise to 47°C without irrigation,[1,6-8] which will not

1 Zhejiang Chinese Medical University, Hangzhou, Zhejiang Province, P.R. China.
2 Shulan (Hangzhou) Hospital, Hangzhou, Zhejiang Province, P.R. China.
3 Jincheng General Hospital, Jincheng, Shanxi Province, P.R. China.
4 Shanghai Songjiang District Central Hospital, Shanghai, P.R. China.

Corresponding author: Dr Shu Hong WANG, Department of Stomatology, Shanghai Songjiang District Central Hospital, Shanghai 201699, P.R. China. Tel: 86-18018577881. Email: wangshh@126.com

This work was supported by the Three-Year Action Plan for Public Health System Construction in Songjiang District, Shanghai (SJGW6-29), the Hospital Project of Songjiang District Central Hospital, Shanghai (2023YJA-7), and the Science and Technology Tackling Key Theme Project in Songjiang District (22SJKJGG71).

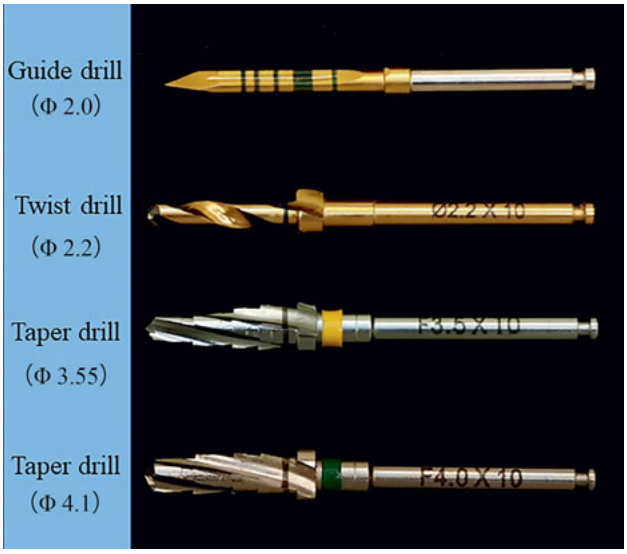

Fig 1 The drills used in the experiment.

cause thermal damage to the bone.[9-11] Additionally, it has no impact on osseointegration or bone loss around implants.[1,12-14] Eliminating the need for irrigation with saline can improve the operator's field of vision and avoid washing away cells, proteins and other soluble substances that play an important role in bone regeneration.[15,16] This process can preserve the autogenous bone graft and maximally restores its osteogenic ability, which is better than conventional drilling with regard to bone regeneration.[16-19] Additionally, the autogenous bone collected during the procedure can be used for bone augmentation to avoid the need for a second surgical site and reduce the use of bone substitutes, thereby also reducing the economic burden on patients. Furthermore, lower drilling speeds can produce greater drilling forces and torques, which can prevent excessive sideways force and minimise the risk of drill bit breakage.[20] Moreover, low-speed drilling without irrigation may provide greater comfort for patients and causes less postoperative pain and inflammation than conventional drilling.[21] These advantages seem to demonstrate that low-speed drilling is superior to other methods.

However, to the best of the present authors' knowledge, there is a lack of evidence regarding the accuracy of implant placement using low-speed drilling. Hence, the aim of this study was to evaluate the accuracy of low-speed drilling and conventional drilling. The secondary aim was to compare the procedure duration and bone chip accumulation.

Materials and methods

The experiments were designed according to a protocol that had been given ethical approval by the Ethics Committee of Shanghai Songjiang District Central Hospital.

Model selection and preparation

Pig ribs obtained from the butcher with a cortical thickness of approximately 2 mm were obtained, and a CBCT scan of each rib was taken before surgery to confirm that an implant (4.2 mm in diameter and 10 mm in length) could be inserted and only penetrated through one layer of cortical bone. The ribs that met the requirements were soaked in sterile normal saline.

DICOM files of the preoperative CBCT scans were imported into the implant planning software (Simplant Pro 17.0, Dentsply Sirona, Charlotte, NC, USA). A group member planned the 3D positions of each intended implant site and changed the implant type to TSIII (4.2 × 10 mm) (Osstem, Seoul, South Korea). The implant templates were manufactured through 3D printing according to the manufacturer's instructions.

Model surgery and deviation detection

All surgical procedures were carried out by a dental postgraduate student (TDL). In order to match the implant models, the surgical procedures were performed using a Taper KIT (Osstem) (Fig 1). The implant sites were located using the implant template and marked with a guide drill at a speed of 800 rpm with irrigation, and the depth of marks was 2.0 mm. Meanwhile, some signposts were placed parallel to the previously planned axis of the implant to indicate the direction (Fig 2). A total of 60 sites were randomly divided into two groups, and different technical conditions (Table 1) were used for each group without a guide template.

The duration of the procedure was recorded for each step. Bone chips generated using low-speed drilling accumulated on the drill surface and near the implantation sites, which could be collected directly; however, the irrigation when using conventional drilling caused difficulty in bone collecting, so bone collection needed to be performed by the surgical assistant.

After the surgery was completed, a postoperative CBCT scan was taken and the data were output as a DICOM file to build the model using Mimics 21. 0 (Materialise, Leuven, Belgium). The virtual preoperative implant positions and the actual postoperative positions were uploaded to Simplant Pro 17.0 and superimposed by manually matching at least three previously made marks.

Table 1 The rotary speed of each drill in model surgery.

Drilling protocol	Guide drilling (φ2.00)	Twist drill (φ 2.20)	Taper drill (φ3.55)	Taper drill (φ4.10)
Low-speed	800 rpm	50 rpm	50 rpm	50 rpm
Conventional	800 rpm	800 rpm	800 rpm	800 rpm

The planned and actual implant positions were represented by the neck centre point and root centre point in spatial coordinates, and each point was measured three times. Lateral neck deviations, lateral apex deviations and vertical apex deviations were calculated according to the distance formula ($d = |a*b|/|a|$), and angular deviations (Fig 3) were calculated according to the vectorial angle formula ($\text{Cos}\theta = a*b/(|a|*|b|)$), and other mathematical methods were used to decrease the measurement error.

Histomorphometric and quantitative analysis of bone chips

After preparation, the bone chips generated in the two groups were collected individually and fixed in 4% paraformaldehyde for 2 days. Following serial dehydration with graded ethanol, the samples were dried using a critical point drier. An electronic balance was employed to measure the dry weight of the samples.

The histomorphometric analysis of bone chips was performed using a sieving method and a scanning electron microscope (SEM). The 30 sites of bone chips collected by low-speed drilling were merged and then screened using sieves with diameters of 200, 400 and 600 μm. The bone chips in both groups were divided into three subgroups: bone chips with sizes of 200 to 400, 400 to 600 and > 600 μm. Almost no chips passed through the 200-mm diameter sieve. The overall weight and the dry weight of each part were measured and recorded. The bone chips gathered using conventional drilling were analysed in the same way.

In the following days, the samples were sputter-coated and analysed microscopically using an SEM (HITACHI, Tokyo, Japan) to determine size variations. The SEM images at ×30 for each group were analysed using ImageJ software (National Institutes of Health, Bethesda, MD, USA). To be defined as "chips", the observed bone particles had to display clear boundaries. Thirty chips from each group were chosen and the projection area and Feret diameter were measured to indicate their size.

Since it was difficult to collect chips when using conventional drilling, a trephine drill (ChengDuPeiYang, Sichuan, China) with an inner diameter of 3 mm and an outer diameter of 4 mm and which had the same depth of preparation was used for the control group for comparison with low-speed drilling (Fig 4). The dry weight of bone blocks generated using a trephine drill were also measured using electronic balance.

Fig 2 The signpost in the rib that served as an indication of nearby implantation sites.

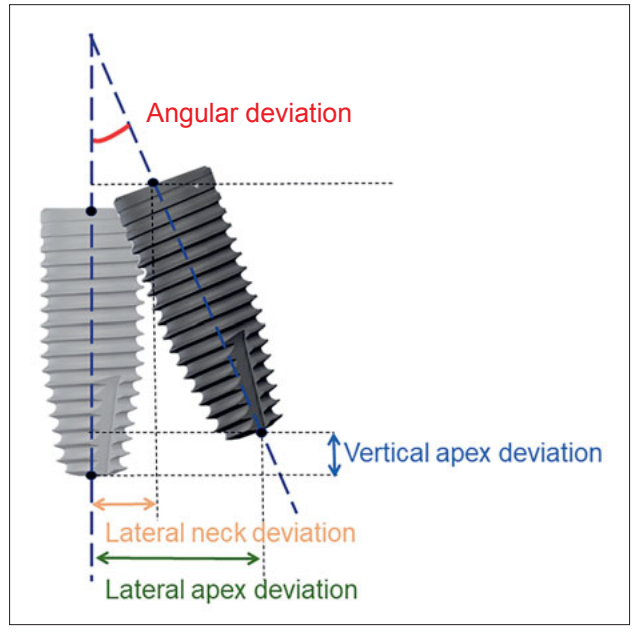

Fig 3 Illustration depicting the method of deviation measurement.

Fig 4 The trephine bur used in the experiment.

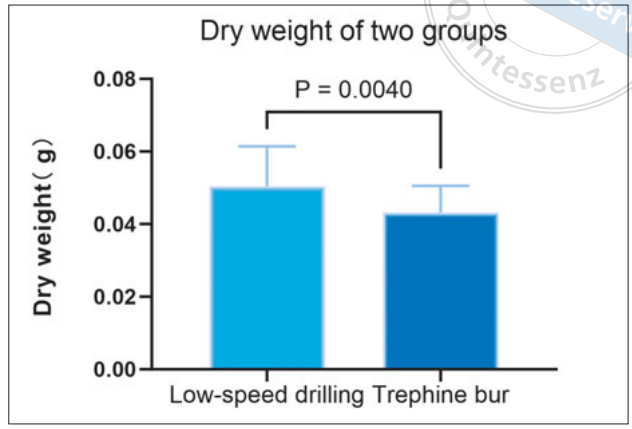

Fig 5 Bar charts representing the dry weight of two technologies.

Table 2 Descriptive statistics (means ± standard) and p-values of the deviation.

3D deviation	Low-speed drilling	Conventional drilling	t (Z)	*P* value
Lateral neck deviation	0.594 ± 0.442	0.590 ± 0.319	0.042	0.967
Lateral apex deviation	1.204 ± 0.556	1.087 ± 0.538	0.829	0.410
Vertical apex deviation	0.474 ± 0.291	0.640 ± 0.354	−1.982	0.052
Angular deviation	5.566 ± 1.964	4.871 ± 2.194	1.293	0.201

Table 3 Procedure time data, mean ± SD. All drilling protocols were repeated 15 times.

Drilling protocol	Final diameter (mm)	Mean ± SD(s)
Low-speed	φ2.2	6.721 ± 1.263
	φ3.5	8.776 ± 1.409
	φ4.0	5.029 ± 1.193
	Total time	20.526 ± 3.009
Conventional	φ2.2	4.153 ± 0.621
	φ3.5	3.692 ± 0.578
	φ4.0	2.865 ± 0.430
	Total time	10.710 ± 1.155

Statistical analyses

Statistical analyses were performed using IBM SPSS 25 (IBM, Armonk, NY, USA). The normality of the data was assessed using histograms and a Shapiro-Wilk test. All data that were normally distributed were compared using an independent samples *t* test, and the rest were compared using a Mann-Whitney U-test.

Results

Precision of the 3D position

In this study, a total of 60 implant surgery procedures were performed on the models: 30 in the low-speed drilling group and 30 in the conventional drilling group. There were no significant differences between the two groups for any of the four primary outcome variables ($P > 0.05$) (Table 2).

Duration of the procedure

The results of the analysis of the duration of the procedure are presented in Table 3. The total duration in the low-speed drilling group was 20.526 ± 3.009 seconds (95% confidence interval [CI] −19.402 to 21.649), whereas that in the conventional drilling group was 10.710 ± 1.155 seconds (95% CI −10.279 to 11.141), which was significantly different ($P < 0.001$).

Accumulation of bone chips

Despite having an assistant to help with bone collection in the conventional drilling group, the collection tended to be less efficient. The dry weight of bone chips was far less than that in the low-speed drilling group. Due to the difficulty in collecting bone chips generated during conventional drilling, a trephine drill was selected for the control group for further evaluation of the bone collecting ability of low-speed drilling. There was a significant difference in the dry weight of the bone chips between the control group (0.0431 ± 0.0074 g, 95% CI −0.0407 to 0.0460) and the low-speed drilling group (0.0504 ± 0.0109 g, 95% CI −0.0463 to 0.0545) ($P = 0.004$). The weight of the chips was greater in the low-speed drilling group (Fig 5).

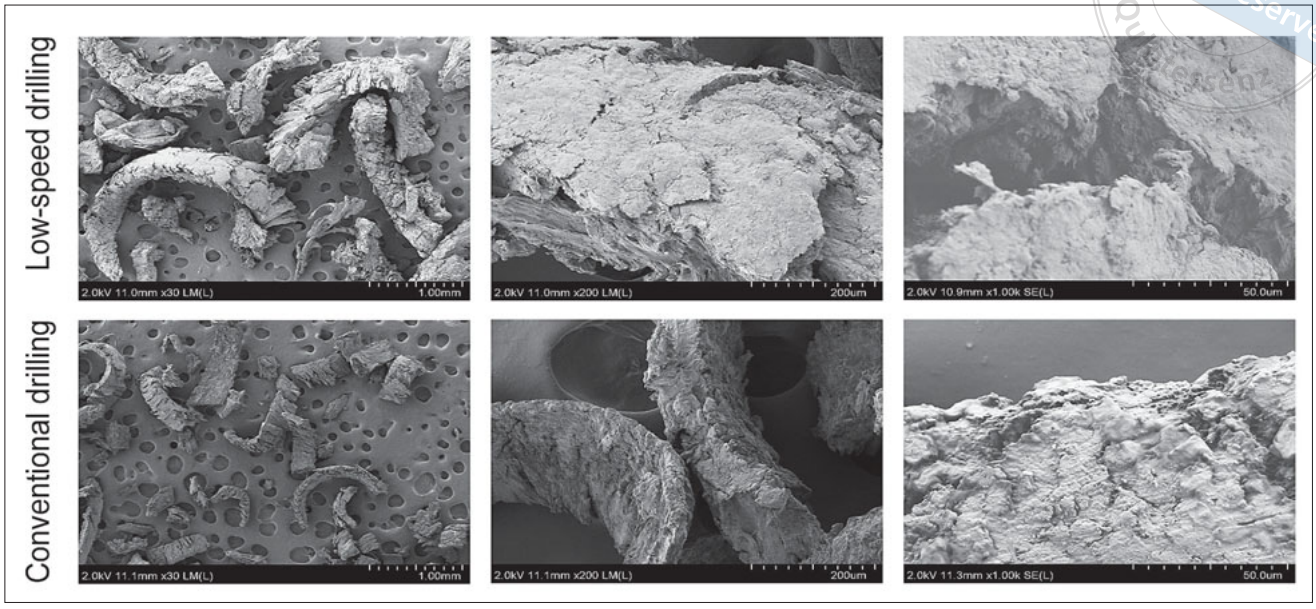

Fig 6 SEM analysis of bone particles harvested by two techniques. The bone particles produced by low-speed drilling were larger than the particles produced by conventional drilling.

Table 4 Characterisation of the average projection area and Feret diameter of bone chips.

Drilling protocol	Area (mm^2, mean ± SD)	Feret diameter (mm, mean ± SD)	Z	*P* value
Low-speed	0.780 ± 0.247	0.154 ± 0.142	−6.446	< 0.001
Conventional	1.769 ± 0.256	0.677 ± 0.313	−6.594	< 0.001

Size of bone chips

SEM analysis of the samples produced by conventional drilling revealed square and rectangular chips. The low-speed drilling samples displayed larger, rectangular chips (Fig 6). The bone chips produced by low-speed drilling were larger than those produced by conventional drilling ($P \leq 0.001$) (Table 4). The large bone chips accounted for a large proportion of the low-speed drilling group, with the percentage of bone chips > 600, 400 to 600, and 200 to 400 μm being 39.1%, 41.2% and 19.7%, respectively. The percentages for the conventional group at > 600, 400 to 600 and < 200 μm were 48.2%, 23.4% and 28.4%, respectively.

Discussion

To confirm whether low-speed drilling without irrigation was safe, the temperature change during drilling was measured using a digital infrared camera and thermocouple.[9-11,22] After ensuring that low-speed drilling did not cause thermal damage, the researchers conducted animal experiments and found that there were no significant differences in crestal bone loss (CBL) or bone–implant contact (BIC) between implants placed via low-speed drilling and those placed via conventional drilling.[1,23] Furthermore, Pellicer-Chover et al[12] and Tabassum et al[13] used low-speed drilling in clinical trials and found no apparent difference in bone loss around the implants between low-speed drilling and conventional drilling after a 12-month follow-up. Low-speed drilling was applied to prepare the sockets for autogenous tooth transplantation, and after a 7-year follow-up, the transplanted teeth remained stable.[24] Low-speed drilling also may provide improved primary stability and cause less postoperative pain and inflammation.[23,25] It appears that low-speed drilling has no impact on the long-term success rate of implants.

To the best of the authors' knowledge, this is the first study evaluating the accuracy of implant preparation using low-speed drilling. In this study, four primary outcome variables were chosen to compare the accuracy between two methods. However, no improvements in accuracy were observed when low-speed drilling was used for preparation compared to conventional drilling, which was inconsistent with the findings of other studies.[26] There are several likely reasons for this discrepancy. First, bone chips that accumulate near implantation sites can interfere with the observa-

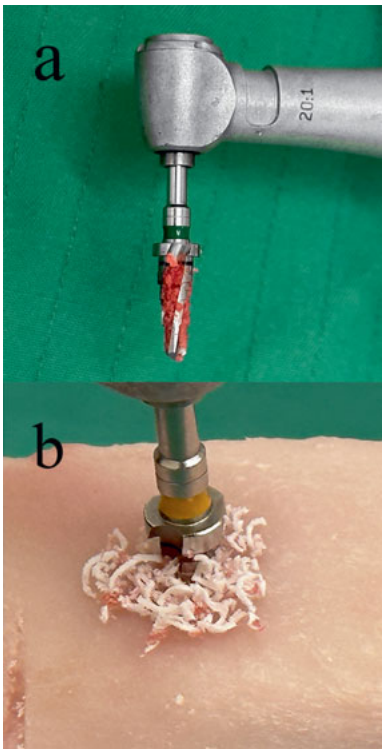

Fig 7 Bone particles accumulate on the drill's surface **(a)** or near the implantation sites **(b)**.

tion of length marks and affect depth control during preparation (Fig 7). Second, the inadequate cutting capability requires operators to apply additional axial force, which increases the risk of the drill slipping and affecting direction. Third, a reduction in rotation speed may affect drill stability. The basic theory behind the design of the tri-spade drill was the inherent stability and self-centring of a tripod.[27] However, as the rotation speed decreases, the chip escape rate and stability decrease accordingly. This could also explain why the operator experienced sideways forces while drilling. Nevertheless, most of these reasons were speculative and largely related to the design of the drills. Further investigation is required to determine whether drills designed specifically for low-speed drilling can improve accuracy during implant bed preparation.

Other differences between low-speed drilling and conventional drilling were also compared in this study. From the perspective of process time, the procedure time of low-speed drilling is approximately 1.9 times that of conventional drilling, which is similar to the finding of Calvo-Guirado et al.[1] The procedure time may be related to bone density and the design of the drill, both of which need further study. Although this approach prolongs the operation time, it provided greater comfort for patients because they did not experience a drowning sensation.[21]

During preparation by low-speed drilling, bone chips accumulate near the implantation sites and on the drill surface (Fig 7), which are heavier than the chips harvested by a trephine bur. Moreover, irrigation during conventional drilling makes it difficult to collect bone debris and leads to bone loss. Therefore, compared to the other two technologies, the slow-speed technique not only provides advantages in bone harvesting but also may avoid a second surgical site when facing small and medium-sized bone defects.

When examining samples under a microscope, Ozcan et al[25] discovered that conventional drilling causes more damage to cancellous bone than low-speed drilling, resulting in bleeding and bone marrow disruption, but there were no significant differences in the morphology of the cortical bone cutting surfaces. As yet, no research has been conducted into whether the method could influence the generation of bone chips. Scholars found that the bone chips harvested by low-speed drilling had better osteogenic potential than conventional drilling, ultrasonic osteotomy and other bone harvesting technologies.[16,17] The size of bone chips is important for osteogenic activity. A clinical study showed that large bovine-derived bone chips (1 to 2 mm) generated a 1.4 times higher volume in sinus augmentation than smaller granules (0.25 to 1 mm).[28] The area and Feret diameter measured in SEM images show that the size of bone chips harvested by low-speed drilling were significantly larger. According to the results of the screening method, 80.3% of the chips collected in the low-speed drilling group and 71.6% of the chips collected in the conventional drilling group were > 400 μm in length, but the proportion that was > 600 μm in length was larger when using conventional drilling. However, according to the result of the SEM method, the Feret diameter of low-speed drilling was much larger than 600 μm. The difference between the two methods was probably due to the fact that the result of the screening method was influenced by the oblong shape of bone chips. Although the volume of the chips was larger, they can pass through small diameter voids because of their slender shape. Therefore, the result of the SEM analysis was extremely serious. In general, low-speed drilling also made it possible to harvest more large bone chips, which may improve bone regeneration and repair.

Finally, this in vitro study is not free of limitations. A major limitation was that the drills used were not designed for low-speed drilling, which could obscure the superiority of this technology. In addition, dead pig ribs can be used to simulate human anatomy, but pig ribs are weaker than the human mandible, which may

affect the results despite the thickness of the cortical bone being homogeneous. Furthermore, all procedures were performed by one experienced operator. Different results might be found by other investigators according to their level of experience.

Conclusion

According to the results of this study and its limitations, low-speed drilling has no influence on the accuracy of implant nest preparation, which may be increased by changing the drill design. Compared to conventional drilling, it offers advantages in terms of bone harvesting, as more and larger bone chips can be collected and osteogenic ability can be maximally restored. It can also reduce the consumption of bone substitutes to alleviate the economic burden on patients. Thus, the authors believe that low-speed drilling has the potential to be an alternative to current methods, and the characteristics of the drill should be further studied to develop a design that suits this technology and expands its advantages.

Conflicts of interest

The authors declare no conflicts of interest related to this study.

Author contribution

Dr Teng Da LIU contributed to the conceptualisation, methodology, project administration and manuscript draft; Drs Jing Jing CHEN and Shu Ya LI contributed to the software data analysis; Dr Shu Hong WANG contributed to the methodology, supervision of the study and revision of the manuscript.

(Received April 08, 2024; accepted Aug 12, 2024)

References

1. Calvo-Guirado JL, Delgado-Peña J, Maté-Sánchez JE, Mareque Bueno J, Delgado-Ruiz RA, Romanos GE. Novel hybrid drilling protocol: evaluation for the implant healing--thermal changes, crestal bone loss, and bone-to-implant contact. Clin Oral Implants Res 2015;26:753–760.
2. Guglielmotti MB, Olmedo DG, Cabrini RL. Research on implants and osseointegration. Periodontol 2000 2019;79: 178–189.
3. Monje A, Ravidà A, Wang HL, Helms JA, Brunski JB. Relationship between primary/mechanical and secondary/biological implant stability. Int J Oral Maxillofac Implants 2019(suppl);34:s7–s23.
4. Al-Sabbagh M, Eldomiaty W, Khabbaz Y. Can osseointegration be achieved without primary stability? Dent Clin North Am 2019;63:461–473.
5. Su YC. Implant Dentistry. Beijing: People's Medical Publishing House, 2014.
6. Jamil M, Rafique S, Khan AM, et al. Comprehensive analysis on orthopedic drilling: A state-of-the-art review. Proc Inst Mech Eng H 2020;234:537–561.
7. Tsiagadigui JG, Ndiwe B, Ngo Yamben MA, Fotio N, Belinga FE, Njeugna E. The effects of multiple drilling of a bone with the same drill bit: thermal and force analysis. Heliyon 2022;8:e08927.
8. Bernabeu-Mira JC, Pellicer-Chover H, Peñarrocha-Diago M, Peñarrocha-Oltra D. In vitro study on bone heating during drilling of the implant site: Material, design and wear of the surgical drill. Materials (Basel) 2020;13:1921.
9. Oh JH, Fang Y, Jeong SM, Choi BH. The effect of low-speed drilling without irrigation on heat generation: an experimental study. J Korean Assoc Oral Maxillofac Surg 2016;42:9–12.
10. Jang HJ, Yoon JU, Joo JY, Lee JY, Kim HJ. Effects of a simplified drilling protocol at 50 rpm on heat generation under water-free conditions: an in vitro study. J Periodontal Implant Sci 2023;53:85–95.
11. Delgado-Ruiz RA, Velasco Ortega E, Romanos GE, Gerhke S, Newen I, Calvo-Guirado JL. Slow drilling speeds for single-drill implant bed preparation. Experimental in vitro study. Clin Oral Investig 2018;22:349–359.
12. Pellicer-Chover H, Peñarrocha-Oltra D, Aloy-Prosper A, Sanchis-Gonzalez JC, Peñarrocha-Diago MA, Peñarrocha-Diago M. Comparison of peri-implant bone loss between conventional drilling with irrigation versus low-speed drilling without irrigation. Med Oral Patol Oral Cir Bucal 2017;22: e730–e736.
13. Tabassum A, Kazmi F, Wismeijer D, Siddiqui IA, Tahmaseb A. A prospective randomized clinical trial on radiographic crestal bone loss around dental implants placed using two different drilling protocols: 12-month follow-up. Int J Oral Maxillofac Implants 2021;36:e175–e182.
14. Tabassum A. Radiographic comparisons of crestal bone levels around implants placed with low-speed drilling and standard drilling protocols: Preliminary results. Saudi Dent J 2021;33:965–971.
15. Chen CH, Coyac BR, Arioka M, et al. A novel osteotomy preparation technique to preserve implant site viability and enhance osteogenesis. J Clin Med 2019;8:170.
16. Liang C, Lin X, Wang SL, Guo LH, Wang XY, Li J. Osteogenic potential of three different autogenous bone particles harvested during implant surgery. Oral Dis 2017;23:1099–1108.
17. Tabassum A, Wismeijer D, Hogervorst J, Tahmaseb A. Comparison of proliferation and differentiation of human osteoblast-like cells harvested during implant osteotomy preparation using two different drilling protocols. Int J Oral Maxillofac Implants 2020;35:141–149.
18. Saulacic N, Bosshardt DD, Jensen SS, Miron RJ, Gruber R, Buser D. Impact of bone graft harvesting techniques on bone formation and graft resorption: a histomorphometric study in the mandibles of minipigs. Clin Oral Implants Res 2015;26:383–391.
19. Anitua E, Troya M, Zalduendo M, Flores J, Tierno R, Alkhraisat MH. The influence of alveolar bone healing degree on its potential as a source of human alveolar bone-derived cells. Ann Anat 2020;232:151578.
20. Alam K, Qamar SZ, Iqbal M, et al. Effect of drill quality on biological damage in bone drilling. Sci Rep 2023;13:6234.

21. Bernabeu-Mira JC, Peñarrocha-Diago M, Peñarrocha-Diago M, Romero-Gavilán F, Camacho-Alonso F, Peñarrocha-Oltra D. Comparison of patient-centered outcomes measures between low-speed drilling without irrigation and high-speed drilling with irrigation: A randomized clinical trial. Clin Oral Implants Res 2024;35:21–30.
22. Kim SJ, Yoo J, Kim YS, Shin SW. Temperature change in pig rib bone during implant site preparation by low-speed drilling. J Appl Oral Sci 2010;18:522–527.
23. Fujiwara S, Botticelli D, Kaneko N, Urbizo Velez J, Tumedei M, Bengazi F. Effect of low-speed drilling without irrigation on osseointegration: an experimental study in dogs. Oral Maxillofac Surg 2022;26:595–601.
24. Anitua E, Piñas L, Alkhraisat MH. A novel technique for preparation of recipient site and autologous bone grafting in autotransplantation of single-rooted teeth: A report of two cases. Cureus 2022;14:e31888.
25. Ozcan M, Salimov F, Temmerman A, Turer OU, Alkaya B, Haytac MC. The evaluation of different osteotomy drilling speed protocols on cortical bone temperature, implant stability and bone healing: An experimental study in an animal model. J Oral Implantol 2022;48:3–8.
26. Soler-Alcaraz S, Guerrero-Sánchez Y, Pérez-Sayáns M, Bernabeu-Mira JC, Peñarrocha-Oltra D, Camacho-Alonso F. Evaluation of change in radiographic fractal dimension around dental implants placed with low-speed drilling and standard drilling protocols. J Clin Med 2023;12:2244.
27. Oh HJ, Kim BI, Kim HY, Yeo IS, Wikesjö UM, Koo KT. Implant drill characteristics: Thermal and mechanical effects of two-, three-, and four-fluted drills. Int J Oral Maxillofac Implants 2017;32:483–488.
28. Yamada M, Egusa H. Current bone substitutes for implant dentistry. J Prosthodont Res 2018;62:152-161.

Prevalence and Characteristics of Taurodontism in Patients with Cleft Lip and Palate Compared to the Healthy Group: a CBCT Study

Fatemeh AKBARIZADEH[1], Mohammad PORDEL[2], Maryam PAKNAHAD[3]

Objective: *To investigate the prevalence and characteristics of taurodontism in patients with cleft lip and palate (CLP) and clarify the relationship between CLP and the frequency and severity of taurodontism.*

Methods: *CBCT scans of 30 patients with bilateral CLP (BCLP), 70 with unilateral CLP (UCLP) and 70 healthy individuals were taken for investigation. In each group, the first and second molars were assessed for the presence of taurodontism. In taurodontic teeth, the severity of taurodontism was measured and classified based on the taurodontic index (TI). The frequency and severity of taurodontism were compared between the three groups.*

Results: *Taurodontism was significantly higher in patients with CLP ($P < 0.001$), and its prevalence was significantly higher in patients with BCLP than those with UCLP ($P = 0.003$) and the control group ($P < 0.001$). There was no difference among the three groups regarding the severity of taurodontism. Additionally, the frequency of taurodontism in the second molars was significantly higher than that in the first molars in the control group ($P = 0.019$).*

Conclusion: *Based on this investigation, clinicians should be aware of the possible complications that may occur when performing dental procedures on patients with BCLP and UCLP due to the higher incidence of taurodontism in these patients.*

Keywords: *CBCT, cleft lip and palate, taurodontism*

Chin J Dent Res 2024;27(4):327–332; doi: 10.3290/j.cjdr.b5860295

Cleft lip and palate (CLP) is considered the most prevalent congenital anomaly developed in the craniofacial region, with a global frequency of 0.45 in every 1,000 newborns.[1] Patients suffer from several functional, psychological and aesthetic problems.[2,3] Dental anomalies are frequent in CLP patients, including missing, hypoplastic or supernumerary teeth, enamel hypoplasia and taurodontism.[4,5]

One of the most prominent dental anomalies that accompanies CLP is taurodontism, or bull-shaped teeth. Taurodontism is the apico-coronal enlargement of the pulp chamber with apical displacement of bifurcation or trifurcation areas of the root.[6] Taurodontic teeth, with their abnormal morphology, affect periodontal, surgical, prosthetic and endodontic treatment planning, as they are characterised by vertically elongated pulp chambers, apically displaced furcation areas, short roots and a lack of cervical constriction.[7,8] Taurodontism is classified based on a well-known radiographic index, the Taurodontic Index (TI), into three main groups: hypotaurodontism, mesotaurodontism and hypertaurodontism.[9] The least severe of these according to this scale is hypotaurotontism, whereas hypertaurodontism is considered the most severe type.[8]

Few studies have assessed the risk of incidence of taurodontism in patients with CLP compared to

1 Department of Oral and Maxillofacial Radiology, School of Dentistry, Shiraz University of Medical Sciences, Shiraz, Iran.
2 Student Research Committee, School of Dentistry, Shiraz University of Medical Sciences, Shiraz, Iran.
3 Oral and Dental Disease Research Center, Department of Oral and Maxillofacial Radiology, School of Dentistry, Shiraz University of Medical Sciences, Shiraz, Iran.

Corresponding author: Dr Maryam PAKNAHAD, Oral and Maxillofacial Radiology Department, Shiraz Dental School, Ghasrodasht Street, Shiraz 7144833586, Iran. Tel: 98-711-2292680. Email: paknahadmaryam@yahoo.com

This study was supported by the School of Dentistry, Shiraz University of Medical Sciences (SUMS), Shiraz, Iran.

unaffected individuals in various populations.[4,10-13] According to the current literature,[4,12] the frequency of taurodontism in patients with CLP varies widely among different populations, ranging from 18.2% to 71.05%.

Moreover, the accuracy of radiographic techniques can greatly impact the outcomes and investigations, which should be considered carefully. Previously published research on the epidemiological characteristics of taurodontism is mostly based on panoramic[14,15] or other conventional radiographic examinations.[16] It has been observed that many taurodontic teeth go undiagnosed even after using conventional two-dimensional (2D) radiography because of its well-known disadvantage of superimposition, especially in maxillary teeth.[8] On the other hand, the application of CBCT, as a viable 3D modality, can be helpful in diagnosis, classification, accurate measurement and the planning of treatment of taurodontism.[4]

To the best of the present authors' knowledge, there are only two studies evaluating the frequency of taurodontism in patients with CLP using CBCT.[4,10] Therefore, the aim of the present study was to compare the frequency and severity of taurodontism in patients with bilateral CLP, unilateral CLP, and healthy individuals using CBCT imaging.

Materials and methods

Study design

This retrospective study was performed on CBCT images of 170 subjects (87 women, 83 men), including 70 with UCLP (37 women, 33 men) and 30 with BCLP (17 women, 13 men), as well as 70 control subjects (33 women, 37 men) who met the eligibility criteria. The sample size was calculated according to the following formula:

$$n = \frac{\left(Z_{1-\alpha/2} + Z_{1-\beta}\right)^2 [P_1(1-P_1) + P_2(1-P_2)]}{(P_1 - P_2)^2}$$

Assuming α = 0.05 and power = 80%, with the use of the above formula, the sample size was calculated as 70 subjects per group. The age range of the participants was between 18 to 67 years. This study was approved by the institutional research committee (IR.SUMS.DENTAL.REC.1401.100). The criterion for inclusion of patients in the CLP and control groups was the presence of fully developed permanent molars. The high-quality images that showed both arches were included. Patients with extensive caries, restorations or crowns and who had undergone endodontic treatment of first and/or second permanent molars were excluded from the study. Finally, the patients were categorised into the UCLP, BCLP and control groups. All participants signed an informed consent so that their anonymous data could be used in further research.

Radiographic assessment of taurodontism

CBCT images were taken using the VGi EVO NNT imaging system (NewTom, Imola, Italy) at 0.3 mm voxel size, 110 kVp, 7.56 mAS, and a standard field of view. To assess the intergroup observer reliability, a dentistry student and an oral and maxillofacial radiologist measured the variables of every CBCT scan separately. Two weeks later, 20% of the studied images were randomly chosen for reassessment to evaluate the intragroup observer reliability of the measurements. To quantitatively assess the inter- and intragroup observer reliability of the outcomes, the Kappa coefficient was estimated for each variable. The diagnosis of taurodontism was based on the TI, which was proposed by Shifman and Chananel.[17] To determine TI, the present authors measured two variables. Variable 1 was the distance from the lowest point of the roof of the pulp chamber to the highest point of the floor of the pulp chamber, whereas variable 2 was the distance from the lowest point of the roof of the pulp chamber to the apex of the longest root. Then variable 1 was divided by variable 2 and multiplied by 100.

The teeth were categorised as being affected by hypotaurodontism if TI was 20% to 30%, mesotaurodontism if it was 30% to 40% and hypertaurodontism if it was 40% to 75% (Fig 1). All measurements and calibrations were performed using the digital scale provided by NewTom NNT software. The presence and severity of taurodontism in eight molar teeth of each subject were assessed in the BCLP, UCLP and control groups.

Statistical analysis

All the obtained values were restored and measured in SPSS (version 26; IBM, Armonk, NY, USA). A chi-square test was used to compare the frequency and severity of taurodontism in the three studied groups. The prevalence of taurodontism between the three groups regarding laterality, tooth number and arch was evaluated. The confidence interval (CI) of 95% and $P < 0.05$ were considered as the level of statistical significance.

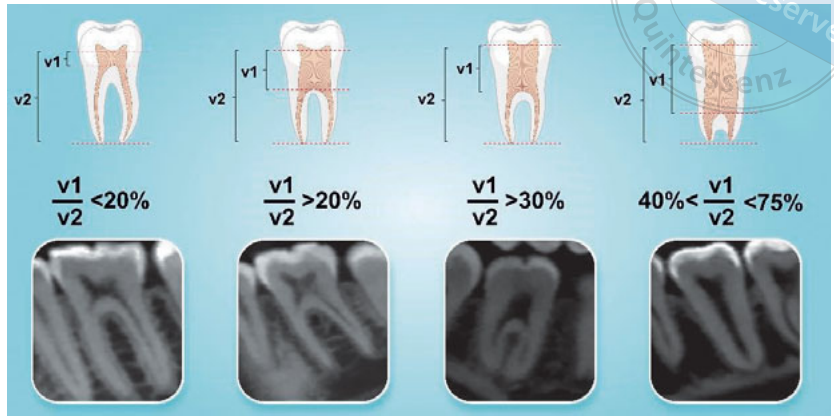

Fig 1 Classification of taurodontism in the CBCT images.

Table 1 Comparison of the frequency of taurodontism in different subtypes of CLP.

	BCLP, n (%)	UCLP, n (%)	Control group, n (%)	*P* value
Taurodontism	48 (41.88%)[a,b]	91 (26%)[a,c]	51 (12.57%)[b,c]	< 0.001*
Normal teeth	69 (58.11%)	259 (74%)	345 (87.12%)	

*Statistically significant.
a, statistically significant difference between the BCLP and UCLP groups ($P = 0.003$); b, statistically significant differences between the BCLP and control groups ($P < 0.001$); c, statistically significant differences between the UCLP and control groups ($P < 0.001$)

Table 2 Comparison of the frequency of occurrence different types of taurodontism among groups

Type of taurodontism	BCLP, n (%)	UCLP, n (%)	Control group, n (%)	*P* value
Hypotaurodontism	117 (81.25%)	78 (85.71%)	45 (88.23%)	0.879
Mesotaurodontism	7 (14.58%)	11 (12.08%)	5 (9.80%)	
Hypertaurodontism	2 (4.16%)	2 (2.19%)	1 (1.96%)	

Table 3 Comparison of the frequency of taurodontism between first and second molars in the CLP and control groups

	BCLP group		UCLP group		Control group	
	1st molar (%)	2nd molar (%)	1st molar (%)	2nd molar (%)	1st molar (%)	2nd molar (%)
Taurodontism	30	18	49	42	17 (8.99%)	34 (16.42%)
P value	0.274		0.115		0.019*	

*Statistically significant.

Results

The prevalence of taurodontism was 139 (12.87%) and 51 (29.76%) in the participants with CLP and healthy individuals, respectively. The analysis of the present results indicated that the presence of CLP was significantly associated with a higher prevalence of taurodontism ($P < 0.001$). Table 1 shows the frequency of taurodontism among the three groups. The frequency of taurodontism was significantly correlated with the type of CLP ($P < 0.001$). In this regard, it was found that taurodontism was significantly higher in the BCLP group than the UCLP ($P = 0.003$) and control groups ($P < 0.001$).

The different classifications of taurodontism (hypo-, meso- and hypertaurodontism) were assessed among patients with BCLP and UCLP and the control group. The results indicated that there was no difference between the three groups regarding the severity of taurodontism (Table 2).

The frequency of taurodontism in second molars in the control group was significantly higher than in first molars ($P = 0.019$); however, this difference was not significant among patients with BCLP and UCLP (Table 3).

The results in Table 4 indicate that in both CLP and control groups, taurodontism was significantly more prevalent in the maxilla compared to the mandible. The estimated *P* value in the BCLP and UCLP groups was < 0.001. The same outcome was obtained in the control group ($P < 0.001$). In both the CLP group and the control group, no statistically significant correlation

Table 4 Association of taurodontism with the arch in both the BCLP and UCLP groups and the control group

	BCLP group		UCLP group		Control group	
	Maxilla, n (%)	Mandible, n (%)	Maxilla, n (%)	Mandible, n (%)	Maxilla, n (%)	Mandible, n (%)
Taurodontism	42 (87.5 %)	6 (12.5%)	72 (79.12 %)	19 (20.88 %)	44 (86.27%)	7 (13.72%)
P value	< 0.001*		< 0.001*		< 0.001*	

*Statistically significant

was observed between the two sides. The *P* value in the BCLP, UCLP and control groups was estimated as 0.233, 0.429 and 0.469, respectively.

Discussion

Taurodontism is one of the dental anomalies commonly observed in molars, and its prevalence varies among different populations. Several systemic disorders have been demonstrated to be associated with taurodontism, including amelogenesis imperfecta, osteogenesis imperfecta, Down syndrome, ectodermal dysplasia, hypophosphatasia and tricho-dento-osseous syndrome.[18] Among the different systemic disorders associated with a higher risk of taurodontism, CLP, being the most common developmental craniofacial anomaly, has been suggested to have possible associations with taurodontism. Taurodontism is a developmental anomaly that can affect several clinical procedures, including endodontic procedures,[16,19] prosthetic treatment[20] and tooth extraction.[16] The large and elongated pulp chamber, as well as the shortened root canals and high proximity of dilated roots, create specific challenges for clinicians to achieve acceptable outcomes in the treatment of teeth with taurodontism.[16,21-23]

The present study indicated that the frequency of taurodontism in patients with CLP was significantly higher than in healthy individuals. This finding is confirmed by previous studies that assessed the frequency of taurodontism in patients with CLP compared with healthy individuals.[10,11,13,24] Moreover, the type of CLP also played a role in this regard, since BCLP was associated with a higher incidence of taurodontism compared to UCLP. One of the possible mechanisms through which CLP can be correlated with taurodontism is through the role of DLX genes. Since these genes are involved in the pathogenesis of both CLP and taurodontism, it can be speculated that the enhanced frequency of teeth affected by taurodontism can be associated with possible genetic factors, including DLX genes.[25,26]

Moreover, the present study demonstrated that the severity of CLP can also be associated with a higher incidence of taurodontism since the frequency of taurodontism in patients with BCLP was significantly higher than the group with UCLP. Thus, the dental care and treatment planning for these patients should be conducted with more caution. In this regard, Küchler et al[12] failed to determine the possible correlation of severity of CLP with taurodontism. This difference could be ascribed to the fact that this study included only patients with the highest severity of taurodontism (hypertaurodontism),[12] whereas the present authors included patients regardless of their level of severity of taurodontism. Furthermore, to obtain the highest precision in our study, we utilised CBCT scans to avoid possible inaccuracies and imprecisions in the diagnosis and measurement of the identified values, whereas the cases evaluated by Küchler et al[12] were examined using conventional techniques.

Concerning the severity of taurodontism, it was found that hypotaurodontism was more commonly detected, followed by mesotaurodontism and hypertaurodontism. The results of the present study are in line with previous studies.[4,11] In this regard, Weckwerth et al[11] stated that in patients with CLP, the frequency of hypotaurodontism, mesotaurodontism and hypertaurodontism was 83.70%, 10.67% and 5.61%, respectively. Similarly to the studies by Sobti et al[4] and Weckwerth et al,[11] we can assume that the frequency of taurodontism subtypes was not affected by the presence of CLP.

Also, we investigated whether the number of taurodontic teeth can also be affected by CLP. The present study demonstrated that in patients with CLP, taurodontism does not exhibit any tendency towards the first or the second molar; however, in participants without CLP, it was more frequently observed in the second molar compared to the first molar. This is in line with the study by Jamshidi et al,[27] which found that taurodontism is more commonly diagnosed in second molars compared to first molars in healthy individuals. Besides, in another study conducted by Aydin and Mobaraki,[7] in healthy individuals, the incidence of taurodontism suggests a predilection towards the second molars.

Concerning the impact of tooth laterality, it was also demonstrated that there was no significant predilection towards the left or the right side in either the control group or the CLP groups. This is in line with previous

studies that reported no significant difference in the frequency of taurodontism on the left or right side in patients without CLP.[22,27,28]

Concerning the impact of the arch on the incidence of taurodontism, the present authors found that in all three groups, the frequency of taurodontism in the maxilla was significantly higher than in the mandible. This is in line with the studies conducted by by Jamshidi et al[27] and Li et al,[29] who reported that taurodontism was more common in the maxilla compared to the mandible in a normal population. In another study, Bharti et al[30] found that taurodontism is much more frequent in the maxilla than the mandible by evaluating the full-mouth periapical radiographs of 1,000 patients. These results are further confirmed by several other studies that assessed the frequency of taurodontism through various radiographic techniques.[7,31,32] The present authors hypothesise that it could be possible that, due to the higher vascularisation of the maxilla compared to the mandible,[33] the genetic background of teeth with taurodontism may have a higher chance of incidence, and therefore the probability of formation of taurodontism may be enhanced in the tooth formation process.

The differences in root and canal morphologies in taurodont molars in the BCLP, UCLP and control group were not evaluated. Therefore, further studies are recommended to examine this topic in taurodont teeth in CLP patients.

Conclusion

The present study showed that the presence of CLP increased the incidence of taurodontism. Moreover, the type of CLP is also a factor that can further increase this phenomenon. The authors also found that the incidence of taurodontism in the maxilla is much higher than in the mandible in all groups. It is important to note that the severity of taurodontism was not affected by the presence or even the type of CLP. Thus, based on the current outcomes, clinicians should be aware of the possible complications in endodontic, prosthodontic and surgical procedures in patients with BCLP and UCLP due to the higher incidence of taurodontism in these patients.

Conflicts of interest

The authors declare no conflicts of interest related to this study.

Author contribution

Drs Maryam Paknahad, Mohammad Pordel and Fatemeh Akbarizadeh contributed to the design and implementation of the research, the analysis of the results and the writing of the manuscript.

(Received Feb 05, 2024; accepted Aug 13, 2024)

References

1. Salari N, Darvishi N, Heydari M, Bokaee S, Darvishi F, Mohammadi M. Global prevalence of cleft palate, cleft lip and cleft palate and lip: A comprehensive systematic review and meta-analysis. J Stomatol Oral Maxillofac Surg 2022;123:110–120.
2. Amiri MA, Lavaee F, Danesteh H. Use of stem cells in bone regeneration in cleft palate patients: Review and recommendations. J Korean Assoc Oral Maxillofac Surg 2022;48:71–78.
3. Farshidfar N, Ajami S, Sahmeddini S, Goli A, Foroutan HR. Epidemiological and spatiotemporal descriptive analysis of patients with nonsyndromic cleft lip and/or palate: A 12-year retrospective study in Southern Iran. Biomed Res Int 2023;2023:7624875.
4. Sobti G, Chaudhry A, Thanvi J, et al. Co-occurrence of taurodontism in nonsyndromic cleft lip and palate patients in subset of Indian population: A case–control study using CBCT. Cleft Palate Craniofac J 2023;60:1053–1060.
5. Jamilian A, Lucchese A, Darnahal A, Kamali Z, Perillo L. Cleft sidedness and congenitally missing teeth in patients with cleft lip and palate patients. Prog Orthod 2016;17:14.
6. Jabali AH, Chourasia HR, Wasli AS, et al. Taurodontism in maxillary and mandibular molars using cone beam computed tomography in a dental center in Saudi Arabia. Ann Saudi Med 2021;41:232–237.
7. Aydın H, Mobaraki S. Comparison of root and canal anatomy of taurodont and normal molar teeth: A retrospective cone-beam computed tomography study. Arch Oral Biol 2021;130:105242.
8. Penukonda R, Pattar H, Siang Lin GS, Kacharaju KR. Cone-beam computed tomography diagnosis and nonsurgical endodontic management of a taurodontic mandibular first premolar with two roots and four canals: A rare case report. J Conserv Dent 2021;24:634–639.
9. Shifman A, Chanannel I. Prevalence of taurodontism found in radiographic dental examination of 1,200 young adult Israeli patients. Community Dent Oral Epidemiol 1978;6:200–203.
10. Öçbe M, Altun BD, Borahan MO, Dumlu A. Evaluation of root dilaceration and taurodontism in children with and without cleft lip and palate. BSJ Health Sci 2023;6:309–315.
11. Weckwerth GM, Santos CF, Brozoski DT, et al. Taurodontism, root dilaceration, and tooth transposition: A radiographic study of a population with nonsyndromic cleft lip and/or palate. Cleft Palate Craniofac J 2016;53:404–412.
12. Küchler EC, da Motta LG, Vieira AR, Granjeiro JM. Side of dental anomalies and taurodontism as potential clinical markers for cleft subphenotypes. Cleft Palate Craniofac J 2011;48:103–108.
13. Melo Filho MR, Nogueira dos Santos LA, Barbosa Martelli DR, et al. Taurodontism in patients with nonsyndromic cleft lip and palate in a Brazilian population: A case control evaluation with panoramic radiographs. Oral Surg Oral Med Oral Pathol Oral Radiol 2015;120:744–750.

14. Hegde V, Anegundi RT, Pravinchandra KR. Biometric analysis - A reliable indicator for diagnosing taurodontism using panoramic radiographs. J Clin Diagn Res 2013;7:1779–1781.
15. Bronoosh P, Haghnegahdar A, Dehbozorgi M. Prevalence of taurodontism in premolars and molars in the South of Iran. J Dent Res Dent Clin Dent Prospects 2012;6:21–24.
16. MacDonald D. Taurodontism. Oral Radiol 2020;36:129–132 [erratum 2020;36:133–134].
17. Shifman A, Chanannel I. Prevalence of taurodontism found in radiographic dental examination of 1,200 young adult Israeli patients. Community Dent Oral Epidemiol 1978;6:200–203.
18. Chetty M, Roomaney IA, Beighton P. Taurodontism in dental genetics. BDJ Open 2021;7:25.
19. Nazari S, Mirmotalebi F. Endodontic treatment of a taurodontism tooth: Report of a case. Iran Endod J 2006;1:114–116.
20. Dineshshankar J, Sivakumar M, Balasubramanium AM, Kesavan G, Karthikeyan M, Prasad VS. Taurodontism. J Pharm Bioallied Sci 2014;6:S13–S15.
21. Bharti R, Chandra A, Tikku AP, Wadhwani KK. "Taurodontism" an endodontic challenge: A case report. J Oral Sci 2009;51:471–474.
22. Einy S, Yitzhaki IH, Cohen O, Smidt A, Zilberman U. Taurodontism-Prevalence, extent, and clinical challenge in Ashkelon, Israel-A retrospective study. Appl Sci. 2022;12:1062.
23. Jafarzadeh H, Azarpazhooh A, Mayhall JT. Taurodontism: A review of the condition and endodontic treatment challenges. Int Endod J 2008;41:375–388.
24. Lasota A. Dental abnormalities in children with cleft lip with or without cleft palate. J Pre-Clinical Clin Res 2020;15:46–49.
25. Dong J, Amor D, Aldred MJ, Gu T, Escamilla M, MacDougall M. DLX3 mutation associated with autosomal dominant amelogenesis imperfecta with taurodontism. Am J Med Genet A 2005;133A:138–141.
26. Sabóia TM, Reis MF, Martins ÂM, et al. DLX1 and MMP3 contribute to oral clefts with and without positive family history of cancer. Arch Oral Biol 2015;60:223–228.
27. Jamshidi D, Tofangchiha M, Jafari Pozve N, Mohammadpour M, Nouri B, Hosseinzadeh K. Prevalence of taurodont molars in a selected Iranian adult population. Iran Endod J 2017;12:282–287.
28. Abosede TY, Efunyemi AV. Prevalence of taurodontism in mandibular molars among patients at a Dental Care Institution in Nigeria. Int J Oral Dent Health 2015;1:4
29. Li Y, Qian F, Wang D, Wang Y, Wang W, Tian Y. Prevalence of taurodontism in individuals in Northwest China determined by cone-beam computed tomography images. Heliyon 2023;9:e15531.
30. Bharti R, Chandra A, Tikku AP, Arya D. Prevalence of taurodont molars in a North Indian population. Indian J Dent 2015;6:27–31.
31. Colak H, Tan E, Bayraktar Y, Hamidi MM, Colak T. Taurodontism in a central anatolian population. Dent Res J (Isfahan) 2013;10:260–263.
32. Darijani M, Ebrahimnejad H, Haghani J, Sharifi M, Jazinizadeh M. Prevalence of taurodont molars and its associated anomalies in dental patients in Kerman in 2019. J Oral Heal Oral Epidemiol 2022;11:134–139.
33. Wu V, Schulten EAJM, Helder MN, Ten Bruggenkate CM, Bravenboer N, Klein-Nulend J. Bone vitality and vascularization of mandibular and maxillary bone grafts in maxillary sinus floor elevation: A retrospective cohort study. Clin Implant Dent Relat Res 2023;25:141–151.

Orthodontic Treatment of an Adult Maxillomandibular Protrusion Case with Impacted Mandibular Second Molars Using the Physiologic Anchorage Spee-wire System: a Case Report

Huan Huan CHEN[1,2], Gui CHEN[1,2], Guang Yao FENG[2,3], Xiu Jing WANG[2,3], Tian Min XU[1,2], Hong SU[2,3]

Impaction of mandibular second molars should be resolved as soon as possible once diagnosed, since it may lead to many functional, periodontal, hygienic and endodontic problems. Treatment options for impacted second molars include orthodontic-assisted eruption following surgical exposure, surgical uprighting and, in some cases, surgical extraction with possible subsequent implant placement if the tooth is deemed non-restorable or the patient prefers an implant restoration. This case report describes the orthodontic treatment of a 21-year-old woman with maxillomandibular protrusion and impacted bilateral mandibular second molars. The Physiologic Anchorage Spee-wire System (PASS) was adopted due to its innovative strategy of physiological anchorage control and unique design involving the multilevel low-friction (MLF) bracket and cross buccal tube (XBT). After 22 months of treatment, a well-aligned dentition, a normal functional occlusion and a harmonious facial profile were obtained, and impaction of the bilateral mandibular second molars was finally resolved. This case report demonstrates a simple and efficient solution to dental impaction. The PASS technique is superior to other preadjusted straight wire appliances in the treatment of maxillomandibular protrusion cases without auxiliary anchorage devices, and the mandibular buccal tube involved in the PASS technique can assist in uprighting the impacted mandibular second molars with NiTi round wire and minimising oral discomfort for the patient.

Keywords: *anchorage, maxillomandibular protrusion, molar impaction, physiological anchorage, Spee-wire system*

Chin J Dent Res 2024;27(4):333–343; doi: 10.3290/j.cjdr.b5860297

1 Department of Orthodontics, Cranial-Facial Growth and Development Center, Peking University School and Hospital of Stomatology, Beijing, P.R. China.

2 National Center of Stomatology & National Clinical Research Center for Oral Diseases & National Engineering Research Center of Oral Biomaterials and Digital Medical Devices & Beijing Key Laboratory for Digital Stomatology & Research Center of Engineering and Technology for Computerized Dentistry Ministry of Health, Beijing, P.R. China.

3 First Clinical Division, Peking University School and Hospital of Stomatology, Beijing, P.R. China.

Corresponding author: Dr Hong SU, No. 37A Xishiku Street, Xicheng District, Beijing 100034, P.R. China. Tel: 86-10-82195737. Email: suhong0309@qq.com

The work was supported by the National Natural Science Foundation of China (no. 82001080), National Clinical Key Discipline Construction Project (PKUSSNKT-T202102) and National Programme for Multidisciplinary Cooperative Treatment on Major Diseases (PKUSSNMP-201902).

Tooth impaction is defined as the cessation of eruption or failure of teeth to erupt into the normal functional position caused by physical barriers in the eruption path.[1] Impaction of permanent second molars is relatively rare and its prevalence is often expressed as the percentage of all retained teeth in a group of patients,[2] which lies between 0.06% and 0.3%, and the prevalence rate is increasing gradually.[3] However, despite the fact that impaction is rarely seen in clinical practice, there are many functional, periodontal, hygienic and endodontic reasons that justify the need for treatment of impacted mandibular molars.[4] For example, oral hygiene in the area surrounding the impacted teeth is usually poor, which can cause caries and periodontal disease. Furthermore, undiagnosed second molar impaction may

initiate distal root resorption of the first molars, causing irreversible damage.[5,6]

The treatment of impacted teeth is very challenging for both the orthodontist and oral surgeon due to the limited access and complexity of the mechanics that needs to be applied.[7] Treatment options depend on multiple factors, such as the degree of tooth inclination, the existence of third molars and the desired type of movement in 3D directions.[8] In contrast to vertically impacted molars that may be associated with ankylosis or other factors that prevent eruption, mesially inclined or horizontally impacted mandibular second molars usually have great eruption potential, since the impaction is often due to the lack of space or abnormal eruption path.[9] Methods for managing impacted or tilted mandibular molars include surgical extraction with or without transplantation of the third molar into the extraction site, surgical uprighting and orthodontic repositioning. Further use of miniscrew as a temporary anchorage device (TAD) in the uprighting of mesially inclined mandibular molars may also be considered.[10] Among the above-mentioned methods for resolving molar impaction, the advantages of orthodontically uprighting impacted molars are functional, periodontal and restorative, showing the most promising efficacy.[11]

In addition to havingimpacted bilateral mandibular second molars, patients with tooth impaction usually display noticeable maxillomandibular protrusion. This is characterised by proclined anterior teeth and protrusive lips.[12] Most of these patients seek orthodontic treatment to improve their dental and profile aesthetics, and maximum anchorage is often required.[13] To attain better treatment outcomes, miniscrews and headgear are frequently utilised for anchorage reinforcement.[14] However, the introduction of the physiological anchorage Spee-wire system (PASS) provides orthodontists with an additional, simplified solution that can reduce the reliance on miniscrew anchorage significantly.[15] The advantages of the PASS to treat maxillomandibular protrusion include the fact that the cross buccal tube (XBT) can be used to prevent molar forward tipping following premolar extraction, and that the multilevel low-friction (MLF) bracket can be employed to facilitate the alignment of anterior teeth.

This case report describes the treatment of a 21-year-old woman with impacted bilateral mandibular second molars and mild maxillomandibular protrusion. The PASS appliance was applied following the extraction of four first premolars and three third molars.

Case report

Diagnosis and aetiology

A 21-year-old woman presented for orthodontic treatment in September 2015 with the chief concerns of occlusal disorder and lip protrusion. Her medical history showed no contraindication for orthodontic treatment.

The pretreatment facial and occlusal photographs showed an asymmetrical midline and chin, moderate maxillomandibular crowding, crossbite of the left anterior teeth, scissor bite involving the right second premolars, early loss of the maxillary left second molar, and impaction of the bilateral mandibular second molars (Fig 1). The mandibular dental midline was deviated 3.0 mm to the left and the maxillary midline was deviated 1.0 mm to the left, and the chin deviated 4.0 mm to the left of the facial midline. The dental casts showed an Angle Class III occlusion on each side with apparent crowding. Horizontal overlap was 2.0 mm, and vertical overlap was shallow (Fig S1, provided on request). The cephalometric analysis (Table 1) showed that the patient had a maxillomandibular protrusive profile relative to the cranial base, and the mandible was more protrusive than the maxilla. The impacted bilateral mandibular second molars were shown to have penetrated the oral mucosa in the intraoral photographs, but showed a severe lack of eruption potential on the panoramic radiograph (Fig 1). Clinical examination of the temporomandibular joint revealed that upon opening the mouth, the patient exhibited a single, audible click, deviation to the left during the opening motion, and a maximum degree of opening of 35 mm, and denied experiencing tenderness and restricted or limited arch movement. The panoramic radiograph demonstrated that the patient had four third molars and asymmetric bilateral joints. Her left condyle was flattened, and the left ascending ramus was shorter than the right. Although there is no definite association between the occlusal disorder caused by impaction of the second molars and temporomandibular disorder,[16] it is important to pay attention to dysfunction of the masticatory musculature.[17]

After analysis of the facial and occlusal photographs, dental casts and cephalometric and panoramic radiographs, the patient's problems were represented as an Angle Class III malocclusion with impaction of the bilateral mandibular second molars, maxillomandibular protrusion, early loss of the maxillary left second molar, and a deviated midline.

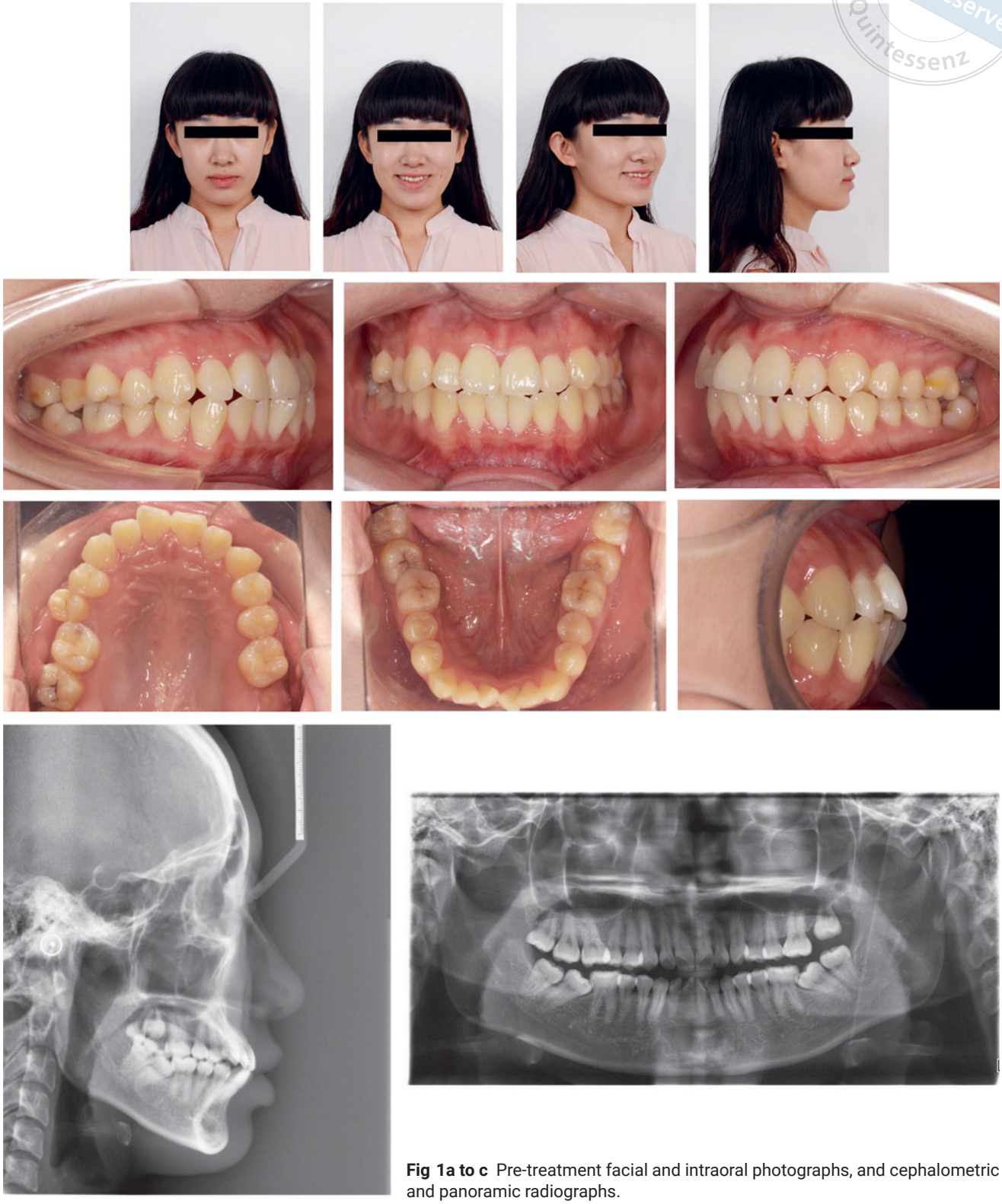

Fig 1a to c Pre-treatment facial and intraoral photographs, and cephalometric and panoramic radiographs.

Table 1 Cephalometric measurements at pre-treatment and post-treatment.

Measurement	Initial value	Final value	Norm	Standard deviation
SNA, degrees	82.2	82.2	81.2	3.5
SNB, degrees	83.3	83.6	79.2	3.2
ANB, degrees	−1.1	−1.3	2.1	1.5
SN-GoGn, degrees	28.9	28	32.8	5.3
FH-GoGn, degrees	24.8	28.5	25.4	5.3
Y axis, degrees	69.5	68.9	66.3	7.1
U1-SN, degrees	115.1	108.7	105.7	6.3
U1-NA, degrees	32.9	26.5	22.8	5.7
U1-NA, mm	11.8	7.8	3.5	6.5
U1-L1, degrees	111.5	134.9	124.2	8.2
L1-NB, degrees	36.7	20	30.5	5.8
L1-NB, mm	7.9	2.9	6.7	2.1
L1-MP, degrees	104.4	88.4	93.9	6.2
UL-EP, mm	−3.7	−6.5	−1.4	1.9
LL-EP, mm	0.8	−3.9	0.6	1.9
L7-MP, degrees	62.0	95.0	NA	NA

NA, not applicable.

Treatment

Treatment objectives

The treatment objectives were to resolve crowding and impaction of the bilateral mandibular second molars, improve the maxillomandibular protrusive profile, replace the early lost maxillary left second molar with the third molar, relieve the crossbite of the left anterior teeth and the scissor bite involving the right second premolars, achieve optimal horizontal and vertical overlap with a Class I relationship, correct the midline and chin asymmetry as far as possible without the need for surgery, and maintain a stable occlusion in the long term.

Treatment options

The following treatment options were presented to the patient and her parents:

1. Comprehensive orthodontic treatment: To resolve the dental crowding, maxillomandibular protrusion, early loss of the maxillary left second molar and molar impaction, extraction of the four first premolars and three third molars (maxillary right and mandibular left and right) was proposed. The dental midline could be corrected, but there was a risk that the chin symmetry might not change significantly without orthognathic surgery. The PASS appliance with no auxiliary anchorage and a conventional fixed appliance with TADs, such as miniscrews, were introduced to the patient separately. In the hope of achieving a better facial profile, aligning the teeth, requiring minimal surgical procedures and experiencing greater comfort during treatment, the patient opted for the PASS appliance for correction.
2. Local orthodontic treatment: This would simply involve extraction of the bilateral mandibular third molars and uprighting of the bilateral impacted second molars with local orthodontic intervention. The patient declined this option.

Written informed consent was obtained from the patient. The treatment was approved by the Institutional Review Board (IRB) of the biomedical ethics committee of Peking University School and Hospital of Stomatology (PKUSSIRB-202163049).

Treatment progress

Prior to orthodontic treatment, periodontal therapy and extraction of the four first premolars and three third molars were completed, then the patient was referred for bonding of the PASS appliance, which was characterised by the innovative design of the MLF bracket and XBT (Fig 2). The MLF brackets were originally designed to reduce friction by cutting the outer walls of the slot into slopes to shift the ligature wire off the archwire to increase the first-order clearance. In the maxilla, the XBT consists of one −25-degree auxiliary round tube that is 0.018 inches in size for thin nickel-titanium (NiTi) wires in the early stage of treatment, which will make a −25-degree tip back angle on the maxillary first molar, and another −7-degree rectangular tube with dimensions of 0.022 × 0.027 inches for thick round wires and rectangular wires in the following stages of treatment. In the mandible, a slot is cut on the occlusal wall of

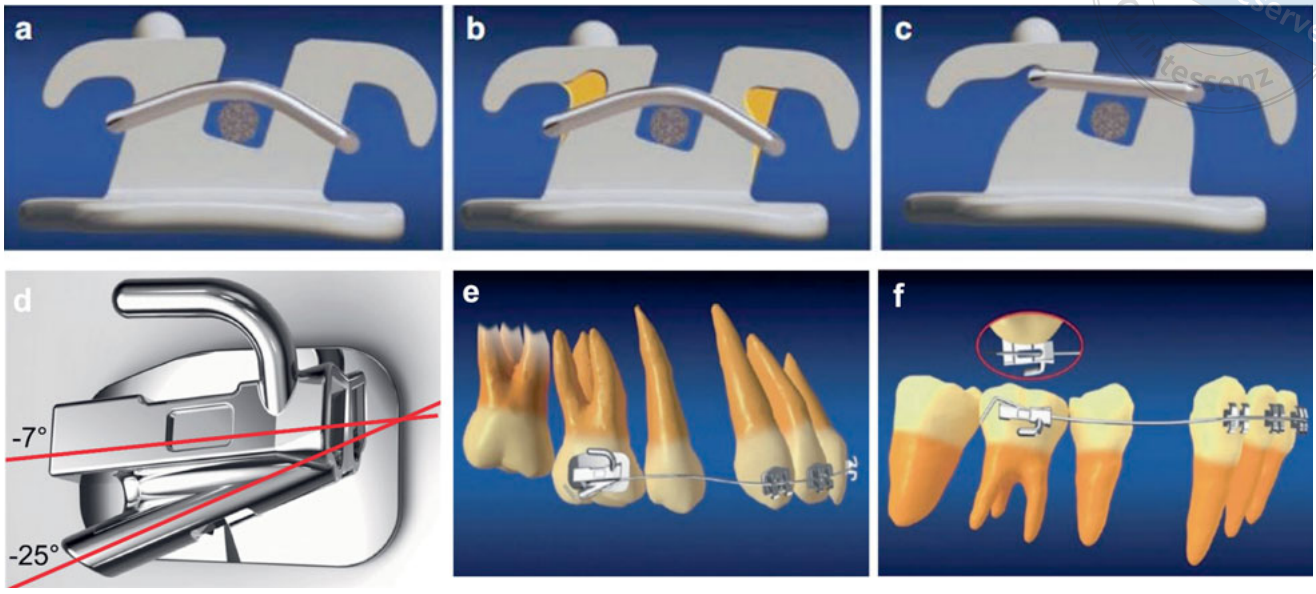

Fig 2a to f Conventional twin bracket **(a)**. Cutting the outer walls of the slot into slopes **(b)**. MLF bracket: the ligature wire was shifted up to increase the wire-slot clearance **(c)**. The XBT consists of one −25-degree auxiliary round tube and another −7-degree rectangular tube **(d)**. Initial setting showing a −25-degree tip back angle on the maxillary first molar **(e)**. A slot was cut on the occlusal wall of the conventional buccal tube and the slot size allowed thin archwires to go through, showing a −20-degree tip back angle on the mandibular first molar **(f)**.

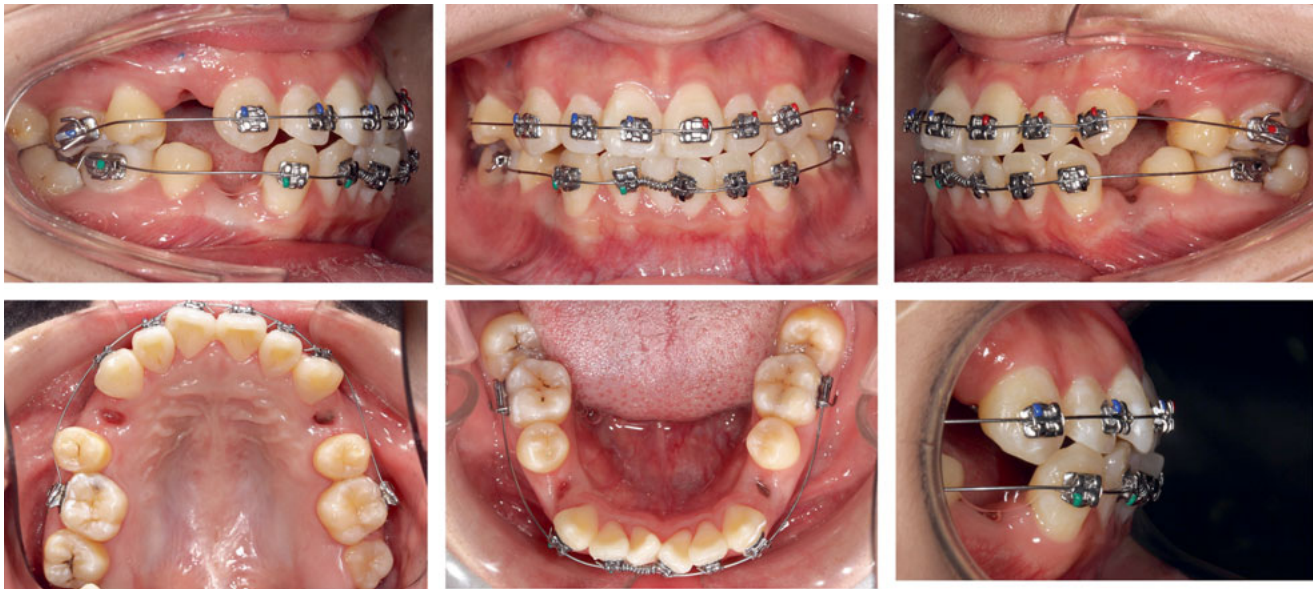

Fig 3 The maxillomandibular canine-to-canine MLF brackets and buccal tubes on the first molars were bonded, and 0.014-inch NiTi wires were engaged separately in a −25-degree tip back tube on the maxillary molars and a −20-degree tip back tube on the mandibular molars.

the conventional buccal tube and the slot size allows thin wires (usually less than 0.018 inches) to go through, which will make a −20-degree tip back angle on the mandibular first molar.18

At the first stage, the maxillomandibular canine-to-canine MLF brackets and XBT on first molars were bonded. Since the residual space for the rmandibular right central incisor was small, its bracket was not bonded and a NiTi coil-spring was used. Then, the 0.014-inch NiTi wires were inserted separately into a −25-degree round tube on the maxillary molar and a −20-degree buccal tube on the mandibular molar (Fig 3). When inserting NiTi wires into −25-degree maxillary XBT and a −20-degree mandibular buccal

Fig 4 The maxillomandibular second premolar brackets and second molar tubes were bonded when the anterior teeth were aligned. Specifically, the 0.012-inch NiTi wire was inserted into the −20-degree mandibular buccal tubes to apply a gentle and constant force to upright the bilateral impacted molars.

tube, the dominant moment was applied to the anchor molars to protect the molars from drifting forwards during the alignment stage. When there was sufficient space for the mandibular right central incisor, the bracket was bonded to align the dentition.

Four months later, the maxillomandibular second premolar brackets and second molar tubes were bonded (the maxillary left third molar had sprouted automatically and was severely twisted). To improve the inclination of the impacted mandibular second molars, the 0.012-inch NiTi wire was inserted into −20-degree mandibular buccal tubes to apply a gentle and constant force to upright the bilateral impacted molars (Fig 4). In addition, since the maxillary posterior teeth would bite the buccal tubes and wires of the mandibular posterior teeth, the pad material was bonded to the occlusal surface of the mandibular first molars. Meanwhile, the 0.016-inch NiTi wires with a normal curve of Spee were changed to the −7-degree rectangular tube of the maxillary first molars. After alignment, 0.018 × 0.025-inch NiTi wires with a normal curve of Spee were used to level irregularities in the third-order direction and prepare the teeth in the third order for engaging rectangular stainless-steel wires.

Eight months later, a 0.018- × 0.025-inch rectangular stainless-steel wire with a normal curve of Spee was used in the maxilla, while a 0.018- × 0.025-inch rectangular stainless-steel wire with a reverse curve of Spee was used in the mandible. Then a power chain and maxillomandibular elastics were employed to close the space and adjust the occlusion.

Treatment was completed in a total of 22 months (Fig 5, Fig S2 [provided on request]). The patient was followed up for 4 years without complications (Fig 6).

Results

After 22 months of treatment, a well-aligned dentition, a normal functional occlusion and a harmonious facial profile were achieved. The early lost maxillary left second molar had been perfectly replaced with the third molar, and the impaction of the bilateral mandibular second molars was resolved successfully, with the teeth having been rotated upright by approximately 33 degrees (Fig 5, Fig S2 [provided on request]). Since the maxillary molars in cases treated with the PASS technique would exhibit a slight backward retroversion, the physiological curve of Spee was maintained after treatment.

Through superimposition of the pre- and post-treatment cephalometric tracings, the lip inclination and protrusion of the maxillomandibular incisors were shown to have decreased significantly, which was also attributed to the improvement of the profile (Fig 7). The decrease in U1-NA and L1-NB indicated the anterior tooth retraction (U1-NA decreased by 4.0 mm, L1-NB decreased by 5.0 mm). In addition, the superimposition of the anterior skull base showed that the

Fig 5 Post-treatment facial and intraoral photographs, and cephalometric and panoramic radiographs (22 months in fixed applicances).

Fig 6 Post-retention facial and intraoral photographs obtained 4 years after debonding.

patient's vertical facial height was controlled properly, and the mandibular plane angle was reduced by just 0.9 degrees. The maxillary superimposition showed a small amount of forward movement of the maxillary molars and a large amount of retraction of the maxillary incisors, whereas the mandibular superimposition revealed a small amount of retroversion and forward movement of the mandibular molars, and a large amount of retraction of the mandibular incisors. The panoramic radiograph after treatment showed that the patient had no obvious root resorption (Fig 5).

The tooth movement was further quantified by superimposing the pre- and post-treatment digital models (Fig 7),[19] which showed that the mean forward movement of the maxillary first molar in a sagittal direction was 1.16 mm, less than one-third of the extraction space, achieving strong sagittal anchorage control. The mean retraction of the maxillary central incisors was 5.15 mm.

From the facial and occlusal photographs, the patient's profile was improved after treatment, from convex to straight. The midline of the maxillomandibular dentition was consistent with the facial midline (Fig 5). When smiling, the relationship between the lips and teeth was harmonious, and the patient displayed noticeable confidence and ease. Overall, the treatment was successful in addressing the patient's chief complaints and post-treatment stability was excellent at the 4-year follow-up (Fig 6).

Discussion

The incidence of impaction of the mandibular second molars is increasing gradually, and early diagnosis and treatment of eruption disturbances contributes to optimal outcomes. In most cases, extraction or uprighting of the impacted molars was the most important decision that determined the treatment planning.[20] The factors that affect this decision are mainly the degree of impaction, the relationship of the tooth with the critical anatomical structures, caries, root dilacerations, periodontal problems and the complexity of the surgical procedure. In this case report, since there was a visible clinical crown that was sufficient to be bonded with buccal tubes, surgical exposure was not necessary, and the PASS technique in this case also seemed to pro-

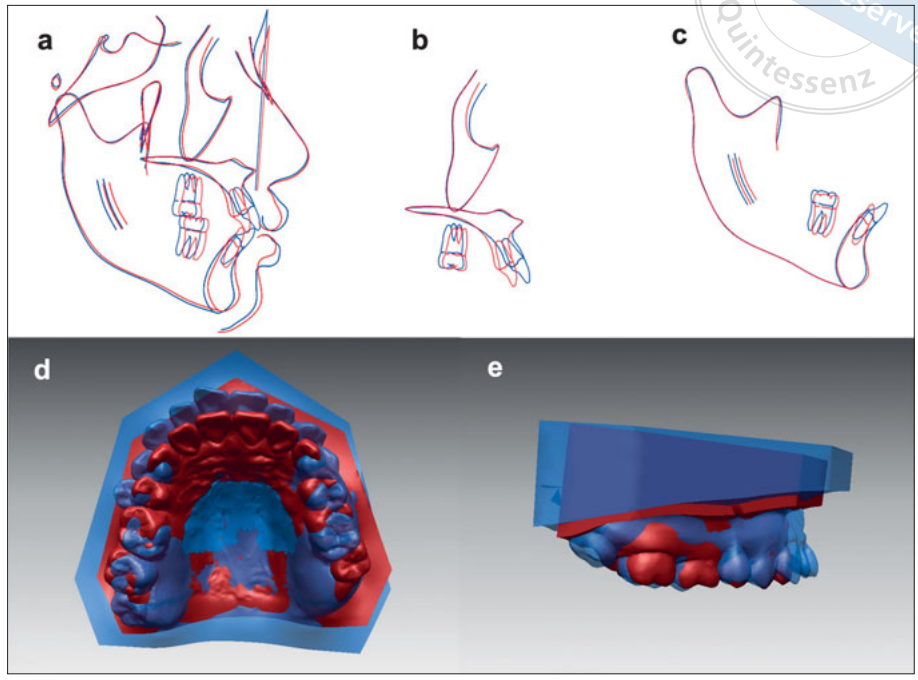

Fig 7a to e Pre- and post-treatment superimposition. Anterior skull base, maxillary, and mandibular superimposition of cephalometric radiographs **(a to c)**. Top and side views of 3D digital model superimposition, pretreatment (blue) and posttreatment (red) **(d and e)**.

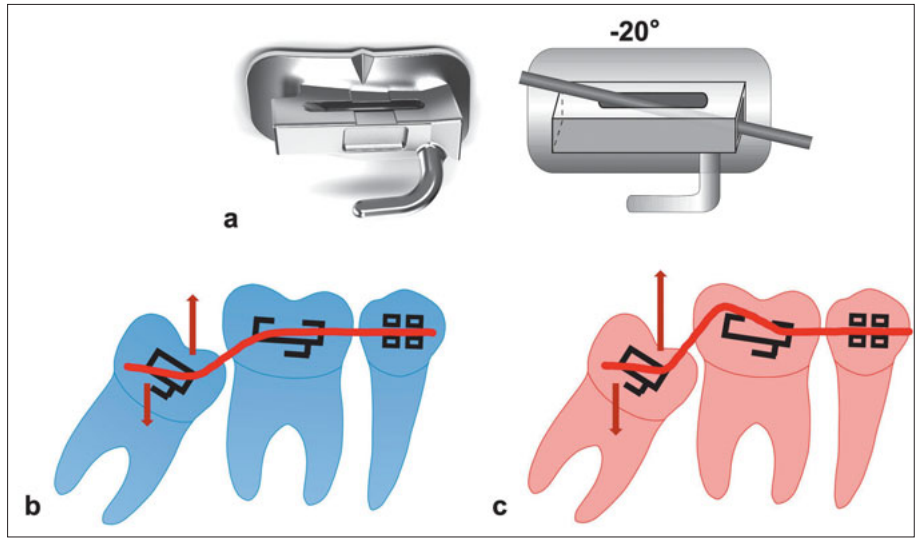

Fig 8a to c Sketch of uprighting of the impacted mandibular second molar. Mandibular buccal tube with a slot cut on the occlusal wall of the conventional buccal tube **(a)**. Insertion of the NiTi wire into the conventional rectangular tube that has a −4-degree prescribed angle **(b)**. Insertion of the NiTi wire into the mesial entrance and out from the slot of a −20-degree tip back angle **(c)**.

vide good control of the mandibular second molars during uprighting, in which just a single buccal tube was effective enough, minimising patient discomfort and reducing chair time. For example, after being bonded with buccal tubes, the mandibular second molars were engaged in 0.012-inch NiTi wire, and instead of engaging in the −4-degree conventional rectangular tube, the −20-degree tip back angle of mandibular buccal tubes were engaged, which could apply an upward and distal force to upright the bilateral impacted molars (Fig 8). The moment applied to the mandibular second molar was greater than other ordinary moments, which could upright the impacted mandibular molars more efficiently and comfortably. In the literature, since molar uprighting requires good anchorage control, multiple uprighting appliances have been applied successively to enhance anchorage and avoid undesirable tooth movements, such as Australian uprighting springs, cantilever springs and prefabricated Sander springs. However, in contrast to those that have a complicated design and relatively massive volume, the retroversion moment of PASS tubes has avoided greater inconvenience and discomfort, such as mucosal swelling, pain and poor oral hygiene. Furthermore, the invasiveness of miniscrew

implantation was avoided, and the bulkiness and inconvenience of extraoral appliances were also eliminated.[21]

Furthermore, in addition to providing good control of the mandibular second molars during uprighting, the PASS technique in this case also appeared to facilitate rapid alignment of crowded teeth and prevention of anchorage loss. The MLF bracket involved in the PASS technique has increased the clearance of the groove in the first-order direction and reduced the friction force, which can facilitate the alignment of crowded dentition at an early stage. Additionally, MLF brackets can also facilitate the "drifting" of anterior teeth back along the archwire when tip back moments are exerted, which may sometimes result in anterior scattered spacing. The PASS technique also made full use of the patient's own physiological anchorage reserve to improve the profile. The XBT buccal tube is equipped with an additional −25-degree round tube, which is used in the early alignment stage to make the molar occupy the dominant moment. The application of conventional straightwire appliances often causes the maxillary molars to tip forward rapidly under the influence of the forward tipping angle, resulting in the loss of anchorage and levelling of the curve of Spee of the maxillary molars, so as to occupy part of the extraction space. However, previous clinical application has shown that the −25 degrees exceeds the greatest tip back angle of the malpositioned teeth. Therefore, the −25-degree tip back angle of the round tube can effectively maintain the backward tipping compensation angle of the maxillary molars and avoid iatrogenic anchorage loss. The backward tipping angles in all posterior brackets and buccal tubes of the PASS appliance also inhibit the forward tipping trend of the posterior teeth due to growth and extraction, while maintaining the posterior curve of Spee, which saves more space for anterior tooth retraction. Chen et al[22] conducted a clinical randomised controlled study and found that compared with the medium or maximum anchorage cases in the McLaughlin-Bennett-Trevisi group using miniscrews, Nance's arch, headgear and other devices, the cases in the PASS group without additional anchorage devices achieved the same effect of sagittal anchorage control.[22]

For patients with maxillomandibular protrusion who are not undergoing orthognathic surgery, torque control of anterior incisors is equally crucial as the anchorage control of molars in maintaining profile aesthetics. Excessive retraction of the anterior incisors and inadequate control of tooth torque can lead to uprighting of the anterior teeth, which adversely affects patients' lip and smile aesthetics, as well as the health of the alveolar bone. In this case, the tooth movement achieved through orthodontic treatment was a controlled oblique movement. At this time, the stress on the root tip was small, and the teeth were finally close to the centre of the alveolar bone, which was the most recommended retraction method for the health of the anterior teeth. The good control of torque during treatment was due to the groove size design of the MLF bracket, which was specifically tailored to the maxillary incisors, with a slot size of 0.020 × 0.027 inches. When 0.018 × 0.025-inch rectangular stainless-steel wire was used to close the extraction space, the residual clearance was only around 2 degrees, and the positive torque could be expressed fully. Moreover, the power of retracting incisors in the PASS technique was relatively gentle, which did not further reduce the height of the labial bone platee. This adherence to gentle forces aligns with the principles of healthy orthodontic correction, effectively preventing complications such as bone dehiscence and fenestration.

Limitations

In orthodontic research, case reports serve as an important method that provides detailed insight into specific cases; however, it is essential to acknowledge the limitations inherent in this approach. For example, case reports typically focus on one or a few cases, which may limit the generalisability of the findings to a larger patient population. Additionally, they often emphasise descriptive analysis and lack a control group or statistical analysis, which makes it difficult to accurately assess the effectiveness of interventions. Therefore, future clinical research requires the collection of a more diverse range of clinical cases to validate the effectiveness of treatment. This approach is crucial for ensuring that the treatment can be applied confidently to a broader patient population.

Conclusion

Taking advantages of the PASS technique's characteristic of physiological anchorage reserve and low friction, the present authors effectively and efficiently solved the problems of maxillomandibular protrusion and dental crowding in this patient. Using the mandibular buccal tube in the PASS technique, we simply and conveniently erected the impacted mandibular second molars with NiTi round wire and minimised the patient's oral discomfort.

Conflicts of interest

The authors declare no conflicts of interest related to this study.

Author contribution

Dr Huan Huan CHEN contributed to the data collection, analysis and manuscript draft; Drs Gui CHEN, Guang Yao FENG, Xiu Jing WANG and Tian Min XU contributed to the case treatment design and supervision; Dr Hong SU contributed to the investigation, conceptualisation and critical revision of the manuscript. All authors gave final approval and agreed to be accountable for all aspects of the work.

(Received Dec 04, 2023; accepted Aug 08, 2024)

References

1. Hanisch M, Hanisch L, Kleinheinz J, et al. Primary failure of eruption (PFE): a systematic review. Head Face Med 2018;14:5.
2. Evans R. Incidence of lower second permanent molar impaction. Br J Orthod 1988;15:199–203.
3. Arevalo SS, Choy R, Rich AP, Felemban O, Bagher SM, Loo CY. Relationship of lower lingual arch appliance use and impaction of second molars: A retrospective study. Pediatr Dent 2020;42:123–125.
4. Magkavali-Trikka P, Emmanouilidis G, Papadopoulos MA. Mandibular molar uprighting using orthodontic miniscrew implants: a systematic review. Prog Orthod 2018;19:1.
5. Shapira Y, Finkelstein T, Shpack N, Lai YH, Kuftinec MM, Vardimon A. Mandibular second molar impaction. Part 1: Genetic traits and characteristics. Am J Orthod Dentofacial Orthop 2011;140:32–37.
6. Hsin-Chung Cheng J, Yi-Hsuan Lee T, Fang CY, De-Shing Chen D. Orthodontic uprighting of horizontally impacted second mandibular molar through innovative use of springs. J Dent Sci 2023;18:939–941.
7. Vedtofte H, Andreasen JO, Kjaer I. Arrested eruption of the permanent lower second molar. Eur J Orthod 1999;21:31–40.
8. Sawicka M, Racka-Pilszak B, Rosnowska-Mazurkiewicz A. Uprighting partially impacted permanent second molars. Angle Orthod 2007;77:148–154.
9. Barros SE, Faria J, Jaramillo Cevallos K, et al. Torqued and conventional cantilever for uprighting mesially impacted molars: A 3-dimensional finite element analysis. Am J Orthod Dentofacial Orthop 2022;162:e203–e215.
10. Park HS, Kyung HM, Sung JH. A simple method of molar uprighting with micro-implant anchorage. J Clin Orthod 2002;36:592–596.
11. Sabuncuoglu FA, Sencimen M, Gülses A. Surgical repositioning of a severely impacted mandibular second molar. Quintessence Int 2010;41:725–729.
12. Rajandram RK, Ponnuthurai L, Mugunam K, Chan YS. Management of bimaxillary protrusion. Oral Maxillofac Surg Clin North Am 2023;35:23–35.
13. Almutairi TK, Albarakati SF, Aldrees AM. Influence of bimaxillary protrusion on the perception of smile esthetics. Saudi Med J 2015;36:87–93.
14. Villela HM. Treatment of bimaxillary protrusion using intra- and extra-alveolar miniscrews associated to self-ligating brackets system. Dental Press J Orthod 2020;25:66–84.
15. Xu T, Vaden J, Johnston L, et al. Physiologic Anchorage Control——A New Orthodontic Concept and its Clinical Application. Cham: Springer International Publishing; 2017.
16. Bales JM, Epstein JB. The role of malocclusion and orthodontics in temporomandibular disorders. J Can Dent Assoc 1994;60:899–905.
17. Shroff B. Malocclusion as a cause for temporomandibular disorders and orthodontics as a treatment. Oral Maxillofac Surg Clin North Am 2018;30:299–302.
18. Xu TM, Zhang X, Oh HS, Boyd RL, Korn EL, Baumrind S. Randomized clinical trial comparing control of maxillary anchorage with 2 retraction techniques. Am J Orthod Dentofacial Orthop 2010;138:544.e1–e9; discussion 544–545.
19. Chen G, Chen S, Zhang XY, et al. Stable region for maxillary dental cast superimposition in adults, studied with the aid of stable miniscrews. Orthod Craniofac Res 2011;14:70–79.
20. la Monaca G, Cristalli MP, Pranno N, Galluccio G, Annibali S, Pippi R. First and second permanent molars with failed or delayed eruption: Clinical and statistical analyses. Am J Orthod Dentofacial Orthop 2019;156:355–364.
21. Lorente C, Lorente P, Perez-Vela M, Esquinas C, Lorente T. Treatment of impacted or retained second molars with the miniscrew-supported pole technique: a prospective follow-up study. Prog Orthod 2022;23:36.
22. Chen H, Han B, Jiang R, et al. PASS versus MBT (TM) for evaluation of anchorage control in three-dimensional measurements: a randomized controlled trial. Eur J Orthod 2021;43:113–119.

THE WHOLE PICTURE

NEW

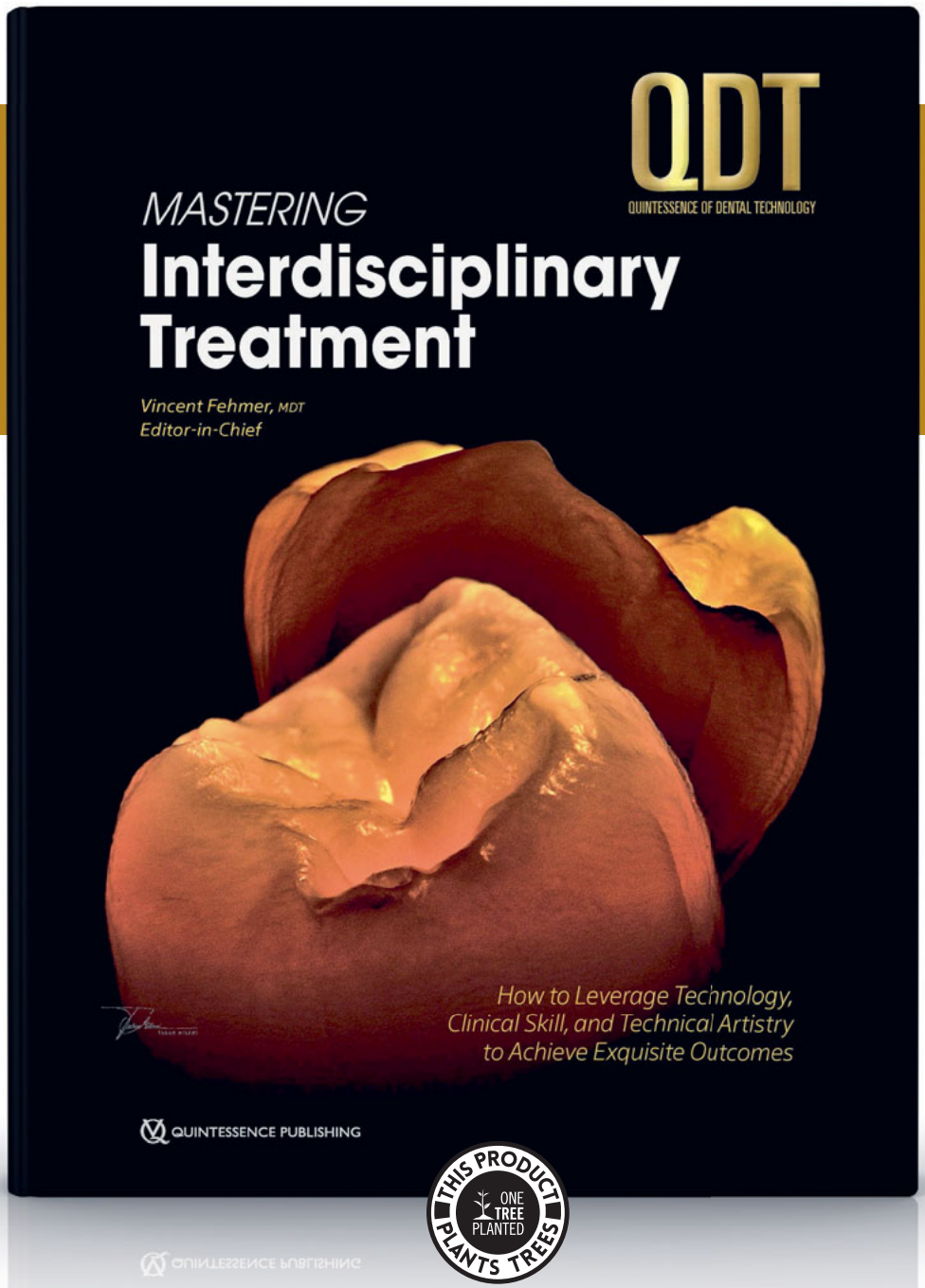

Vincent Fehmer (Ed)

Mastering Interdisciplinary Treatment

How to Leverage Technology, Clinical Skill, and Technical Artistry to Achieve Exquisite Outcomes

276 pages, 742 illus
ISBN 978-1-64724-201-5, €168

QDT has always served dental technicians with the best of the best work being done in the field. But technical artistry is only half of the equation, which is why QDT 2025 focuses on the whole picture of interdisciplinary dentistry, highlighting how clinician and technician work together to achieve predictable and esthetic outcomes. This year's issue is stacked with several articles on FP1 prostheses and the digital workflows and procedures required for their planning and delivery, as well as multiple articles on minimally invasive laminate veneers and other topics relevant to daily practice, such as the fabrication of digital complete dentures, shade matching zirconia crowns, and managing the single central incisor. Throughout the issue, the latest technologies and their capabilities are emphasized, truly reflecting this era of digital dentistry while always relying on the foundation of manual skills and artistry, which can never fully be replaced by digital tools. With such a stellar group of contributing authors, this may just be the best issue of QDT yet.

www.quint.link/qdt25
books@quintessenz.de
+49 (0)30 761 80 667

QUINTESSENCE PUBLISHING

GET A HANDLE ON EVERYTHING

Perfect training with Quintessence e-books: compact, portable, always available

We offer our e-books on numerous platforms (including Apple Books, Google Play Books and Amazon Kindle Store), so you can read them on the device of your choice: smartphone, tablet, e-reader, laptop, or PC. You can find all our e-books here: www.quint.link/e-books.

QUINTESSENCE PUBLISHING